Ph. D. Thesis

Discrete flavor symmetry for lepton mixing and quark mixing

Department of Physics, Kyoto University

Atsushi Ogasahara

May 2014

Abstract

We study non-Abelian discrete flavor symmetries, whose breaking produce the lepton mixing and the quark mixing. By using the Hernandez-Smirnov method, we systematically search symmetries in von Dyck groups and derive possible patterns of the mixing matrix at the leading order in some cases. Then, we propose some groups to generate the $\theta_{13} \neq 0$ in the lepton mixing and the quark mixing. We also discuss embedding these symmetries into a finite flavor group such as $\Delta(6N^2)$.

Contents

Chapter 1

Introduction

The study of particle phenomenology is now entering into a new frontier. In 2012, the Large Hadron Collider (LHC) experiment [1] discovered a Higgs boson, and all the components in the Standard Model (SM) are finally present. The result of the LHC experiment up to the present is consistent with the SM and does not include any strong indications for physics beyond the SM. Now we can confidently say that the SM is an effective model which faithfully re-creates particle phenomena at the electroweak scale.

Although the SM is successful in the collider experiments, other experiments have reported physics beyond the SM. For example, the experiments for the "neutrino oscillation" discovered the evidence of the nonzero neutrino masses and the lepton flavor mixing, which do not appear in the SM. They imply that there exists an underlying new theory in the lepton sector. On the other hand, the SM itself has theoretical mysteries. One of the mysteries of the SM is about the origin of parameters. For example, the Yukawa couplings have different values between flavors. However, the SM does not tell anything about the fact. From the theoretical side, we also eager an underlying theory of the SM, which describes particle physics more naturally.

For the purpose of generating the lepton flavor mixing, one of the attempts to improve the SM is to introduce an extra non-Abelian flavor symmetry and its breaking. The breaking of the flavor symmetry gives relations between three generations, which make it possible to predict the pattern of the Pontecorvo-Maki-Nakagawa-Sakata (PMNS) matrix. The PMNS matrix measured in the neutrino oscillation experiments has large mixing angles except θ_{13} [2]. In the work of the flavor symmetry models, the approximate tri-bimaximal pattern of the PMNS matrix with $\theta_{13} = 0$ is a quite interesting Ansatz for the lepton sector [3]. The tri-bimaximal mixing matrix has certain symmetries. Then, a number of studies have been carried out to derive it by using non-Abelian discrete flavor symmetries such as D_4 [4], D_7 [5], S_3 [6], S_4 [7], A_4 [8], T' [9], $PSL(2, Z_7)$ [10, 11], A_5 [12], T_7 [13], $\Delta(27)$ [14] and $SU(3)$ [15]. (See for review Ref. [16, 17, 18].) In those studies, first a non-Abelian flavor symmetry $G_f^{(\ell)}$ for the lepton sector is assumed. Then, such a symmetry is broken to G_ℓ (G_ν) in the mass terms of the charged lepton (neutrino) sector. It was also found that inherent symmetries $G_\nu = Z_2 \times Z_2$ and $G_\ell = Z_3$ in a certain basis are important to derive the tri-bimaximal mixing matrix [19].

Recent neutrino experiments show that θ_{13}^ℓ angle is not zero and relatively large [20,

21, 22, 23, 24]. However, the above approach to use flavor symmetries is still interesting to derive experimental values of lepton mixing angles (see e.g. Ref. [25]), although we need some modifications. For example, G_ℓ was often extended from Z_3 to Z_m.

Hernandez and Smirnov developed a model-independent way of screening out possible flavor symmetries in the lepton sector to derive experimental values [26]. (See also Ref. [27].) They figured out necessary conditions for ensuring that the inherent symmetries $G_\nu = Z_2(\times Z_2)$ and $G_\ell = Z_m$ can be embedded into a single discrete group. In particular, the lepton mixing angles are written interestingly in terms of a small number of integers by requiring that the product g between the Z_m element in G_ℓ and the Z_2 in G_ν should satisfy $g^p = 1$, that is, g is a Z_p element.

The mixing angles in the quark sector, the Cabibbo-Kobayashi-Maskawa (CKM) matrix, are another issue to study. These patterns are quite different from those in the lepton sector. The Cabibbo angle is as large as θ_{13} in the lepton sector, and other mixing angles are rather small. For the small mixing angles, the CKM matrix is not often generated at the leading order of the flavor symmetry breaking in models for tri-bimaximal lepton mixing. However, in the cases of large flavor symmetries, the CKM matrix could also be generated. Especially, it is expected that the Cabibbo angle is generated as well as θ_{13} in the lepton sector while the other small mixing angles in the CKM matrix are generated at the next to leading order.

There is no Ansatz to figure out underlying symmetries behind the CKM matrix like the tri-bimaximal mixing Ansatz. Here we study systematically the symmetries of the CKM matrix following Hernandez-Smirnov's analysis on the lepton sector. We assume that the flavor symmetry $G_f^{(q)}$ in the quark sector is broken to G_u (G_d) in the mass terms of the up-type quark (down-type quark) sector, where $G_u = Z_n$ and $G_d = Z_m$. Then, following Hernandez and Smirnov, we assume that the product g between the Z_m element in G_d and the Z_n in G_u should satisfy $g^p = 1$, that is, g is a Z_p element. That leads to constraints on three angles and one phase in the CKM matrix depending on m, n and p. Then, we would figure out what Abelian symmetries are important to realize the CKM matrix as $Z_2 \times Z_2$ and Z_3 symmetries are important to realize the tri-bimaximal mixing matrix. Such an analysis is useful to investigate candidates for the quark flavor symmetry $G_f^{(q)}$, which includes Z_n, Z_m and Z_p.

This paper is organized as follows. In chapter 2, we briefly review on the related part of the SM and list the values of the CKM matrix in experiments. We give simple explanations for neutrino masses and lepton mixing and list the experimental values in chapter 3. In chapter 4, we show how the flavor symmetry works for generating the lepton mixing with examples. For searching flavor symmetries to generate $\theta_{13} \neq 0$, we introduce Hernandez-Smirnov's analysis and revisit their results more carefully in chapter 5. In chapter 6, we apply their method to the quark sector and derive conditions on the CKM parameters. For some special cases, we consider the conditions and derive possible residual symmetries. In chapter 7, we consider cases that some residual symmetries in the lepton sector and the quark sector are the same, which could happen in the model for GUT. Possibilities of embedding the residual symmetries into the $\Delta(6N^2)$ groups are discussed in chapter 8. Charpter 6 and 8 are based on Ref. [28]. We summarize our discussions in chapter 9. In appendix, we review general topics about group theory and

list properties of non-Abelian symmetries such as A_4, S_4, $\Delta(6N^2)$, $PSL(2, Z_7)$ and the von Dyck group.

Chapter 2

The Standard Model

The SM is the established and confirmed model in particle physics. The SM is simple but describes the experimental result well in large part at the electroweak scale. Thereby the SM could be a base model for studying physics at the higher energy scale.

The SM is gauged under the local $\mathrm{SU}(3)_C \times \mathrm{SU}(2)_W \times \mathrm{U}(1)_Y$ symmetry. The components of the SM are summarized in Table 2.1, which shows representations of fields under $\mathrm{SU}(3)_C$, $\mathrm{SU}(2)_W$, $\mathrm{U}(1)_Y$ and their spins. In the table, the index of the $\mathrm{SU}(3)_C$ symmetry is abbreviated. The indices $i = (1, 2, 3)$ and $l = (e, \mu, \tau)$, represent flavors of the three generations. The $U_{iL(R)}$ is the up-type quark and $D_{iL(R)}$ is the down-type quark charged under the $\mathrm{SU}(3)_C$ symmetry. The $l_{L(R)}$ and ν_l are called leptons. They are called the charged leptons and neutrinos, respectively. Note that the right-handed neutrinos have not been found yet, and do not appear in the SM. The scalar field H is the Higgs field. The G, W and B are the $\mathrm{SU}(3)_C$, $\mathrm{SU}(2)_W$ and $\mathrm{U}(1)_Y$ gauge bosons, respectively.

The hypercharges Y are determined for satisfying the following Gell-Mann Nishijima formula between the $\mathrm{U}(1)_{EW}$ charge Q, the isospin T^3 of $\mathrm{SU}(2)_W$ and the hypercharge Y of $\mathrm{U}(1)_Y$,

$$Q = \frac{Y}{2} + T^3 \,. \tag{2.1}$$

The relation (2.1) comes from the phenomenological requirement that the $\mathrm{U}(1)_{EW}$ charge of the charged leptons is $Q = 1$ while the neutrino is not charged $Q = 0$. However, the theoretical requirement for the relation Eq. (2.1) has not been known yet.

The symmetry breaking of $\mathrm{SU}(2)_W \times \mathrm{U}(1)_Y$ to $\mathrm{U}(1)_{EW}$ is spontaneously driven by the Higgs mechanism. That is, the minimum of the Higgs potential

$$\mathcal{L}_H = -\frac{\lambda}{2}|H|^4 - \mu_H^2 |H|^2 \tag{2.2}$$

$$= -\frac{\lambda}{2}\left(|H|^2 + \frac{\mu_H^2}{\lambda}\right)^2 + \frac{\mu_H^4}{2\lambda^2}\,, \qquad (\mu_H^2 < 0) \tag{2.3}$$

is not at the origin $H \neq 0$. Then, the Higgs field has vacuum expectation value (vev) as

$$\langle H^+ \rangle = 0\,, \qquad \langle H^0 \rangle = v \equiv -\sqrt{\frac{\mu_H^2}{\lambda}}\,, \tag{2.4}$$

Field	$\mathrm{SU}(3)_C$	$\mathrm{SU}(2)_W$	$\mathrm{U}(1)_Y$	Spin
$Q_{iL} = \begin{pmatrix} U_{iL} \\ D_{iL} \end{pmatrix}$	$\mathbf{3}$	$\mathbf{2}$	$\frac{1}{3}$	$\frac{1}{2}$
U^*_{iR}	$\bar{\mathbf{3}}$	1	$-\frac{4}{3}$	$\frac{1}{2}$
D^*_{iR}	$\bar{\mathbf{3}}$	1	$\frac{2}{3}$	$\frac{1}{2}$
$L_{lL} = \begin{pmatrix} \nu_{lL} \\ l_L \end{pmatrix}$	1	$\mathbf{2}$	-1	$\frac{1}{2}$
l^*_R	1	1	2	$\frac{1}{2}$
$H = \begin{pmatrix} H^+ \\ H^0 \end{pmatrix}$	1	$\mathbf{2}$	1	0
G	$\mathbf{8}$	1	0	1
$W = \begin{pmatrix} W^1 \\ W^2 \\ W^3 \end{pmatrix}$	1	$\mathbf{3}$	0	1
B	1	1	0	1

Table 2.1: Field content of the SM.

which breaks $\mathrm{SU}(2)_W \times \mathrm{U}(1)_Y$ and gives masses to the gauge fields. The mass eigenstates of the massive gauge fields become

$$W^+ \equiv (W^1 + iW^2)/\sqrt{2}\,, \qquad W^- \equiv (W^1 - iW^2)/\sqrt{2}\,, \tag{2.5}$$

and

$$Z \equiv \cos\theta_W W^3 + \sin\theta_W B\,, \tag{2.6}$$

where

$$\cos\theta_W = \frac{g_2}{(g_1^2+g_2^2)^{1/2}}\,, \qquad \sin\theta_W = \frac{g_1}{(g_1^2+g_2^2)^{1/2}}\,, \tag{2.7}$$

and g_1 and g_2 are the gauge couplings of $\mathrm{U}(1)_Y$ and $\mathrm{SU}(2)_W$. The other gauge boson

$$A \equiv -\sin\theta_W W^3 + \cos\theta_W B\,, \tag{2.8}$$

which behaves as the electroweak gauge field, is massless.

The Higgs mechanism also gives masses to the quarks and charged leptons through Yukawa interactions. The Yukawa terms in the Lagrangian are written by

$$\begin{aligned}\mathcal{L}_y = &-\sum_{l,l'=e,\mu,\tau} y_L^{ll'} \overline{L}_{lL} H l'_R \\ &- \sum_{i,j=1,2,3} y_U^{ij} \overline{Q}_{iL} (i\sigma^2 H^*) U_{jR} - \sum_{i,j=1,2,3} y_D^{ij} \overline{Q}_{iL} H D_{jR} + h.c.\,,\end{aligned} \tag{2.9}$$

where $y_{L,U,D}$ are the dimensionless Yukawa couplings. The $(i\sigma^2 H^*)$ is an isospin doublet with $Y=-1$. When the Higgs field has the vev, the Dirac mass terms are read as

$$\mathcal{L}_y^{(\mathrm{mass})} = -\sum_{l,l'=e,\mu,\tau} y_L^{ll'} v \bar{l}_L l'_R - \sum_{i,j}^{3} y_U^{ij} v \overline{U}_{iL} U_{jR} - \sum_{i,j}^{3} y_D^{ij} v \overline{D}_{iL} D_{jR} + h.c.\,. \tag{2.10}$$

Note that the neutrinos are massless in the SM.

The charged current interactions come from the terms $\bar{L}\gamma^\mu D_\mu L$ and $\bar{Q}\gamma^\mu D_\mu Q$. The lepton part of the charged current interaction is

$$\mathcal{L}_{cc}^{l} = \sum_l \frac{g_2}{\sqrt{2}} \bar{l}_L \gamma^\mu W_\mu^+ \nu_{lL} + h.c.\,, \tag{2.11}$$

and the quark part is

$$\mathcal{L}_{cc}^{q} = \sum_i \frac{g_2}{\sqrt{2}} \bar{U}_{iL} \gamma^\mu W_\mu^+ D_{iL} + h.c.\,. \tag{2.12}$$

2.1 Flavor mixing of the quark masses

The flavor mixing in the quark sector is a property described in the framework of the SM. Quark masses in both up and down sectors are given via the Yukawa interactions with the Higgs field. In Eq. (2.10) and Eq. (2.12), the quark masses and the charged current weak interactions are written in the flavor basis. Taking the diagonal basis of the up sector, the mass terms and charged current weak interaction of the quark sector are written by

$$\mathcal{L}^q = -\frac{g_2}{\sqrt{2}}\bar{U}_L V_{\rm CKM}\gamma^\mu W^+_\mu D_L - \bar{U}_R\hat{M}_U U_L - \bar{D}_R V_{\rm CKM}\hat{M}_D V^\dagger_{\rm CKM} D_L + h.c.\,, \tag{2.13}$$

where

$$\hat{M}_U \equiv {\rm diag}\{m_u, m_c, m_t\}\,, \qquad \hat{M}_D = {\rm diag}\{m_d, m_s, m_b\}\,. \tag{2.14}$$

The fields of the up and down sectors in the flavor basis are $U_{L(R)} \equiv (u, c, t)^T_{L(R)}$ and $D_{L(R)} \equiv (d, s, b)^T_{L(R)}$, respectively. The quark flavor mixing $V_{\rm CKM}$ is called the Cabibbo-Kobayashi-Maskawa (CKM) matrix, which is a 3×3 unitary matrix and parametrized by the following three mixing angles (θ_{12}, θ_{23}, θ_{13}) and a CP-violating phase δ as

$$V_{\rm CKM} \equiv \begin{pmatrix} V_{ud} & V_{us} & V_{ub} \\ V_{cd} & V_{cs} & V_{cb} \\ V_{td} & V_{ts} & V_{tb} \end{pmatrix} \tag{2.15}$$

$$= \begin{pmatrix} c_{12}c_{13} & s_{12}c_{13} & s_{13}e^{-i\delta} \\ -s_{12}c_{23} - c_{12}s_{23}s_{13}e^{i\delta} & c_{12}c_{23} - s_{12}s_{23}s_{13}e^{i\delta} & s_{23}c_{13} \\ s_{12}s_{23} - c_{12}c_{23}s_{13}e^{i\delta} & -c_{12}s_{23} - s_{12}c_{23}s_{13}e^{i\delta} & c_{23}c_{13} \end{pmatrix}\,, \tag{2.16}$$

where s_{ij} and c_{ij} represent $\sin\theta_{ij}$ and $\cos\theta_{ij}$, respectively. The CP-violating phase δ appearing in the CKM matrix is the only CP-violation which has ever been confirmed in the SM. One often uses the Jarlskog invariant J_{CP} for representing the CP-violation instead of the δ,

$$\begin{aligned} J_{CP} &\equiv {\rm Im}\,(V_{us}V_{cb}V^*_{ub}V^*_{cs}) \\ &= \sin\theta_{12}\cos\theta_{12}\sin\theta_{23}\cos\theta_{23}\sin\theta_{13}\cos^2\theta_{13}\sin\delta\,, \end{aligned} \tag{2.17}$$

which is independent of phase convention of the quarks.

A similar mixing appears in the lepton sector, if the neutrinos are massive. Otherwise, mixing angles in the lepton sector vanish.

Experimental data for quark mixing

The values of the quark mixing CKM matrix elements are well measured in the experiments. The magnitudes of the CKM matrix are [2]

$$V_{\rm CKM} = \begin{pmatrix} 0.97427 \pm 0.00015 & 0.22534 \pm 0.00065 & 0.00351^{+0.00015}_{-0.00014} \\ 0.22520 \pm 0.00065 & 0.97344 \pm 0.00016 & 0.0412^{+0.0011}_{-0.0005} \\ 0.00867^{+0.00029}_{-0.00031} & 0.0404^{+0.0011}_{-0.0005} & 0.999146^{+0.000021}_{-0.000046} \end{pmatrix}\,, \tag{2.18}$$

and the Jarlskog invariant is $J = (2.96^{+0.20}_{-0.16}) \times 10^{-5}$. In the thesis, we use the following values

$$(\sin\theta_{12},\, \sin\theta_{23},\, \sin\theta_{13},\, \cos\delta) = (0.225, 0.0412, 0.00341, 0.355) \tag{2.19}$$

as the central experimental values.

2.2 RGE corrections to the quark mixing

The CKM matrix is influenced by the renormalization group equation (RGE) effect. The RGEs for the CKM matrix have been evaluated in, for examples, Ref. [29, 30].

The RGEs for the CKM matrix is approximately written by [30]

$$\frac{d}{d\ln\mu}\theta_{23}^2 = \frac{3}{8\pi^2}y_t^2(\mu)\theta_{23}^2\,, \qquad \frac{d}{d\ln\mu}\theta_{13}^2 = \frac{3}{8\pi^2}y_t^2(\mu)\theta_{13}^2\,, \tag{2.20}$$

and θ_{12} and δ do not vary. Here, μ is a renormalization scale and y_t is the top Yukawa coupling. According to the analysis at the two-loop order [30], corrections to θ_{12} and δ are about a few percents at the Planck scale.

The 1-loop RGEs for the top Yukawa coupling and gauge couplings in the SM are the followings (For the 3-loop RGEs of the SM, see Ref. [31].)

$$\frac{d}{d\ln\mu}y_t^2 = \frac{9}{2}\frac{y_t^2}{8\pi^2}\left[y_t^2 - \frac{17}{54}g_1^2 - \frac{1}{2}g_2^2 - \frac{16}{9}g_3^2\right]\,, \tag{2.21}$$

$$\frac{d}{d\ln\mu}g_1^2 = \frac{g_1^4}{8\pi^2}\left[\frac{10n_f}{9} + \frac{1}{6}\right]\,, \qquad \frac{d}{d\ln\mu}g_2^2 = \frac{g_2^4}{8\pi^2}\left[\frac{2n_f}{3} - \frac{43}{6}\right]\,, \tag{2.22}$$

$$\frac{d}{d\ln\mu}g_3^2 = \frac{g_3^4}{8\pi^2}\left[\frac{2n_f}{3} - 11\right]\,, \tag{2.23}$$

where n_f is the number of quarks appearing at the scale μ.

In our notation, the top Yukawa coupling y_t is derived from the Higgs vev v and the top quark mass m_t as

$$y_t = \frac{m_t}{v}\,, \qquad v = \sqrt{\frac{2}{g_1^2 + g_2^2}}m_z\,. \tag{2.24}$$

We use the following input data at the scale $m_z = 91.2$ GeV

$$m_t(m_z) = 164.4 \text{ GeV}\,, \qquad \alpha_s(m_z) = 0.1185\,, \tag{2.25}$$

$$\alpha(m_z) = \frac{1}{129}\,, \qquad \sin\theta_W = 0.231\,. \tag{2.26}$$

and $n_f = 6$. Note that the Higgs vev becomes $v \simeq 174$ in our notation. The results of the RG flows of θ_{23} and θ_{13} are depicted in Fig. 2.1. We find that the mixing angles do not drastically vary at the high energy scale in the SM.

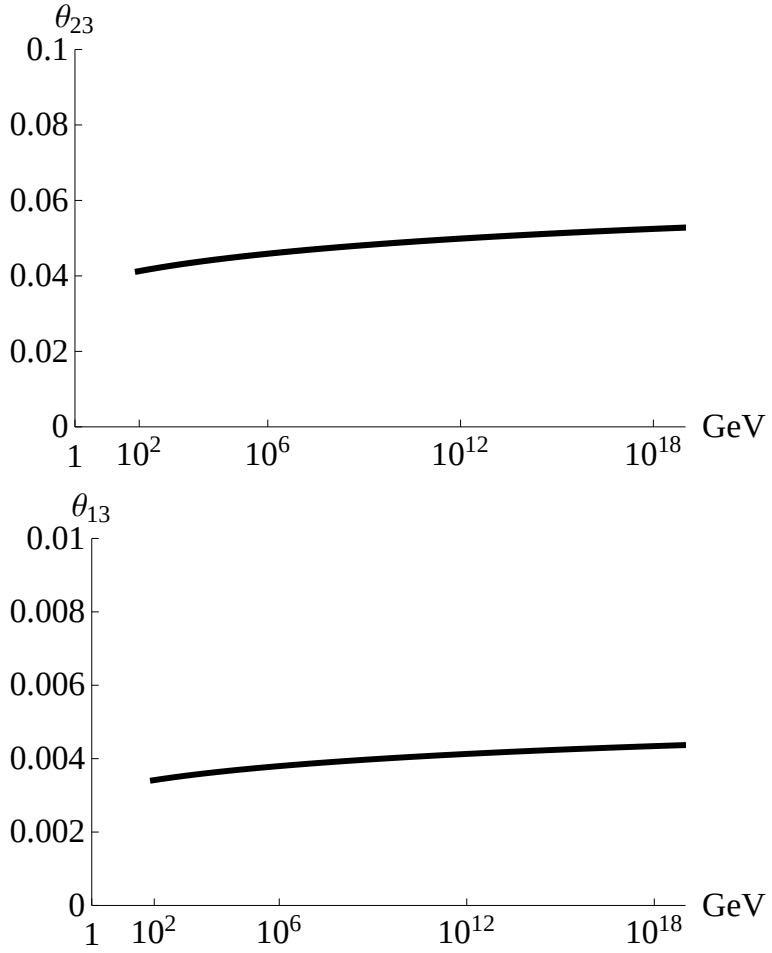

Figure 2.1: The RG flows of θ_{23} (upper graph) and θ_{13} (lower graph) in the SM.

Chapter 3

Neutrino Mass and Lepton Mixing

In the SM, there are 3 flavors of left-handed neutrinos, ν_e, ν_μ, ν_τ. The left-handed neutrinos are charged under $SU(2)_W$ and are produced by charged current weak interactions with charged leptons. The process of producing a neutrino is going within each flavor. That is the produced neutrino and the interacting charged lepton are in the same flavor state, for examples, ν_e is produced with e^+, ν_μ is produced with μ^+, and ν_τ is produced with τ^+ in the β^+ decay. In the SM, neutrinos are massless particles, and each flavor is conserved in the lepton sector.

If neutrinos have non-zero masses, neutrinos in the mass diagonal basis become different from that in the flavor basis. It leads to the lepton flavor mixing. The most experimentally important phenomenon caused by the neutrino flavor mixing is the "neutrino oscillation." The neutrino oscillation is a quantum mechanical phenomenon, in which neutrinos vary their flavors during propagation.

Recently, the experiments have revealed the existence of neutrino oscillations in detail. They strongly suggest that neutrinos have non-zero masses and 3 flavors are largely mixing.

In this chapter, we review on the neutrino masses, the lepton flavor mixing and the neutrino oscillation. Then, we list the recent experimental results. We also discuss the RG effect to the lepton flavor mixing at the high energy scale.

3.1 Neutrino mass

3.1.1 Majorana mass

The origin of the neutrino masses have not been known yet. When constructing a neutrino mass term with only the left-handed neutrino ν_L, we must prepare a right-handed function, which is a charge conjugation of ν_L. The charge conjugation operator C is given by $C \equiv i\gamma^2\gamma^0$ and the charge conjugation of a Dirac field ψ is represented by

$$\psi^c = C\bar{\psi}^T . \tag{3.1}$$

Then, using the following charge conjugation of the left-handed neutrino,

$$\nu_L^c = C\bar{\nu}_L^T = i\sigma^2\nu_L^* \,, \tag{3.2}$$

we define the neutrino Majorana field as

$$\nu = \begin{pmatrix} \nu_L \\ \nu_L^c \end{pmatrix} \,, \tag{3.3}$$

which satisfies $\nu^c = \nu$. It allows to build a neutrino Majorana mass term as

$$\bar{\nu} M_\nu \nu = \overline{\nu_L^c} M_\nu \nu_L + h.c. \,. \tag{3.4}$$

Note that the neutrino Majorana mass term breaks the lepton number. Under the following U(1) transformation,

$$\nu_L \to e^{i\varphi}\nu_L \,, \qquad \overline{\nu_L^c} \to e^{i\varphi}\overline{\nu_L^c} \,, \tag{3.5}$$

the Eq. (3.4) is not invariant.

In the SM, the neutrino mass term is forbidden in a renormalizable Lagrangian due to the charge assignment of the fields. A simple way to represent the neutrino masses is to introduce an effective Majorana mass term with a higher dimensional operator such as

$$\mathcal{L}_\nu^M \sim y_\nu \frac{1}{\Lambda}(\overline{L_L^c}\sigma^2 H)(H^T\sigma^2 L_L) \sim y_\nu \frac{1}{\Lambda}\overline{\nu_L^c} H^0 H^0 \nu_L \,. \tag{3.6}$$

where y_ν is the dimensionless coupling and Λ is a high energy scale of the new theory beyond the SM. The Higgs mechanism gives $\langle H^0 \rangle = v$ and the neutrino Majorana mass is given by

$$M_\nu = \frac{y_\nu v^2}{\Lambda} \,. \tag{3.7}$$

If $\Lambda \sim 10^{16}$GeV, $y = O(1)$ and $v = 174$GeV, the Majorana mass is of $O(0.01)$eV which is consistent with the experimental result.

3.1.2 Dirac mass

Another way to generate the neutrino mass is to introduce the right-handed neutrino ν_R. For the condition of the gauge anomaly, the right-handed neutrino is singlet under the symmetry $\mathrm{SU}(3)_C \times \mathrm{SU}(2)_W$ and has vanishing $\mathrm{U}(1)_Y$ charge. Then, we sometimes call the right-handed neutrino as the sterile neutrino. The left- and right-handed neutrinos construct a Dirac mass term as

$$y_\nu \overline{L_L}(i\sigma^2 H^*)\nu_R + h.c. = y_\nu \bar{\nu}_L H^0 \nu_R + h.c. \,. \tag{3.8}$$

The Higgs mechanism gives $\langle H^0 \rangle = v$, and the Dirac mass term is diagonalized by the bi-unitary matrices.

The order of the above Dirac neutrino masses are $M_{\nu D} \sim y_\nu v$. However, the neutrino masses in the experiments are much smaller than the Higgs vev $v = 174\text{GeV}$. Then, we need a small Yukawa coupling $y_\nu \lesssim 10^{-12}$ or another mechanism for the small neutrino mass.

The seesaw mechanism is a well-known method for the small neutrino mass. The simplest seesaw model is to consider both the Dirac mass and Majorana mass term of the right-handed neutrino. As the right-handed neutrino is not charged under gauge symmetries, we can construct the Majorana mass term as

$$\overline{\nu_R^c} M_{\nu R} \nu_R + h.c.\,. \tag{3.9}$$

The neutrino mass matrix $\mathcal{M}$ in the basis of $\nu' = (\nu_L, \nu_R^c)^T$ is

$$\overline{\nu'^c} \mathcal{M} \nu' + h.c.\,, \tag{3.10}$$

$$\mathcal{M} = \begin{pmatrix} 0 & y_\nu v \\ y_\nu v & M_{\nu R} \end{pmatrix}. \tag{3.11}$$

The mass matrix is diagonalized by the unitary matrix U as $U\mathcal{M}U^T$. As the right-handed neutrino does not couple to the SM Higgs field, the scale of the Majorana mass of the right-handed neutrino is not given by the SM Higgs mechanism. Instead, we assume that $M_{\nu R}$ is the order of a high energy theory beyond the SM. In the approximation of $M_{\nu R} \gg y_\nu v$, the mass eigenvanlues $M_{\nu 1}$, $M_{\nu 2}$ of the neutrinos are

$$M_{\nu 1} = -\frac{(y_\nu v)^2}{M_{\nu R}}\,, \qquad M_{\nu 2} = M_{\nu R} + \frac{(y_\nu v)^2}{M_{\nu R}}\,. \tag{3.12}$$

The minus sign of the first solution can be absorbed by the phase definition of ν'. Then light neutrino mass is given by

$$m = \frac{(y_\nu v)^2}{M_{\nu R}}\,. \tag{3.13}$$

The form of the neutrino mass in this see-saw mechamism is similar to that of the 5 dimensional operator of the Majorana neutrino Eq. (3.7), which naturally gives the order of the neutrino mass observed in the experiments.

3.2 Lepton mixing

We consider the case that neutrinos have non-zero masses and are Majorana fermions. The case that neutrinos are Dirac fermions can be treated in a similar way.

Charged leptons acquire masses from the Yukawa interaction with the Higgs field in the SM. In the flavor basis, the mass terms and charged current weak interaction of the lepton sector can be written by

$$\mathcal{L}^l = -\frac{g}{\sqrt{2}} \bar{l}_L \gamma^\mu W_\mu^+ \nu_{lL} - \bar{l}_R \hat{M}_l l_L - \bar{\nu}_{lL}^c U_{\text{PMNS}}^* \hat{M}_\nu U_{\text{PMNS}}^\dagger \nu_{lL} + h.c.\,, \tag{3.14}$$

where

$$\hat{M}_l \equiv \mathrm{diag}\{m_e,\, m_\nu,\, m_\tau\}\,, \qquad \hat{M}_\nu \equiv \mathrm{diag}\{m_1,\, m_2,\, m_3\}\,. \tag{3.15}$$

Here $l_{L(R)} \equiv (e,\, \mu,\, \tau)^T_{L(R)}$ are the 3 flavors of charged leptons, and neutrinos are in the flavor basis $\nu_{lL} \equiv (\nu_e, \nu_\mu, \nu_\tau)^T$.

As Eq. (3.14) is in the diagonal basis of the charged leptons, one can not simultaneously diagonalize the neutrino mass term while maintaining the other terms. Then, there remains a difference between neutrinos in the mass diagonal basis ν_{iL} $(i = 1, 2, 3)$ and that in the flavor basis ν_{lL} $(l = e,\, \mu,\, \tau)$

$$\nu_{lL} = U_{\mathrm{PMNS}} \nu_{iL}\,, \tag{3.16}$$

where U_{PMNS} is called the Pontecorvo-Maki-Nakagawa-Sakata (PMNS) matrix. When neutrinos are Majorana fermions, the PMNS matrix is a product of a unitary 3×3 matrix V, and Majorana phases P,

$$U_{\mathrm{PMNS}} = VP\,, \tag{3.17}$$

where V and P are parametrized as

$$V = \begin{pmatrix} 1 & 0 & 0 \\ 0 & c_{23} & s_{23} \\ 0 & -s_{23} & c_{23} \end{pmatrix} \begin{pmatrix} c_{13} & 0 & s_{13}e^{-i\delta^l} \\ 0 & 1 & 0 \\ -s_{13}e^{i\delta^l} & 0 & c_{13} \end{pmatrix} \begin{pmatrix} c_{12} & s_{12} & 0 \\ -s_{12} & c_{12} & 0 \\ 0 & 0 & 1 \end{pmatrix} \tag{3.18}$$

$$= \begin{pmatrix} c_{12}c_{13} & s_{12}c_{13} & s_{13}e^{-i\delta^l} \\ -s_{12}c_{23} - c_{12}s_{23}s_{13}e^{i\delta^l} & c_{12}c_{23} - s_{12}s_{23}s_{13}e^{i\delta^l} & s_{23}c_{13} \\ s_{12}s_{23} - c_{12}c_{23}s_{13}e^{i\delta^l} & -c_{12}s_{23} - s_{12}c_{23}s_{13}e^{i\delta^l} & c_{23}c_{13} \end{pmatrix}\,, \tag{3.19}$$

and $P = \mathrm{diag}\{1,\, e^{i\alpha_1},\, e^{i\alpha_2}\}$. Here s_{ij} and c_{ij} represent $\sin\theta^l_{ij}$ and $\cos\theta^l_{ij}$, respectively. Parameters in the unitary matrix are three Euler angles
$(\theta^l_{12},\, \theta^l_{23},\, \theta^l_{13})$ and a Dirac CP-violating phase δ^l. Note that Majorana CP-violating phases P do not appear if neutrinos are Dirac fermions.

3.3 Neutrino oscillations

The facts that neutrinos have non-degenerate masses and the lepton flavors are mixing are experimentally confirmed by the neutrino oscillations. Here we review a simplified explanation for the neutrino oscillations [32, 2].

Since neutrinos are always produced by charged current weak interactions, we consider a system to begin in a neutrino flavor state $|\nu_l\rangle$ $(l = e, \mu, \tau)$ at $(x, t) = (0, 0)$. Then we assume that the neutrino propagates in vacuum.

When neutrinos have non-zero masses, the neutrinos in the flavor state $|\nu_l\rangle$ can be written by a superposition of the mass eigenstates $|\nu_i\rangle$ $(i = 1, 2, 3)$ with the PMNS matrix U as

$$|\nu_l\rangle = \sum_{j=1}^{3} U^*_{lj} |\nu_j, \tilde{p}_j\rangle\,, \tag{3.20}$$

where $\tilde{p}_j \equiv (E_j, \mathbf{p}_j)$. In this case, the amplitude A of the probability that we find the neutrino with a flavor eigenstate $|\nu_{l'}\rangle$ at $(x,t) = (\mathbf{L}, T)$ is

$$\begin{aligned} A(\nu_l \to \nu_{l'}) &= \langle \nu_{l'} | \nu_l(\mathbf{L}, t) \rangle \\ &= \sum_j U_{l'j} e^{-i(E_j T - \mathbf{p}_j \cdot \mathbf{L})} U^\dagger_{jl} \,. \end{aligned} \tag{3.21}$$

As the probability is $P = |A|^2$, let us focus on the phase difference $\delta\varphi_{jk}$ in the following

$$\begin{aligned} \delta\varphi_{jk} &= (E_j - E_k)T - (p_j - p_k)L \\ &= (E_j - E_k)\left[T - \frac{E_j + E_k}{p_j + p_k} L\right] + \frac{m_j^2 - m_k^2}{p_j + p_k} L \,, \end{aligned} \tag{3.22}$$

where $L \equiv \hat{\mathbf{p}} \cdot \mathbf{L}$. Here we assume the directions of momenta are the same, $\mathbf{p}_j = \hat{\mathbf{p}} p_j$, $\mathbf{p}_k = \hat{\mathbf{p}} p_k$ for simplicity. In the relativistic limit, the first term in the right-hand-side is negligible. Then the phase can be approximated as

$$\delta\varphi_{jk} \sim \frac{\Delta m_{jk}^2}{p_j + p_k} L \,, \tag{3.23}$$

where $\Delta m_{jk}^2 \equiv m_j^2 - m_k^2$. Therefore, the probability P for the $\nu_l \to \nu_{l'}$ oscillation is estimated by

$$\begin{aligned} P(\nu_l \to \nu_{l'}) &= \sum_j |U_{l'j}|^2 |U_{lj}|^2 \\ &\quad + 2 \sum_{j>k} |U_{lk} U^*_{l'k} U_{l'j} U^*_{lj}| \cos\left[\frac{\Delta m_{jk}^2}{p_j + p_k} L - \arg\left(U_{lk} U^*_{l'k} U_{l'j} U^*_{lj}\right)\right] . \end{aligned} \tag{3.24}$$

Similarly, the probability for the $\bar{\nu}_l \to \bar{\nu}_{l'}$ oscillation becomes

$$\begin{aligned} P(\bar{\nu}_l \to \bar{\nu}_{l'}) &= \sum_j |U_{l'j}|^2 |U_{lj}|^2 \\ &\quad + 2 \sum_{j>k} |U_{lk} U^*_{l'k} U_{l'j} U^*_{lj}| \cos\left[\frac{\Delta m_{jk}^2}{p_j + p_k} L + \arg\left(U_{lk} U^*_{l'k} U_{l'j} U^*_{lj}\right)\right] . \end{aligned} \tag{3.25}$$

From the above equations Eq. (3.24) and Eq. (3.25), we can see that the probability for neutrino oscillations depends on the PMNS matrix U and the neutrino masses.

The CP-violation can be evaluated by considering the following value

$$P(\nu_l \to \nu_{l'}) - P(\bar{\nu}_l \to \bar{\nu}_{l'}) = 4 \sum_{j>k} \mathrm{Im}\left(U_{lk} U^*_{l'k} U_{l'j} U^*_{lj}\right) \sin \frac{\Delta m_{jk}^2}{p_j + p_k} L \,. \tag{3.26}$$

As the U is a unitary 3×3 matrix, all the magnitudes of $\mathrm{Im}\left(U_{lk} U^*_{l'k} U_{l'j} U^*_{lj}\right)$ are the same for any $l \neq l'$ $(j \neq k)$. Then, the CP violation in $\nu_e \to \nu_\mu$ is written by

$$\begin{aligned} &P(\nu_e \to \nu_\mu) - P(\bar{\nu}_e \to \bar{\nu}_\mu) \\ &\quad = 4\mathrm{Im}\left(U_{e2} U^*_{\mu 2} U_{\mu 3} U^*_{e3}\right) \left(\sin \frac{\Delta m_{32}^2}{p_3 + p_2} L + \sin \frac{\Delta m_{21}^2}{p_2 + p_1} L + \sin \frac{\Delta m_{13}^2}{p_1 + p_3} L\right) . \end{aligned} \tag{3.27}$$

The magnitudes of Eq. (3.26) with $\nu_e \to \nu_\mu$, $\nu_\mu \to \nu_\tau$, $\nu_e \to \nu_\tau$ and their inverse processes are all the same. Therefore, one often defines

$$J^l_{CP} \equiv \mathrm{Im}\left(U_{e2}U^*_{\mu 2}U_{\mu 3}U^*_{e3}\right) \tag{3.28}$$

$$= \sin\theta^l_{12}\cos\theta^l_{12}\sin\theta^l_{23}\cos\theta^l_{23}\sin\theta^l_{13}\cos^2\theta^l_{13}\sin\delta^l\,, \tag{3.29}$$

as the variable for measuring the CP violation effects instead of the Dirac CP phase δ^l.

3.4 Experimental data for neutrinos

There are many experiments for neutrino oscillations. Often the neutrino oscillations are observed as the neutrino "disappearance" and "appearance". In 1960s, the lack of the amount of the solar ν_e was first reported in the Homestake experiment [33]. Then in 1998, the Super-Kamiokande [34] observed the atmospheric ν_μ disappearance consistent with $\nu_\mu \to \nu_\tau$ oscillation, which is the first evidence for the neutrino oscillation. In 2003, the Kamland [35] reported the detection of the reactor $\bar{\nu}_e$ disappearance. In 2011, T2K [20] reported the $\nu_\mu \to \nu_e$ appearance of 2.5σ, which is consistent with the MINOS report [21] in later. In 2011, the DOUBLE-CHOOZ [22] reported the indications of the reactor $\bar{\nu}_e$ disappearance. Then in 2012, DAYA-BAY [23] and RENO [24] reported the reactor $\bar{\nu}_e$ disappearance of 5.2σ and 4.9σ, respectively.

During the above history, there are many other experiments for supporting the neutrino oscillations. Through all the experiments, the neutrino masses and lepton mixing are confirmed.

According to the Particle Data Group [2], in the case of 3-neutrino lepton flavor mixing, the best-fit values of lepton mixing angles are

$$\sin^2(2\theta^l_{12}) = 0.857 \pm 0.024\,, \tag{3.30}$$

$$\sin^2(2\theta^l_{23}) > 0.95\,, \tag{3.31}$$

$$\sin^2(2\theta^l_{13}) = 0.095 \pm 0.010\,, \tag{3.32}$$

and there are no experimental data on the CP-violating phases, $(\delta^l, \alpha_1, \alpha_2)$ yet. From the above data, the magnitude of the PMNS matrix is about

$$|U_{\mathrm{PMNS}}| \simeq \begin{pmatrix} 0.82 & 0.55 & 0.16 \\ 0.42 & 0.54 & 0.64 \\ 0.36 & 0.54 & 0.75 \end{pmatrix}\,. \tag{3.33}$$

On the other hand, neutrino mass squared differences are

$$\Delta m^2_{21} = (7.50 \pm 0.20) \times 10^{-5}\mathrm{eV}^2\,, \tag{3.34}$$

$$|\Delta m_{32}|^2 = (2.32^{+0.12}_{-0.08}) \times 10^{-3}\mathrm{eV}^2\,, \tag{3.35}$$

Neutrino masses are bounded from above. However, the constraint on each neutrino mass is very weak. Stringent constraint on the sum of three neutrino masses comes from the

data of the cosmological experiments, which is

$$\sum_{j=1}^{3} m_j \lesssim (0.3 - 1.3)\,\mathrm{eV}. \tag{3.36}$$

3.5 RGE corrections to the lepton mixing

The neutrino mass and the lepton mixing are influenced by a Renormalization Group Equation (RGE) effect. However, if an unknown physics appear at a high energy scale, we cannot evaluate unknown RGE effects beyond the scale of the new physics. Below the scale of such a high energy physics, the RGE effect can be discussed [36].

When the neutrinos are Majorana fermions whose mass terms are written by Eq. (3.6), the effective neutrino mass matrix $\mathcal{M}_\nu$ evolves with the following RGE,

$$\frac{d\mathcal{M}_\nu}{dt} = \mathcal{M}_\nu F + F^T \mathcal{M}_\nu + S\mathcal{M}_\nu\,, \qquad t \equiv \frac{1}{16\pi^2}\log\mu\,, \tag{3.37}$$

where

$$F \equiv -\frac{1}{2} y_l^\dagger y_l\,, \qquad S \equiv 2\lambda - 3g_2^2 + 2\mathrm{tr}[3y_U^\dagger y_U + 3y_D^\dagger y_D + y_l^\dagger y_l]\,, \tag{3.38}$$

and μ represents an renormalization scale.

From Eq. (3.37), the RGE of the PMNS matrix is derived in the following way. At the one-loop order, the charged lepton mass term maintain the diagonal form. Then, we consider only the neutrino mass terms when deriving the RGE of the lepton mixing. In the diagonal basis of the charged lepton, $\mathcal{M}_\nu$ can be diagonalized as $\mathcal{M}_\nu = U^* \hat{\mathcal{M}}_\nu U^\dagger$ where U is the PMNS matrix. Mutiplying U^T from the left and U from the right side in Eq. (3.37), we find

$$U^T \dot{U}^* \hat{\mathcal{M}}_\nu + \dot{\hat{\mathcal{M}}}_\nu + \hat{\mathcal{M}}_\nu \dot{U}^\dagger U = \frac{1}{16\pi^2}\left(\hat{\mathcal{M}}_\nu F' + F'^T \hat{\mathcal{M}}_\nu + S\hat{\mathcal{M}}_\nu\right) \tag{3.39}$$

where $F' \equiv U^\dagger F U$ and the dot represents the derivative with respect to t, i.e. $\dot{U} \equiv dU/dt$. On the other hand, U, which is an unitary matrix, flows by the following RGE,

$$\dot{U} = UX\,, \tag{3.40}$$

where X is an anti-Hermite matrix. Using the relation (3.40), the RGE for the diagonal neutrino mass matrix $\hat{\mathcal{M}}_\nu$ becomes

$$\dot{\hat{\mathcal{M}}}_\nu = \frac{1}{16\pi^2}\left(\hat{\mathcal{M}}_\nu F' + F'^T \hat{\mathcal{M}}_\nu + S\hat{\mathcal{M}}_\nu\right) - X^* \hat{\mathcal{M}}_\nu + \hat{\mathcal{M}}_\nu X\,. \tag{3.41}$$

In the above equation, the diagonal parts give the RG flow of the neutrino masses

$$\dot{m}_{\nu i} = \frac{1}{16\pi^2}\left(2m_{\nu i}F'_{ii} + m_{\nu i}S\right) + 2m_{\nu i}X_{ii}\,. \tag{3.42}$$

The X_{ii} is a pure imaginary and influences the Majorana phase, which is not determined in this way.

The off diagonal part gives a relation between X and F' as

$$\frac{1}{16\pi^2}\left(m_i F'_{ij} + m_j (F'^*)_{ij}\right) + m_i X_{ij} - m_j (X^*)_{ij} = 0\,. \tag{3.43}$$

It can be decomposed into the real and imaginary parts as

$$\mathrm{Re}[X_{ij}] = \frac{1}{16\pi^2}\frac{m_j + m_i}{m_j - m_i}\mathrm{Re}[F'_{ij}]\,, \tag{3.44}$$

$$\mathrm{Im}[X_{ij}] = \frac{1}{16\pi^2}\frac{m_j - m_i}{m_j + m_i}\mathrm{Im}[F'_{ij}]\,. \tag{3.45}$$

Then, we can see the RG flows of the neutrino masses $m_{\nu i}$ and the lepton mixing U by using the above equations.

In the SM, the effect of RGE to the lepton sector is small. The RG flow of the PMNS matrix is dominantly influenced by the largest Yukawa couplings of the charged lepton, which is $y_\tau \simeq 10^{-2}$. The magnitude of Eq. (3.44) becomes largest when

$$m_j + m_i \simeq 1\mathrm{eV}\,, \qquad m_j - m_i \simeq 10^{-2}\mathrm{eV}\,, \tag{3.46}$$

$$\frac{m_j + m_i}{m_j - m_i} \simeq 10^2\,. \tag{3.47}$$

In this case, the RG flow of the PMNS matrix is

$$\dot{U} \simeq -\frac{1}{2}\frac{y_\tau^\dagger y_\tau}{16\pi^2} U \frac{m_j + m_i}{m_j - m_i}\mathrm{Re}[U_{i\tau}^\dagger U_{\tau j}] \simeq -\frac{10^{-2}}{32\pi^2} U \mathrm{Re}[U_{i\tau}^\dagger U_{\tau j}]\,. \tag{3.48}$$

It implies that the RGE effect to the PMNS matrix is small. Then, when we consider the model for generating the PMNS matrix in the following sections, we assume that the effect of the RGE is small and can be ignored.

When the neutrinos are Dirac fermions, which mass terms are written by Eq. (3.8) and Eq. (3.9), we follow a similar discussion and can evaluate the RGE effect [37]. In the case of the neutrino Dirac fermions, we can also see the small RGE effect to the neutrino masses and lepton mixing due to the small Yukawa couplings.

Chapter 4

Flavor Symmetry

"Flavor symmetry" is a symmetry which gives relations between different flavors. The structure of the symmetry leads to various properties beyond the SM. Especially, it is known that a model with a non-Abelian discrete flavor symmetry may predict the lepton mixing and the quark mixing. In this chapter, we show how a flavor symmetry predicts the lepton mixing angle. Then, we review on an example model for deriving the tri-bimaximal pattern of the PMNS matrix.

4.1 Flavor symmetry for lepton mixing

In this section, we show that how a flavor symmetry predicts the lepton mixing angle.

We consider the case that flavor symmetry G_f breaks at a high energy scale, and in result, there exist residual symmetries G_l in the charged lepton massse and G_ν in the neutrino masses as shown in Fig. 4.1. We assume that the flavor symmetry is a subgroup of SU(3). Besides, we assume that residual symmetries G_l and G_ν are Abelian symmetries.

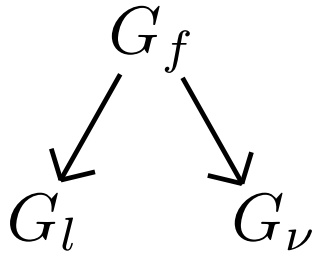

Figure 4.1: A relation between the flavor symmetry and residual symmetries.

We consider the case that neutrinos are Majorana fermions. The Lagrangian relevant in the discussion is the following lepton part,

$$\mathcal{L}^l = -\frac{g}{\sqrt{2}}\bar{l}_L\gamma^\mu W^+_\mu \nu_{lL} - \bar{l}_R M_l l_L - \bar{\nu}^c_{lL} M_\nu \nu_{lL} + h.c.\,. \tag{4.1}$$

The masses can be diagonalized by the unitary matrices,

$$M_l = V_l \hat{M}_l U_l^\dagger, \qquad M_\nu = U_\nu^* \hat{M}_\nu U_\nu^\dagger \,. \tag{4.2}$$

Redefining the fields as

$$l_L \equiv U_l^\dagger l_L, \qquad l_R \equiv V_l^\dagger l_R, \qquad \nu_{lL} \equiv U_l^\dagger \nu_{lL} \,, \tag{4.3}$$

and comparing with Eq. (3.14), the PMNS matrix $U_{\rm PMNS}$ is represented as

$$U_{\rm PMNS} = U_l^\dagger U_\nu \,. \tag{4.4}$$

On the other hand, in Eq. (4.1), the charged lepton mass term is invariant under $T\,(T') \in G_l$, and the neutrino mass is invariant under $S \in G_\nu$ for the residual flavor symmetries. That is, under the transformations

$$l_L \to T l_L \,, \qquad l_R \to T' l_R \,, \tag{4.5}$$

$$\nu_{lL} \to S \nu_{lL} \,, \tag{4.6}$$

the following mass is invariant

$$T^\dagger M_l^\dagger M_l T = M_l^\dagger M_l \,, \qquad S^T M_\nu S = M_\nu \,. \tag{4.7}$$

As the residual symmetries G_l, G_ν are Abelian symmetries, the elements $T \in G_l$, $S \in G_\nu$ are diagonalized by the unitary matrices

$$T = U_T T_0 U_T^\dagger \,, \qquad S = U_S S_0 U_S^\dagger \,, \tag{4.8}$$

where T_0, S_0 are the diagonal matrix. From the second equation in Eq. (4.7), the possible element of the symmetries in the neutrino mass $S_0 \in G_\nu$ are explicitly written as the following

$$S_0^{(i)} = \left\{ \begin{pmatrix} 1 & 0 & 0 \\ 0 & -1 & 0 \\ 0 & 0 & -1 \end{pmatrix}, \begin{pmatrix} -1 & 0 & 0 \\ 0 & 1 & 0 \\ 0 & 0 & -1 \end{pmatrix}, \begin{pmatrix} -1 & 0 & 0 \\ 0 & -1 & 0 \\ 0 & 0 & 1 \end{pmatrix} \right\} , \tag{4.9}$$

where the index (i) $(i = 1, 2, 3)$ represents the choice of the elements. One element in Eq. (4.9) can be generated by the product of the other symmetries such as $S_0^{(3)} = S_0^{(1)} S_0^{(2)}$, so the maximum symmetry in the neutrino mass is the Klein group $Z_2 \times Z_2$.

An important feature of the flavor symmetries is that the unitary matrices U_T, U_S simultaneously diagonalize the mass matrices $M_l^\dagger M_l$ and M_ν. Then we can identify

$$U_l \equiv U_T \,, \qquad U_\nu \equiv U_S \,. \tag{4.10}$$

The PMNS matrix is derived through the following equation,

$$U_{\rm PMNS} = U_T^\dagger U_S \,. \tag{4.11}$$

Note that the unitary matrices U_T, U_S are identified upto diagonal unitary matrices K_T, K_S and permutations P_T, P_S,

$$U_T \to U_T K_T P_T \,, \qquad U_S \to U_S K_S P_S \,. \tag{4.12}$$

It implies that there is the freedom of exchanging the rows and columns in the PMNS matrix. Therefore, the Dirac CP-phase δ is determined upto π. Also, we can not get any predictions for the neutrino masses and Majorana CP-phases in the discussion.

4.2 The tri-bimaximal pattern

In the study of flavor symmetry, the tri-bimaximal pattern

$$||U_{\rm PMNS}|| = \begin{pmatrix} \frac{2}{\sqrt{6}} & \frac{1}{\sqrt{3}} & 0 \\ \frac{1}{\sqrt{6}} & \frac{1}{\sqrt{3}} & \frac{1}{\sqrt{2}} \\ \frac{1}{\sqrt{6}} & \frac{1}{\sqrt{3}} & \frac{1}{\sqrt{2}} \end{pmatrix} . \tag{4.13}$$

is an important candidate for the leading-order contribution to the experimental value Eq. (3.33). The tri-bimaximal pattern is derived under the assumptions that the charged lepton mass symmetry is $G_l = Z_3$ and the neutrino mass symmetry is $G_\nu = Z_2 \times Z_2$ in a certain basis. For example, when there are residual symmetries $T \in G_l = Z_3$ and $S^{(3)}$, $S^{(1)} \in G_\nu = Z_2 \times Z_2$ as follows

$$T = \begin{pmatrix} 0 & 1 & 0 \\ 0 & 0 & 1 \\ 1 & 0 & 0 \end{pmatrix} ,$$
$$S^{(3)} = \begin{pmatrix} 0 & 0 & -1 \\ 0 & -1 & 0 \\ -1 & 0 & 0 \end{pmatrix} , \qquad S^{(1)} = \begin{pmatrix} 0 & 0 & 1 \\ 0 & -1 & 0 \\ 1 & 0 & 0 \end{pmatrix} , \tag{4.14}$$

the unitary matrices U_T, U_S for diagonalizing T, $S^{(3)}$, $S^{(1)}$ are

$$U_T = \frac{1}{\sqrt{3}} \begin{pmatrix} 1 & \omega^2 & \omega \\ 1 & 1 & 1 \\ 1 & \omega & \omega^2 \end{pmatrix} , \qquad U_S = \begin{pmatrix} \frac{1}{\sqrt{2}} & 0 & -\frac{1}{\sqrt{2}} \\ 0 & 1 & 0 \\ \frac{1}{\sqrt{2}} & 0 & \frac{1}{\sqrt{2}} \end{pmatrix} , \tag{4.15}$$

where U_S simultaneously diagonalizes $S^{(3)}$ and $S^{(1)}$. The diagonalized matrices of T, S_1, S_2 are $T_0 = \mathrm{diag}\{1, \omega, \omega^2\}$, $S_0^{(3)} = \mathrm{diag}\{-1, -1, 1\}$, $S_0^{(1)} = \mathrm{diag}\{1, -1, -1\}$.

Then, the PMNS matrix becomes the tri-bimaximal pattern,

$$U_{\rm PMNS} = U_T^\dagger U_S = \begin{pmatrix} \sqrt{\frac{2}{3}} & \frac{1}{\sqrt{3}} & 0 \\ -\frac{1}{\sqrt{6}} & \frac{1}{\sqrt{3}} & -\frac{i}{\sqrt{2}} \\ -\frac{1}{\sqrt{6}} & \frac{1}{\sqrt{3}} & \frac{i}{\sqrt{2}} \end{pmatrix} . \tag{4.16}$$

When the neutrinos are Dirac fermions, phases $i = e^{i\pi/2}$ in columns can be removed by redefining neutrinos.

Next, we conversely start a discussion from the tri-bimaximal pattern. In the diagonal basis of the charged lepton mass in Eq. (3.14), the effect of the symmetry in the charged lepton has already been included in the neutrino mass term. The unitary matrix U_S for diagonalizing the neutrino masses exactly become the PMNS matrix. From the conditions $S^{(i)} = U_S S_0^{(i)} U_S^\dagger$ and

$$U_S = U_{\rm PMNS} = \begin{pmatrix} \sqrt{\frac{2}{3}} & \frac{1}{\sqrt{3}} & 0 \\ -\frac{1}{\sqrt{6}} & \frac{1}{\sqrt{3}} & -\frac{1}{\sqrt{2}} \\ -\frac{1}{\sqrt{6}} & \frac{1}{\sqrt{3}} & \frac{1}{\sqrt{2}} \end{pmatrix} , \tag{4.17}$$

the forms of the $S^{(i)}$ are the followings

$$S^{(1)} = \frac{1}{3}\begin{pmatrix} 1 & -2 & -2 \\ -2 & -2 & 1 \\ -2 & 1 & -2 \end{pmatrix}, \quad S^{(2)} = -\frac{1}{3}\begin{pmatrix} 1 & -2 & -2 \\ -2 & 1 & -2 \\ -2 & -2 & 1 \end{pmatrix},$$
$$S^{(3)} = \begin{pmatrix} -1 & 0 & 0 \\ 0 & 0 & -1 \\ 0 & -1 & 0 \end{pmatrix}. \tag{4.18}$$

As noted in Eq. (4.9), one of $S^{(i)}$ in Eq. (4.18) is a product of the other two elements, e.g., $S^{(1)} = S^{(2)}S^{(3)}$. When generating the PMNS matrix from $S^{(i)}$, one $S^{(i)}$ determines only the i-th column of the PMNS matrix and the other columns are not fully determined because of the degeneracy of the eigenvalue -1 of $S^{(i)}$. Therefore, for deriving the exact tri-bimaximal pattern, we need $Z_2 \times Z_2$ symmetry written by two elements of Eq. (4.18) in a charged lepton mass diagonal basis.

4.3 Example model for the tri-bimaximal pattern

We assume a non-Abelian discrete flavor symmetry G_f, in which the residual symmetries G_l and G_ν are embedded. The flavor symmetry G_f is spontaneously broken into G_l and G_ν at the high energy scale. Although the flavor symmetry breaking alone does not gives masses to the SM particles, the residual symmetries determine the pattern of the effective terms at the electroweak scale. Then particles gain masses through Yukawa interactions by the Higgs mechanism at the electroweak scale. The resulting pattern of the PMNS matrix is constrained by the residual symmetries at the LO.

So far, many models for the tri-bimaximal pattern of the PMNS matrix are proposed such as D_n, S_3, S_4, A_4, A_5, $\Delta(3N^2)$, $\Delta(6N^2)$. Here we review an A_4 model proposed in Ref. [38] as an example for realizing the tri-bimaximal pattern with a flavor symmetry.

4.3.1 A_4 model

The non-Abelian discrete symmetry A_4 is constructed by even permutation elements of S_4. The algebraic relation is given by

$$S^2 = T^3 = (ST)^3 = 1\,. \tag{4.19}$$

The details of A_4 are in Appendix. The irreducible representations are the following. There are three singlets written by

$$1 \qquad S = 1 \qquad T = 1 \tag{4.20}$$
$$1' \qquad S = 1 \qquad T = \omega \tag{4.21}$$
$$1'' \qquad S = 1 \qquad T = \omega^2\,. \tag{4.22}$$

The triplets in a diagonal basis of T are

$$T = \begin{pmatrix} 1 & 0 & 0 \\ 0 & \omega & 0 \\ 0 & 0 & \omega^2 \end{pmatrix}, \qquad S = \frac{1}{3}\begin{pmatrix} -1 & 2 & 2 \\ 2 & -1 & 2 \\ 2 & 2 & -1 \end{pmatrix}. \tag{4.23}$$

The product of the two triplet **3** can be decomposed as

$$\mathbf{3} \times \mathbf{3} = \mathbf{1} + \mathbf{1}' + \mathbf{1}'' + \mathbf{3} + \mathbf{3}'. \tag{4.24}$$

The multiple rules for the two triplets $x = (x_1, x_2, x_3)$, $y = (y_1, y_2, y_3)$ are the following.

$$(xy)_1 = x_1y_1 + x_2y_3 + x_3y_2, \tag{4.25}$$
$$(xy)_{1'} = x_1y_3 + x_3y_1 + x_2y_2, \tag{4.26}$$
$$(xy)_{1''} = x_1y_2 + x_2y_1 + x_3y_3, \tag{4.27}$$
$$(xy)_3 = \frac{1}{3}(2x_1y_1 - x_2y_3 - x_3y_2,\ 2x_3y_3 - x_1y_2 - x_2y_1,\ 2x_2y_2 - x_1y_3 - x_3y_1), \tag{4.28}$$
$$(xy)_{3'} = \frac{1}{2}(x_2y_3 - x_3y_2,\ x_1y_2 - x_2y_1,\ x_1y_3 - x_3y_1), \tag{4.29}$$

and products of the singlets z, z', z'' under **1**, **1**$'$, **1**$''$ and triplets x are given by

$$zx = (zx_1,\ zx_2,\ zx_3), \tag{4.30}$$
$$z'x = (z'x_2,\ z'x_3,\ z'x_1), \tag{4.31}$$
$$z''x = (z''x_3,\ z''x_1,\ z''x_2), \tag{4.32}$$

respectively. Note that the **3** and **3**$'$ are symmetric and anti-symmetric under the exchange of $x \leftrightarrow y$, respectively. The A_4 symmetry is broken by the vev of the scalar triplet ϕ. If $\langle\phi\rangle = (v, v, v)$, the $\langle\phi\rangle$ under the A_4 transformation is

$$S\langle\phi\rangle = \frac{1}{3}\begin{pmatrix} -1 & 2 & 2 \\ 2 & -1 & 2 \\ 2 & 2 & -1 \end{pmatrix}\begin{pmatrix} v \\ v \\ v \end{pmatrix} = \begin{pmatrix} v \\ v \\ v \end{pmatrix} = \langle\phi\rangle, \tag{4.33}$$

$$T\langle\phi\rangle = \begin{pmatrix} 1 & 0 & 0 \\ 0 & \omega & 0 \\ 0 & 0 & \omega^2 \end{pmatrix}\begin{pmatrix} v \\ v \\ v \end{pmatrix} = \begin{pmatrix} v \\ \omega v \\ \omega^2 v \end{pmatrix} \neq \langle\phi\rangle. \tag{4.34}$$

It means that the A_4 symmetry breaks down into $S \in G_S$. On the other hand, if the triplet vev is $\langle\phi\rangle = (v, 0, 0)$,

$$S\langle\phi\rangle \neq \langle\phi\rangle, \qquad T\langle\phi\rangle = \langle\phi\rangle, \tag{4.35}$$

the A_4 symmetry breaks down into $T \in G_T$.

From the above observation, we can construct the model in Ref. [38] to generate the tri-bimaximal pattern of the lepton mixing. We assume the neutrinos are Majorana fermions. The fields relevant to the flavor mixing are the lepton doublets and right-handed charged

leptons. We assign the left-handed leptons L_{lL} as a triplet of **3** in terms of $l = (e, \mu, \tau)$, and the right-handed charged leptons $\overline{e_R}$, $\overline{\mu_R}$, $\overline{\tau_R}$ are singlets **1**, **1′**, **1″**, respectively. For the flavor symmetry breaking, we prepare the scalar fields, triplets ϕ_S, ϕ_T and a singlet χ. They are not charged under the SM gauge symmetry. The reason of preparing χ is evading the degeneracy of the neutrino mass in later. In addition, we introduce two A_4 singlet Higgs fields H_u, H_d, which are $\mathrm{SU}(2)_W$ doublets and are charged $Y = +1, -1$, respectively.

Here, we do not concern about the detail of the Higgs mechanism. We assume that the scalar fields have vev as $\langle\phi_S\rangle = (v_S, v_S, v_S)$, $\langle\phi_T\rangle = (v_T, 0, 0)$, $\langle\chi\rangle = v_\chi$ and $\langle H^0_{u,d}\rangle = v_{u,d}$, respectively. The lepton mass terms are written by the following non-renormalizable terms

$$\begin{aligned}\mathcal{L}^l_y =& y_e\overline{e_R}(\phi_T L_L)_1\frac{H_d}{\Lambda} + y_\mu\overline{\mu_R}(\phi_T L_L)_{1''}\frac{H_d}{\Lambda} + y_\tau\overline{\tau_R}(\phi_T L_L)_{1'}\frac{H_d}{\Lambda}\\ &+ y_1\chi\frac{1}{\Lambda^2}((\overline{L^c_L}\sigma^2 H_u)(H_u^T\sigma^2 L_L))_1 + y_2\frac{1}{\Lambda^2}(\phi_S(\overline{L^c_L}\sigma^2 H_u)(H_u^T\sigma^2 L_L))_1\\ &+ h.c. + \cdots . \end{aligned} \tag{4.36}$$

where the forms $(\,\cdot\,)_{1,1',1''}$ represent components in the product. In Eq. (4.36), terms of exchanging $\phi_S \leftrightarrow \phi_T$ are excluded, because they break the residual symmetries in the mass term and we can not get the tri-bimaximal pattern. Also we do not write Majorana neutrino mass terms without χ under the assumption that the effect is small. The charged lepton mass is given at $O(\frac{1}{\Lambda})$ while the neutrino mass is of $O(\frac{1}{\Lambda^2})$. The ellipsis denotes terms with higher dimensional operators, which give small corrections to the leading order.

The Dirac masses of the charged leptons and the Majorana masses of the neutrinos are written by

$$M_l = \frac{v_d v_T}{\Lambda}\begin{pmatrix} y_e & 0 & 0\\ 0 & y_\mu & 0\\ 0 & 0 & y_\tau\end{pmatrix}, \tag{4.37}$$

$$M_\nu = \frac{2y_1 v_u^2 v_\chi}{\Lambda^2}\begin{pmatrix} 1 & 0 & 0\\ 0 & 0 & 1\\ 0 & 1 & 0\end{pmatrix} + \frac{2y_2 v_u^2 v_S}{3\Lambda^2}\begin{pmatrix} 2 & -1 & -1\\ -1 & 2 & -1\\ -1 & -1 & 2\end{pmatrix}. \tag{4.38}$$

The PMNS matrix U_{PMNS} diagonalizes the Majorana neutrino matrix as $\hat{M}_\nu = U^T_{\mathrm{PMNS}} M_\nu U_{\mathrm{PMNS}}$. Then, we found that the U_{PMNS} is the tri-bimaximal pattern, and the neutrino masses are

$$\frac{2v_u^2}{\Lambda^2}(-y_1 v_\chi + y_2 v_S), \qquad \frac{2y_1 v_u^2 v_\chi}{\Lambda^2}, \qquad \frac{2v_u^2}{\Lambda^2}(y_1 v_\chi + y_2 v_S). \tag{4.39}$$

In this model, the term with χ plays a crucial role for the neutrino mass splitting and determining the PMNS matrix uniquely. Note that the A_4 model is a special model that the additional Z_2 symmetry in the neutrino mass term comes from the multiple rule in Eq. (4.25). It is not a general situation of the flavor symmetry model. We often need two Z_2 symmetries in the flavor group to generate the fixed lepton mixing in many other models.

We can also build a simple seesaw model where the neutrinos are Dirac particles. We introduce the right-handed neutrinos as a A_4 triplet $\nu_R = (\nu_{Re}, \nu_{R\mu}, \nu_{R\tau})$, which is not

charged under the SM gauge symmetry. Instead of the Majorana masses of the left-handed neutrinos such as LH_uH_uL in Eq. (4.36), we can write the Yukawa interactions which give the Dirac mass term and the Majorana mass term of the right-handed neutrinos as follows,

$$\mathcal{L}_y^\nu = y_{\nu D}(\overline{L_L}(i\sigma^2 H_u^*)\nu_R)_1 + y_{\nu R}^{(1)}\chi(\overline{\nu_R^c}\nu_R)_1 + y_{\nu R}^{(2)}(\phi_S\overline{\nu_R^c}\nu_R)_1 + h.c.\,. \tag{4.40}$$

Then, the Dirac mass matrix M_D and the right-handed Majorana mass matrix M_R become

$$M_D = y_{\nu D}v_u \begin{pmatrix} 1 & 0 & 0 \\ 0 & 0 & 1 \\ 0 & 1 & 0 \end{pmatrix}\,, \tag{4.41}$$

$$M_R = 2y_{\nu R}^{(1)}v_\chi \begin{pmatrix} 1 & 0 & 0 \\ 0 & 0 & 1 \\ 0 & 1 & 0 \end{pmatrix} + \frac{2y_{\nu R}^{(2)}v_S}{3}\begin{pmatrix} 2 & -1 & -1 \\ -1 & 2 & -1 \\ -1 & -1 & 2 \end{pmatrix}\,. \tag{4.42}$$

The overall neutrino mass matrix $\mathcal{M}$ is

$$\mathcal{M} = \begin{pmatrix} 0 & M_D \\ M_D & M_R \end{pmatrix}\,. \tag{4.43}$$

When $M_D \ll M_R$, the light neutrino mass matrix is given by

$$M_{\nu 1} = -M_D M_R^{-1} M_D^T\,. \tag{4.44}$$

We have already known that the right-handed Majorana mass matrix in the form of Eq. (4.42) is diagonalized by the tri-bimaximal unitary matrix U i.e. $M_R = U\hat{M}_R U^T$. Then, U also diagonalize M_D as $M_D = U\hat{M}_D U^T$. From Eq. (4.44), it implies that the light neutrino mass matrix is diagonalized by U

$$M_{\nu 1} = U\hat{M}_{\nu_1}U^T\,, \tag{4.45}$$

Therefore, we find that the PMNS matrix is $U_{\rm PMNS} = U$ and has the tri-bimaximal pattern.

In the model, we expect that corrections to the tri-bimaximal pattern are given from the next to leading order effect. For examples, the effects come from the higher dimensional operators, the deviation of the vev of the Higgs fields, and so on. They give corrections of $O(\frac{1}{\Lambda^3})$ to the PMNS matrix.

In general, the exact amount of such corrections is different in each model. However, the corrections are to be small in many models. Then it is often difficult to generate the large θ_{13} from the NLO corrections from the tri-bimaximal pattern. Therefore, many attempts of improving the flavor symmetry model to generate the experimental large θ_{13} have been proposed so far.

Chapter 5

Searching Flavor Symmetries

So far, we assume that the flavor symmetry generates the PMNS matrix with the tri-bimaximal pattern at the leading order and the next to leading order corrections generate θ_{13}. However, the recent experiments show that the θ_{13} in the PMNS matrix is relatively large. It is difficult to generate such a large θ_{13} from the NLO corrections to the tri-bimaximal pattern. Then, it drives us to search other flavor symmetries generating the PMNS matrix nearer to the experimental value at the LO.

Recently, Hernandez and Smirnov develop a model-independent method of systematically searching necessary conditions of flavor symmetries for the experimental lepton mixing [26]. Their method helps us to find flavor symmetries generating the favored PMNS matrix at the LO, which is useful for the model building in future.

In this chapter, we review the method of Hernandez and Smirnov [26] and revisit their results more carefully.

5.1 Model independent search for flavor symmetries

The assumption of the model is as follows. The neutrinos are Majorana fermions and construct Majorana mass terms. There exists a discrete flavor symmetry G_f in a high energy theory, and it breaks down into the residual symmetries, G_l of the charged lepton mass term and G_ν of the neutrino mass term. The G_f is a subgroup in SU(3) and a finite group. If the G_f is an infinite group, there exist infinite number of elements and we can construct any model generating arbitrary patterns of the PMNS matrix, which means that the model is not predictive. The residual symmetries in the charged lepton mass G_l is Z_m while that in the neutrino mass G_ν is a subgroup of a Klein group $Z_2 \times Z_2$.

The lepton part in the Lagrangian is given by Eq. (3.14). The charged lepton mass term has a residual symmetry $T_0 \in G_l = Z_m$. Under the following transformation, the charged lepton mass term is invariant

$$l_L \to T_0 l_L \,, \qquad l_R \to T_0 l_R \,. \tag{5.1}$$

As the Lagrangian is in the diagonal basis of the charged lepton, T_0 is generally written

by

$$T_0 = \mathrm{diag}\{e^{i\phi_e},\, e^{i\phi_\mu},\, e^{i\phi_\tau}\}\,, \tag{5.2}$$

$$\phi_e \equiv 2\pi\frac{k_e}{m}\,, \qquad \phi_\mu \equiv 2\pi\frac{k_\mu}{m}\,, \qquad \phi_\tau \equiv 2\pi\frac{k_\tau}{m}\,, \tag{5.3}$$

where $(k_e,\, k_\mu\,, k_\tau)$ are integers. From the condition that the symmetry G_l is a subgroup of SU(3),

$$k_e + k_\mu + k_\tau \equiv 0 \mod m\,. \tag{5.4}$$

On the other hand, the neutrino mass term has a residual symmetry as a subgroup of $Z_2 \times Z_2$. Here, we assume that $G_\nu = Z_2$. The neutrino mass is invariant under transformation by a element $S \in G_\nu$,

$$\nu_L \to S\nu_L\,, \tag{5.5}$$

As the S operates the PMNS matrix in the neutrino mass term, we can decompose the S as

$$S = U_{\rm PMNS} S_0 U_{\rm PMNS}^\dagger\,, \tag{5.6}$$

where S_0 is explicitly wrriten by one of Eq. (4.9). Then, we rename $S_0^{(i)}$, where the index (i) represents the element of Z_2 in Eq. (4.9) with the eigenvalue of i-th column is positive.

From the necessary condition that the flavor symmetry G_f is a finite group, the elements generating from $T_0 \in G_l$ and $S \in G_\nu$ must be closed. It requires that $W \equiv ST_0$ is in Z_p,

$$W^p = 1 \qquad p \in Z\,. \tag{5.7}$$

The three eigenvalues λ_j $(j = 1, 2, 3)$ of W are p-th roots of unity, which are parameterized by

$$\lambda_j = e^{2\pi i \frac{q_j}{p}} \qquad q_j \in Z\,. \tag{5.8}$$

From the condition of a subgroup of SU(3),

$$q_1 + q_2 + q_3 \equiv 0 \qquad \mod p\,. \tag{5.9}$$

The trace a of W is

$$a \equiv \mathrm{tr}[W] = \sum_{j=1}^{3} \lambda_j = e^{2\pi i \frac{q_1}{p}} + e^{2\pi i \frac{q_2}{p}} + e^{2\pi i \frac{q_3}{p}}\,, \tag{5.10}$$

which is generally a complex value. On the other hand, using Eq. (5.3) and Eq. (5.6), the trace of W is explicitly written by

$$\begin{aligned}
\mathrm{tr}[W] &= (U_{\rm PMNS} S_0^{(i)} U_{\rm PMNS}^\dagger T_0) \\
&= \sum_{\alpha=e,\mu,\tau} e^{i\phi_\alpha}(e^{i\phi_1}|U_{\alpha 1}|^2 + e^{i\phi_2}|U_{\alpha 2}|^2 + e^{i\phi_3}|U_{\alpha 3}|^2) \\
&= \sum_{\alpha=e,\mu,\tau} e^{i\phi_\alpha}(2|U_{\alpha i}|^2 - 1)\,,
\end{aligned} \tag{5.11}$$

where ϕ_j $(j = 1, 2, 3)$ is 0 if $j = i$, otherwise π. Combining Eq. (5.10) and (5.11), the condition $\mathrm{tr}[W] = a$ leads in general two real equations with two parameters $|U_{i\alpha}|^2$. They can be solved and leads to the relations about the i-th column of the PMNS matrix,

$$\begin{aligned}
|U_{ei}|^2 &= \frac{\mathrm{Re}[a]\cos\frac{\phi_\mu+\phi_\tau}{2} + \cos\frac{\phi_\mu+\phi_\tau-2\phi_e}{2} + \mathrm{Im}[a]\sin\frac{\phi_\mu+\phi_\tau}{2}}{4\sin\frac{\phi_\mu-\phi_e}{2}\sin\frac{\phi_e-\phi_\tau}{2}}\,, \\
|U_{\mu i}|^2 &= \frac{\mathrm{Re}[a]\cos\frac{\phi_e+\phi_\tau}{2} + \cos\frac{\phi_e+\phi_\tau-2\phi_\mu}{2} + \mathrm{Im}[a]\sin\frac{\phi_e+\phi_\tau}{2}}{4\sin\frac{\phi_e-\phi_\mu}{2}\sin\frac{\phi_\mu-\phi_\tau}{2}}\,, \\
|U_{\tau i}|^2 &= \frac{\mathrm{Re}[a]\cos\frac{\phi_e+\phi_\mu}{2} + \cos\frac{\phi_e+\phi_\mu-2\phi_\tau}{2} + \mathrm{Im}[a]\sin\frac{\phi_e+\phi_\mu}{2}}{4\sin\frac{\phi_\tau-\phi_e}{2}\sin\frac{\phi_\mu-\phi_\tau}{2}}\,,
\end{aligned} \tag{5.12}$$

Then, when we fix the $T \in G_l$, $S \in G_S$ and $W = ST \in G_f$, we can get a possible lepton mixing pattern from the necessary condition that the flavor group G_f is a finite one. Note that in this method, the PMNS matrix can not fully determined. In the lepton mixing, it seems reasonable because we introduce only Z_2 in the neutrino mass term G_ν. For fully determining the PMNS matrix, we need to consider $G_\nu = Z_2 \times Z_2$ or a specific model. We discuss about the case of $G_\nu = Z_2 \times Z_2$ in later.

A group with algebraic relations

$$T^m = S^n = (ST)^p = 1 \qquad m,\, n,\, p \in Z\,, \tag{5.13}$$

is called the von Dyck group. Therefore, in this method, we search a von Dyck group with $n = 2$ for generating the PMNS matrix. The existence of finite flavor groups with patterns derived from Eq. (5.12) is not guaranteed. As the condition of the finiteness of the von Dyck group is

$$\frac{1}{n} + \frac{1}{m} + \frac{1}{p} > 1\,, \tag{5.14}$$

the group with large m, p is a infinite von Dyck group. However, some group could be a finite subgroup introducing the other algebraic relation, then we need to consider each case carefully.

5.2 Calculations

The i-th column of the PMNS matrix is determined through Eq. (5.12) by fixing an integer set $(n, p; k_e, k_\mu, q_1, q_2)$. In finite groups which satisfying Eq. (5.14), we list all the useful patterns of the PMNS matrix in Table 5.1. Permutations of $(|U_{ei}|, |U_{\mu i}|, |U_{\tau i}|)$ are also possible with appropriate integer sets. Note that there are some integer sets which generate the same pattern in the list. For example, a group with $(p,\, k_e,\, k_\mu) = (4,\, 0,\, 1)$ also generates $(|U_{ei}|, |U_{\mu i}|, |U_{\tau i}|) = (0,\, 0.71,\, 0.71)$. In the sense, we list a typical integer sets for each pattern in Table 5.1.

From Table 5.1, we find that the bimaximal pattern (0, 0.71, 0.71) and the trimaximal pattern (0.58, 0.58, 0.58) are derived from flavor symmetries. They are consistent with

$(\lvert U_{ei}\rvert, \lvert U_{\mu i}\rvert, \lvert U_{\tau i}\rvert)$	n	p	k_e	k_μ	q_1	q_2	$(\mathrm{Re}[a], \mathrm{Im}[a])$
(0, 0.71, 0.71)	3	2	0	1	0	1	$(-1, 0)$
(0.58, 0.58, 0.58)	3	3	0	1	0	1	$(0, 0)$
(0.82, 0.41, 0.41)	3	4	0	1	0	1	$(1, 0)$
(0.36, 0.66, 0.66)	3	5	0	1	0	2	$(-0.62, 0)$
(0.93, 0.25, 0.25)	3	5	0	1	0	1	$(1.62, 0)$
(0.71, 0.50, 0.50)	4	3	0	1	0	1	$(0, 0)$

Table 5.1: Possible patterns from the finite von Dyck groups.

.

the previous discussion, where some symmetries with $Z_2 \in G_\nu$ and $Z_3 \in G_l$ generate the tri-bimaximal pattern of the PMNS matrix. Also, there is (0.82, 0.41, 0.41), which represents the first column of the PMNS matrix with the tri-bimaximal approximation.

If we assign $i = 3$, the pattern (0.36, 0.66, 0.66) with $p = 5$ implies $\theta_{13} \neq 0$ and $|U_{\mu 3}| = |U_{\tau 3}|$. It seems a good structure to approximate the PMNS matrix. However, $|U_{e3}| = 0.36$ in $p = 5$ is slightly larger than that of the experimental result. Then, we fix $n = 3$ and consider larger p for smaller $|U_{e3}|$. We list the patterns useful for the purpose upto $p = 12$ in Table 5.2.

$(\lvert U_{ei}\rvert, \lvert U_{\mu i}\rvert, \lvert U_{\tau i}\rvert)$	n	p	k_e	k_μ	q_1	q_2	$(\mathrm{Re}[a], \mathrm{Im}[a])$
(0.26, 0.68, 0.68)	3	7	0	1	0	3	$(-0.80, 0)$
(0.44, 0.63, 0.63)	3	8	0	1	0	3	$(-0.41, 0)$
(0.20, 0.69, 0.69)	3	9	0	1	0	4	$(-0.88, 0)$
(0.36, 0.66, 0.66)	3	10	0	1	0	4	$(-0.62, 0)$
(0.16, 0.70, 0.70)	3	11	0	1	0	5	$(-0.92, 0)$
$(0.30, 0.67, 0.67)$	3	12	0	1	0	5	$(-0.73, 0)$

Table 5.2: In the cases of $n = 3$ and $6 < p < 13$, favorable patterns are listed.

All the patterns in Table 5.2 have the properties with $k_e = 0$, $k_\mu = 1$ and $\mathrm{Im}[a] = 0$. Then, we substitute $(\phi_e, \phi_\mu, \phi_\tau, \mathrm{Im}[a]) = (0, \frac{2\pi}{3}, \frac{4\pi}{3}, 0)$ to Eq. (5.12) and find

$$|U_{ei}|^2 = \frac{\mathrm{Re}[a] + 1}{3}\,, \tag{5.15}$$

$$|U_{\mu i}|^2 = |U_{\tau i}|^2 = \frac{-\frac{\mathrm{Re}[a]}{2} + 1}{3}\,. \tag{5.16}$$

For any p, we can find solutions q_1, q_2, q_3 satisfying the relation $\mathrm{Im}[a] = 0$. Some solutions

are given by

$$q_1 = q\,, \qquad q_2 = \bar{q}\,, \qquad q_3 = 0 \tag{5.17}$$

$$q = e^{2\pi i \frac{s}{p}} \qquad s \in Z_p\,, \tag{5.18}$$

and

$$\mathrm{Re}[a] = 2\cos\frac{2\pi s}{p} + 1\,. \tag{5.19}$$

We plot the solutions in terms of p and s in Figure 5.1. Note that groups with $p > 5$ are in the region of infinite von Dyck groups $\frac{1}{n} + \frac{1}{m} + \frac{1}{p} \leq 1$. To let groups finite, we need additional relations to the von Dyck relation. Then in practice, we can not realize all the points in Figure 5.1 but can partly. In the followings, we consider infinite von Dyck groups, in which finite groups can be embedded.

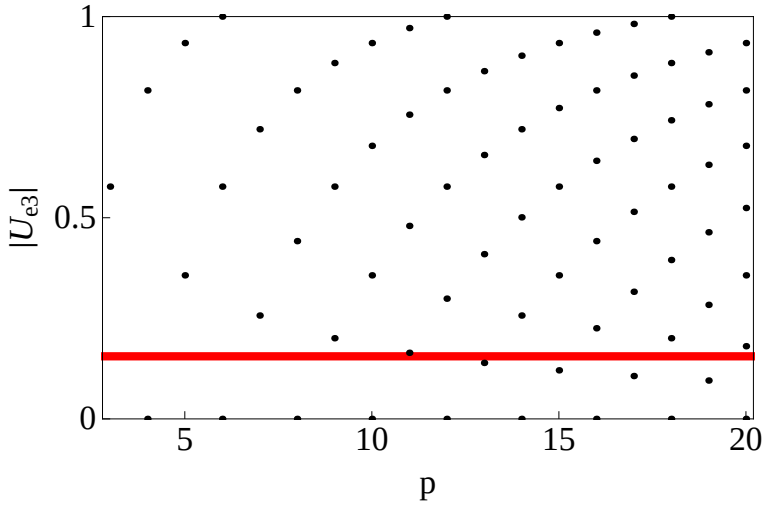

Figure 5.1: Distribution of $|U_{e3}|$ as a function of p. The red line represents the experimental value $|U_{e3}| = 0.156$ with the 1σ error.

5.2.1 Finite subgroups

Some infinite von Dyck groups have finite subgroups. For examples, the inhomogeneous finite modular groups [39, 40]

$$\Gamma_N = SL(2, N)/\{\pm 1\}\,, \tag{5.20}$$

with $N = 7, 8, 16$ have 3-dimensional representations and are subgroups of the von Dyck groups. These modular groups have the same algebraic relations as those of the von Dyck groups,

$$S^2 = T^n = (ST)^p = 1\,, \tag{5.21}$$

and additional relation in the form of

$$(ST^{-1}ST)^r = 1 \quad r \in Z\,, \tag{5.22}$$

which makes the group finite. Regardless of the additional relation Eq. (5.22), we can extend the same discussion about Eq. (5.21) and derive patterns of the PMNS matrix. Then, the additional relation (5.22) gives a new condition that the elements (S, T) could be generators of the modular groups. We explicitly calculate trace of $ST^{-1}ST$ and find

$$\begin{aligned}\mathrm{tr}[ST^{-1}ST] =& |a|^2 + a(e^{-i\phi_e} + e^{-i\phi_\mu} + e^{-i\phi_\tau}) + a^\dagger(e^{i\phi_e} + e^{i\phi_\mu} + e^{i\phi_\tau}) \\ &+ 2 + 2\cos(\phi_e - \phi_\mu) + 2\cos(\phi_\mu - \phi_\tau) + 2\cos(\phi_\tau - \phi_e)\,,\end{aligned} \tag{5.23}$$

while Eq. (5.22) implies the trace of $ST^{-1}ST$ is a sum of three r-th root of unity

$$\mathrm{tr}[ST^{-1}ST] = e^{2\pi i\frac{s_1}{r}} + e^{2\pi i\frac{s_2}{r}} + e^{-2\pi i\frac{-s_1-s_2}{r}}\,. \tag{5.24}$$

From Eq. (5.23) and Eq. (5.24), we can get a condition to be a group given by Eq. (5.21) and Eq. (5.22).

Note that the relation Eq. (5.22) is rewritten by

$$ST^{-1}ST = S(ST)^{-1}S(ST)\,. \tag{5.25}$$

We define $T' \equiv ST$, the algebraic relations become

$$S^2 = (ST')^n = T'^p = 1\,, \qquad (ST'^{-1}ST')^r = 1\,. \tag{5.26}$$

It implies that a permutation of n and p leads to the same group.

In the following subsections, we consider the finite modular group with $N = 7, 8, 16$ based on the above discussion.[1]

5.2.2 $\Gamma_7 \simeq PSL(2, Z_7)$

Let us consider the case of $N = 7$, which is $\Gamma_7 \simeq PSL(2, Z_7)$. The algebraic relations are given by

$$S^2 = T^7 = (ST)^3 = 1\,, \qquad (ST^{-1}ST)^4 = 1\,. \tag{5.27}$$

Considering the equality of Eq. (5.23) and Eq. (5.24), we can get the useful patterns of the PMNS matrix from the group Γ_7 which are listed in Table 5.3.

All patterns given by permutations of (0.81, 0.36, 0.45) are possible with proper assignments of (k_e, k_μ). Note that the assignment (k_e, k_μ) = (5, 6) also gives (0.81, 0.36, 0.45) and (k_e, k_μ) = (5, 3) gives (0.81, 0.45, 0.36). When we assign $i = 1$, the pattern (0.81, 0.45, 0.36) is consistent with the experimental values. Therefore, we conclude that the symmetry $\Gamma_7 \simeq PSL(2, Z_7)$ is a good candidate for the flavor symmetry.

As discussed in the previous subsection, we consider a permutation in Eq. (5.27) as another Γ_7 description, which is written by

$$S^2 = T^3 = (ST)^7 = 1\,, \qquad (ST^{-1}ST)^4 = 1\,. \tag{5.28}$$

$(\lvert U_{ei}\rvert, \lvert U_{\mu i}\rvert, \lvert U_{\tau i}\rvert)$	k_e	k_μ	q_1	q_2	$(\mathrm{Re}[a], \mathrm{Im}[a])$
(0.81, 0.36, 0.45)	2	1	0	1	$(0, 0)$
(0.81, 0.45, 0.36)	2	4	0	1	$(0, 0)$

Table 5.3: Patterns derived from the elements in $PSL(2, Z_7)$ with Eq. (5.27).

$(\lvert U_{ei}\rvert, \lvert U_{\mu i}\rvert, \lvert U_{\tau i}\rvert)$	k_e	k_μ	q_1	q_2	$(\mathrm{Re}[a], \mathrm{Im}[a])$
(0.89, 0.41, 0.19)	1	0	1	2	$(-0.5, 1.32)$
(0.89, 0.19, 0.41)	1	2	1	2	$(-0.5, 1.32)$

Table 5.4: Patterns derived from the elements in $PSL(2, Z_7)$ with Eq. (5.28).

All patterns derived from the relations are in Table 5.4. Patterns of their permutaitons are also possible. Assigning $i = 1$, the patterns are near to the experimental values.

The $PSL(2, Z_7)$ has another description, which is written by

$$S^2 = T^7 = (ST)^4 = 1\,, \qquad (ST^{-1}ST)^4 = 1\,. \tag{5.29}$$

It leads to the same patterns as ones in Table 5.3.

The permuted description is

$$S^2 = T^4 = (ST)^7 = 1\,, \qquad (ST^{-1}ST)^4 = 1\,, \tag{5.30}$$

which gives $(\lvert U_{ei}\rvert, \lvert U_{\mu i}\rvert, \lvert U_{\tau i}\rvert) = (0.84, 0.50, 0.21)$ and its permutations. The pattern seems to be slightly deviated from the experimental values.

5.2.3 $\Gamma_8 \simeq \Delta(6 \times 4^2)$

The $\Gamma_8 \simeq \Delta(6 \times 4^2)$ is a finite group with the following algebraic relations

$$S^2 = T^8 = (ST)^3 = 1\,, \qquad (ST^{-1}ST)^3 = 1\,. \tag{5.31}$$

The relation between Eq. (5.31) and another presentation Eq. (A.23) is given by

$$\begin{aligned} a &= ST^2ST^4\,, & a' &= ST^2ST^6\,, \\ b &= T^5ST^4\,, & c &= ST^2ST^5\,. \end{aligned} \tag{5.32}$$

The patterns derived from the relation Eq. (5.31) are $(\lvert U_{ei}\rvert, \lvert U_{\mu i}\rvert, \lvert U_{\tau i}\rvert) = (0.71, 0.50, 0.50)$ and its permutations.

[1]Note that there are cases that a product of S and T is a residual symmetry of the mass term, which may generate patterns not appearing in the discussion.

The permuted description of Γ_8 is

$$S^2 = T^3 = (ST)^8 = 1\,, \qquad (ST^{-1}ST)^3 = 1\,. \tag{5.33}$$

The resulting patterns are listed in Table 5.5. When we use the pattern (0.79, 0.58, 0.21)

$(\lvert U_{ei}\rvert, \lvert U_{\mu i}\rvert, \lvert U_{\tau i}\rvert)$	k_e	k_μ	q_1	q_2	(Re[a], Im[a])
(0, 0.71, 0.71)	0	1	0	4	$(-1, 0)$
(0.82, 0.41, 0.41)	0	1	0	2	$(1, 0)$
(0.79, 0.58, 0.21)	1	0	1	2	$(0, 1)$

Table 5.5: Patterns derived from the elements in $\Gamma_8 \simeq \Delta(6 \times 4^2)$ with Eq. (5.33).

with $i = 1$, we need some corrections to get the experimental results.

5.2.4 $\Gamma_{16} \simeq \Delta(6 \times 8^2)$

The $\Gamma_{16} \simeq \Delta(6 \times 8^2)$ is a finite group with the following algebraic relations

$$S^2 = T^{16} = (ST)^3 = 1\,, \qquad (ST^{-1}ST)^3 = 1\,. \tag{5.34}$$

The relation between Eq. (5.34) and another presentation Eq. (A.23) is given by [42]

$$\begin{aligned} a &= ST^2ST^4\,, \qquad a' = ST^2ST^{14}\,, \\ b &= T^{15}ST^8\,, \qquad c = ST^6ST^3\,. \end{aligned} \tag{5.35}$$

The resulting patterns are permutations of (0.71, 0.5, 0.5).

The permuted description is

$$S^2 = T^3 = (ST)^{16} = 1\,, \qquad (ST^{-1}ST)^3 = 1\,. \tag{5.36}$$

The resulting patterns are listed in Table 5.6. When $i = 3$, the pattern (0.11, 0.65, 0.75) is consistent with the experiments. When $i = 2$, the obtained values (0.81, 0.50, 0.31) are near to the experiments. Therefore, the $\Delta(6 \times 8^2)$ is a good candidate for the lepton mixing.

5.3 Klein group

We consider the case that the Klein group $Z_2 \times Z_2$ remains in the neutrino mass term. That is often used in flavor symmetry models. The neutrino mass is invariant under S_1, $S_2 \in Z_2 \times Z_2$ and the charged lepton mass is invariant under $T \in Z_n$. We assume that S_1 and S_2 are in different Z_2 symmetries and their diagonal matrices are

$$\hat{S}_1 = \mathrm{diag}\{1, -1, -1\}\,, \qquad \hat{S}_2 = \mathrm{diag}\{-1, 1, -1\}\,. \tag{5.37}$$

$(\lvert U_{ei}\rvert, \lvert U_{\mu i}\rvert, \lvert U_{\tau i}\rvert)$	k_e	k_μ	q_1	q_2	$(\mathrm{Re}[a], \mathrm{Im}[a])$
(0, 0.71, 0.71)	0	1	0	8	$(-1, 0)$
(0.82, 0.41, 0.41)	0	1	0	4	$(1, 0)$
(0.79, 0.58, 0.21)	1	0	2	4	$(0, 1)$
(0.11, 0.75, 0.65)	1	0	5	13	$(0.71, -0.71)$
(0.11, 0.65, 0.75)	1	2	5	13	$(0.71, -0.71)$
(0.81, 0.31, 0.50)	1	0	1	6	$(-0.71, 0.71)$
(0.81, 0.50, 0.31)	1	2	1	6	$(-0.71, 0.71)$

Table 5.6: Patterns derived from the elements in $\Gamma_8 \simeq \Delta(6 \times 4^2)$ with Eq. (5.36).

The S_1 and S_2 satisfy the following relation

$$S_1 S_2 = S_2 S_1 = S_3 \,, \tag{5.38}$$

where S_3 is another Z_2 generating from two Z_2 symmetries, that is

$$\hat{S}_3 = \mathrm{diag}\{-1, -1, 1\} \,. \tag{5.39}$$

The necessary condition that these residual symmetries are in the same finite flavor gorup is written by

$$S_1^2 = S_2^2 = T^n = (S_1 T)^{p_1} = (S_2 T)^{p_2} = (S_1 S_2 T)^{p_3} = 1 \qquad n,\, p_1,\, p_2,\, p_3 \in Z \,. \tag{5.40}$$

We consider

$$\mathrm{tr}[S_1 T] = a_1 \,, \qquad \mathrm{tr}[S_2 T] = a_2 \,, \tag{5.41}$$

where $a_{1(2,3)}$ is a sum of three $p_{1(2,3)}$-th roots of unity. From Eq. (5.41) we can find the formulae for determining two columns of the PMNS matrix in the form of Eq. (5.12) as discussed before. To be more precise, Eq. (5.12) with $a = a_1$ determines first column of the PMNS matrix while Eq. (5.12) with $a = a_2$ determines second column of the PMNS matrix. Note that the phases of the charged lepton residual symmetry $(\phi_e,\, \phi_\mu,\, \phi_\tau)$ are not different between both formulae Eq. (5.12) with $a = a_1$ and a_2. Considering the unitarity condition $|U_{\alpha 1}|^2 + |U_{\alpha 2}|^2 + |U_{\alpha 3}|^2 = 1$, the formulae fully determine the PMNS matrix.

However, in this case, a_1 and a_2 must satisfy another condition. The condition comes from $\mathrm{tr}[S_1 S_2 T]$, which can be rewritten by

$$\begin{aligned} \mathrm{tr}[S_1 S_2 T] &= \mathrm{tr}[S_3 T] \\ &= \sum_{\alpha = e,\,\mu,\,\tau} e^{i\phi_\alpha} (2|U_{\alpha 3}|^2 - 1) \\ &= -a_1 - a_2 - \sum_{\alpha} e^{i\phi_\alpha} = a_3 \,. \end{aligned} \tag{5.42}$$

The a_1 and a_2 must satisfy the last non-trivial equality. If the above equation is satisfied, we can write the third column of the PMNS matrix by Eq. (5.12) with $a = -a_1 - a_2 - \sum_\alpha e^{i\phi_\alpha}$ and the resulting PMNS matrix automatically becomes the unitary matrix.

Though we can search the possible PMNS matrices from the $Z_2 \times Z_2$ symmetry, the variety of patterns is reduced from the case of one Z_2 symmetry. We systematically search patterns from $(n,\, p_1,\, p_2,\, p_3) = (3,\, 2,\, 2,\, 2)$ to $(8,\, 8,\, 8,\, 8)$ and show the results in the followings.[2]

The tri-bimaximal pattern often appears in the small parameter regions. For example, when we set $(n,\, p_1,\, p_2;\, k_e,\, k_\mu,\, a_1,\, a_2) = (3,\, 4,\, 3;\, 0,\, 1,\, 1,\, 0)$, the first column of tri-bimaximal pattern $(0.82, 0, 42, 0.42)^T$ comes from a_1 and the second column $(0.58,\, 0.58,\, 0.58)^T$ comes from a_2.

We find the following pattern as

$$\begin{pmatrix} 0.93 & 0.36 & 0 \\ 0.25 & 0.66 & 0.71 \\ 0.25 & 0.66 & 0.71 \end{pmatrix}, \tag{5.43}$$

with $(n,\, p_1,\, p_2;\, k_e,\, k_\mu,\, a_1,\, a_2) = (3,\, 5,\, 5;\, 0,\, 1,\, 1.62,\, -0.62)$. The pattern is derived from A_5 symmetry and reported in Ref. [41].

We find the following pattern as

$$\begin{pmatrix} 0.89 & 0.41 & 0.19 \\ 0.41 & 0.82 & 0.41 \\ 0.19 & 0.41 & 0.89 \end{pmatrix} \tag{5.44}$$

with $(n,\, p_1,\, p_2;\, k_e,\, k_\mu,\, a_1,\, a_2) = (3,\, 7,\, 4;\, 1,\, 0,\, -0.5+1.3i,\, 1)$. The θ_{13} angle is near to the experimental. However, we need a slightly large corrections to the solar and atmosphere angles. The pattern is derived from $PSL(2, Z_7)$ symmetry.

We find the following pattern as

$$\begin{pmatrix} 0.79 & 0.58 & 0.21 \\ 0.58 & 0.58 & 0.58 \\ 0.21 & 0.58 & 0.79 \end{pmatrix}, \tag{5.45}$$

with $(n,\, p_1,\, p_2;\, k_e,\, k_\mu,\, a_1,\, a_2) = (3,\, 8,\, 3;\, 1,\, 0,\, i,\, 0)$. The θ_{13} angle is near to the experiments while the solar and atmosphere angle need slightly large corrections. The pattern is derived from $\Delta(6 \times 4^2)$, which is discussed in Ref. [42].

We find the following pattern as

$$\begin{pmatrix} 0.71 & 0.71 & 0 \\ 0.5 & 0.5 & 0.71 \\ 0.5 & 0.5 & 0.71 \end{pmatrix} \tag{5.46}$$

[2]In this method, we just consider necessary conditions of a finite group and it is not guaranteed that the following patterns are truly realized by finite groups. Fortunately, however, it happens that all the following patterns can be generated by finite groups in Ref. [40].

with $(n,\, p_1,\, p_2;\, k_e,\, k_\mu,\, a_1,\, a_2) = (4,\, 3,\, 3;\, 0,\, 1,\, 0,\, 0)$. The pattern is derived from S_4 symmetry.

We find the following pattern as

$$\begin{pmatrix} 0.84 & 0.5 & 0.21 \\ 0.5 & 0.71 & 0.5 \\ 0.21 & 0.5 & 0.84 \end{pmatrix} \tag{5.47}$$

with $(n,\, p_1,\, p_2;\, k_e,\, k_\mu,\, a_1,\, a_2) = (4,\, 7,\, 3;\, 1,\, 0,\, -0.5 + 1.32i,\, 0)$. The θ_{13} angle is near to the experiments while the solar and atmosphere angle need slightly large corrections. The pattern is derived from $PSL(2, Z_7)$ symmetry.

We find the following pattern as

$$\begin{pmatrix} 0.85 & 0.53 & 0 \\ 0.37 & 0.60 & 0.71 \\ 0.37 & 0.60 & 0.71 \end{pmatrix} \tag{5.48}$$

with $(n,\, p_1,\, p_2;\, k_e,\, k_\mu,\, a_1,\, a_2) = (5,\, 3,\, 5;\, 0,\, 1,\, 0,\, -0.62)$. The pattern is derived from the A_5 symmetry and reported in Ref. [12, 43, 44].

We find the following pattern as

$$\begin{pmatrix} 0.81 & 0.36 & 0.45 \\ 0.45 & 0.81 & 0.36 \\ 0.36 & 0.45 & 0.81 \end{pmatrix} \tag{5.49}$$

with $(n,\, p_1,\, p_2;\, k_e,\, k_\mu,\, a_1,\, a_2) = (7,\, 3,\, 7;\, 2,\, 4,\, 0,\, -0.5 - 1.32i)$. The pattern need large corrections. The pattern is derived from $PSL(2, Z_7)$ symmetry.

In our calculation, other patterns near to the experiments are not derived upto $(n,\, p_1,\, p_2,\, p_3) = (8,\, 8,\, 8,\, 8)$. We need larger $(n,\, p)$ if we want better patterns for the PMNS matrix.

Chapter 6

CKM Matrix

The values of the CKM matrix is a mysterious matter in the SM. Although the mixing angles in the CKM matrix is much smaller than that of the PMNS matrix, the flavor symmetry could be a candidate for explaining the quark mixing as well as the lepton mixing. In this chapter, we apply Hernandez-Smirnov method to the quark sector and see the possibility of the flavor symmetry.

6.1 Searching for flavor symmetries to the quark mixing

The quark sector of Lagrangian is given by Eq. (2.13). In general, each quark mass term inherently and maximally respects three $U(1)$ symmetries corresponding to three generations. For instance, in the basis of Eq. (2.13), the down quark mass term is invariant under transformations

$$D_R \to S_D D_R\,, \qquad D_L \to S_D D_L\,, \tag{6.1}$$

where

$$S_0 \equiv \mathrm{diag}\{e^{i\phi_d}, e^{i\phi_s}, e^{i\phi_b}\}\,, \qquad S_D = V_{\mathrm{CKM}} S_0 V_{\mathrm{CKM}}^\dagger\,. \tag{6.2}$$

We regard S_D as an element of a residual symmetry G_d arising from spontaneous breaking of a full flavor symmetry $G_f^{(q)}$ at a high energy scale. Here, for simplicity, we assume that $G_f^{(q)}$ and G_d are discrete subgroups of $SU(3)$ and that G_d is Z_m. Then S_D satisfies

$$S_D^m = \mathbb{1}\,. \tag{6.3}$$

The phases in S_D are described as

$$\phi_d \equiv 2\pi\frac{k_d}{m}\,, \qquad \phi_s \equiv 2\pi\frac{k_s}{m}\,, \qquad \phi_b \equiv 2\pi\frac{k_b}{m}\,, \tag{6.4}$$

where $(k_d,\, k_s,\, k_b)$ represent Z_m charges and are restricted to be

$$k_d + k_s + k_b \equiv 0 \qquad \mathrm{mod}\ m\,, \tag{6.5}$$

because of the assumption $G_d \subset SU(3)$.

Similarly, in the up quark mass term, we postulate $G_u = Z_n$ and define Z_n transformations as

$$U_L \to TU_L\,, \qquad U_R \to TU_R\,, \tag{6.6}$$

where

$$T \equiv \mathrm{diag}\{e^{i\phi_u}, e^{i\phi_c}, e^{i\phi_t}\}\,, \tag{6.7}$$

$$T^n = \mathbb{1}\,, \tag{6.8}$$

$$\phi_u \equiv 2\pi\frac{k_u}{n}\,, \qquad \phi_c \equiv 2\pi\frac{k_c}{n}\,, \qquad \phi_t \equiv 2\pi\frac{k_t}{n}\,, \tag{6.9}$$

and, from the assumption $G_u \subset SU(3)$,[1] we obtain

$$k_u + k_c + k_t \equiv 0 \qquad \mathrm{mod}\ n\,. \tag{6.10}$$

In order for both G_u and G_d to be residual symmetries of $G_f^{(q)}$, products of S_D and T must also belong to $G_f^{(q)}$ and have a finite order. Hence, we here introduce a new element

$$W \equiv S_D T\,, \tag{6.11}$$

and require that W is an element of Z_p, leading to

$$W^p = (S_D T)^p = \mathbb{1}\,. \tag{6.12}$$

Thus, in total, $G_f^{(q)}$ should contain three elements, S_D, T and W, satisfying

$$S_D^m = T^n = W^p = \mathbb{1}\,, \tag{6.13}$$

and groups composed of such elements are also called von Dyck group. The groups have the finite number of elements if $1/n + 1/m + 1/p > 1$, whereas it is infinite in the case of $1/n + 1/m + 1/p \leq 1$.

The requirement of $W^p = \mathbb{1}$ gives two constraints on the CKM matrix elements. In order to demonstrate that, let us consider the trace of W. On one hand, $\mathrm{tr}[W]$ can directly be written down with

$$W = V_{\mathrm{CKM}} S_0 V_{\mathrm{CKM}}^\dagger T\,. \tag{6.14}$$

On the other hand, $\mathrm{tr}[W]$ is equal to a sum of the eigenvalues of W. From $W^p = \mathbb{1}$, the sum, a, is given by

$$a = e^{2\pi i\frac{q_1}{p}} + e^{2\pi i\frac{q_2}{p}} + e^{2\pi i\frac{q_3}{p}}\,, \qquad q_1 + q_2 + q_3 \equiv 0 \qquad \mathrm{mod}\ p\,, \tag{6.15}$$

[1]Note that since eqs. (6.5) and (6.10) lead to $\det S_0 = \det S_D = \det T = 1$, these Z_m and Z_n symmetries are anomaly-free (see Ref. [45] and references therein).

where (q_1, q_2, q_3) represent Z_p charges. As a result, one obtains

$$\begin{aligned} tr[W] \,=& e^{i\phi_u}\left[|V_{ud}|^2 e^{i\phi_d} + |V_{us}|^2 e^{i\phi_s} + |V_{ub}|^2 e^{i\phi_b}\right] \\ &+ e^{i\phi_c}\left[|V_{cd}|^2 e^{i\phi_d} + |V_{cs}|^2 e^{i\phi_s} + |V_{cb}|^2 e^{i\phi_b}\right] \\ &+ e^{i\phi_t}\left[|V_{td}|^2 e^{i\phi_d} + |V_{ts}|^2 e^{i\phi_s} + |V_{tb}|^2 e^{i\phi_b}\right] \,=\, a\,, \end{aligned} \tag{6.16}$$

where V_{ij} stands for the ij element of the CKM matrix. Since a is a complex parameter, Eq. (6.16) generally yields two constraints on the CKM matrix elements with a fixed integer set (n, k_u, k_c, m, k_d, k_s, p, q_1, q_2). Since the CKM matrix is characterized by the four parameters (θ_{12}, θ_{13}, θ_{23}, δ), the above two constraints can not determine the whole CKM matrix. However, by setting some of the CKM parameters by hand, one can predict the remaining CKM parameters. In the following section, under several cases, we systematically search the integer sets (n, k_u, k_c, m, k_d, k_s, p, q_1, q_2), which predict the experimental data.

6.2 Calculations

6.2.1 $\theta_{13} = \theta_{23} = 0$ case

By fixing at least two of the four CKM parameters by hand, one can predict the remaining CKM parameters with Eq. (6.16) for given
(n, k_u, k_c, m, k_d, k_s, p, q_1, q_2). Since θ_{13} and θ_{23} are much smaller than θ_{12}, they are often taken to be vanishing at zero-th order in some flavor models. We here adopt the same stance and concentrate on predicting the Cabibbo angle θ_{12}. Note that we do not aim at precisely reproducing the Cabibbo angle and others. Small perturbations are expected to occur, because a breaking scale of the full flavor symmetry is supposed to be very high.

In the case of $\theta_{13} = \theta_{23} = 0$, the Dirac phase δ is also disappeared from the CKM matrix, then Eq. (6.16) is reduced to be

$$e^{i(\phi_u+\phi_d)} + e^{i(\phi_c+\phi_s)} + e^{i(\phi_t+\phi_b)} - s_{12}^2(e^{i\phi_u} - e^{i\phi_c})(e^{i\phi_d} - e^{i\phi_s}) \,=\, a\,. \tag{6.17}$$

This yields two conditions on θ_{12}:

$$\sin^2\theta_{12} \,=\, \frac{-\mathrm{Re}[a] + \cos(\phi_b+\phi_t) + \cos(\phi_d+\phi_u) + \cos(\phi_s+\phi_c)}{\cos(\phi_d+\phi_u) - \cos(\phi_d+\phi_c) - \cos(\phi_s+\phi_u) + \cos(\phi_s+\phi_c)}\,, \tag{6.18}$$

from the real part while

$$\sin^2\theta_{12} \,=\, \frac{-\mathrm{Im}[a] + \sin(\phi_b+\phi_t) + \sin(\phi_d+\phi_u) + \sin(\phi_s+\phi_c)}{\sin(\phi_d+\phi_u) - \sin(\phi_d+\phi_c) - \sin(\phi_s+\phi_u) + \sin(\phi_s+\phi_c)}\,, \tag{6.19}$$

from the imaginary part. In general, these conditions are independent of each other and must simultaneously be satisfied. However, in some cases, restrictions on θ_{12} become reduced. For example, when the denominator of Eq. (6.18) (or Eq. (6.19)) is zero, the real (or the imaginary) part of Eq. (6.17) becomes free from θ_{12}, which implies that Eq. (6.18)

(or Eq. (6.19)) gives no constraint on θ_{12}. Furthermore, in certain cases, both conditions, eqs. (6.18) and (6.19), provide no constraints on θ_{12}, e.g. the denominators are vanishing in both conditions; we will omit such cases in what follows.

We perform a numerical search for a possible integer set
$(n,\, k_u,\, k_c,\, m,\, k_d,\, k_s,\, p,\, q_1,\, q_2)$ upto $(n,\, m,\, p) = (6,\, 6,\, 12)$.[2] Figure 6.1 shows $\sin\theta_{12}$ near the experimental value as a function of p. We also list solutions near to the experiments in Table 6.1 and find that all the solutions are within the region of $0.21 < \sin\theta_{12} < 0.24$. In the table, only the case of $(n,\, m,\, p) = (2,\, 2,\, 7)$ can be a finite von Dyck group, which is D_7 and discussed in Ref. [46], while all the other cases compose infinite von Dyck groups. Some of the latter cases may be embedded into finite subgroups of infinite von Dyck groups [40, 26].

Let us study more on the case with $n = m = 2$. We consider a special case with $n = m = 2$, $k_u = k_s = q_1 = 0$, and $k_c = k_d = 1$. Then, the mixing angle in Eq. (6.18) can be expressed by a simple form of

$$\sin^2\theta_{12} = \cos^2\frac{\pi q_2}{p}\,. \tag{6.20}$$

The mixing angle in this form can be derived by the finite group $\Delta(6N^2)$ as discussed in section 8.1. Experimentally, the center value $\sin\theta_{12}$ is 0.225, so we need $q_2/p = 0.428$. Also, the range $\sin\theta_{12} = [0.224, 0.226]$ corresponds to $q_2/p = [0.427, 0.428]$. To express this value approximately by integer sets, the combination of $p = 7$ and $q_2 = 3$ is the simplest, i.e. $3/7 = 0.4286$, as it appeared in our numerical analysis. For $p < 89$, there is no intergers to fit better than $p = 7$ except $(p, q_2) = (7r, 3r)$. Taking greater number for p, we can better fit to the experimental value, for instance $(p, q_2) = (89, 38),\ (96, 41),\ (103, 44)$, i.e. $38/89 = 0.4270$, $41/96 = 0.4271$, $44/103 = 0.4272$. Thus, $p = 7$ is much simpler to fit the experiemental value in this scheme and it seems that the Z_{7r} symmetry is favorable.

6.2.2 $\theta_{13} = 0$ case

Next, we lift the restriction of $\theta_{23} = 0$. Then, the expression of $\mathrm{tr}[W]$ is given as follows:

$$\begin{aligned} &e^{i(\phi_u+\phi_d)} + e^{i(\phi_c+\phi_s)} + e^{i(\phi_t+\phi_b)} - s_{12}^2(e^{i\phi_u} - e^{i\phi_c})(e^{i\phi_d} - e^{i\phi_s}) \\ &- s_{23}^2(e^{i\phi_c} - e^{i\phi_t})(e^{i\phi_s} - e^{i\phi_b}) - s_{12}^2 s_{23}^2(e^{i\phi_c} - e^{i\phi_t})(e^{i\phi_d} - e^{i\phi_s}) \;=\; a\,. \end{aligned} \tag{6.21}$$

As in Subsection 6.2.1, we focus only on solutions in which θ_{12} and θ_{23} are uniquely determined. In addition, we here omit solutions predicting $\theta_{23} = 0$ since they are included in the results of Subsection 6.2.1[3].

Similar to Subsection 6.2.1, we search for possible integer sets upto
$(n,\, m,\, p) = (6,\, 6,\, 12)$. We plot $\sin\theta_{23}$ as a function of $\sin\theta_{12}$ in Figure 6.2 and pick out

[2]When $n = 2$ or $m = 2$, one needs to introduce an additional Z_2 symmetry to keep the mass matrix diagonal in their diagonal basis. The additional Z_2 can be chosen not to affect θ_{12}.

[3]However, the opposite is not always true. For example, the solution of $(n,\, m,\, p) = (2,\, 2,\, 7)$ in Table 6.1 does not derive $\theta_{23} = 0$ in Eq. (6.21). This is because the terms associated with θ_{23} are dropped from Eq. (6.21), and thus θ_{23} is not determined.

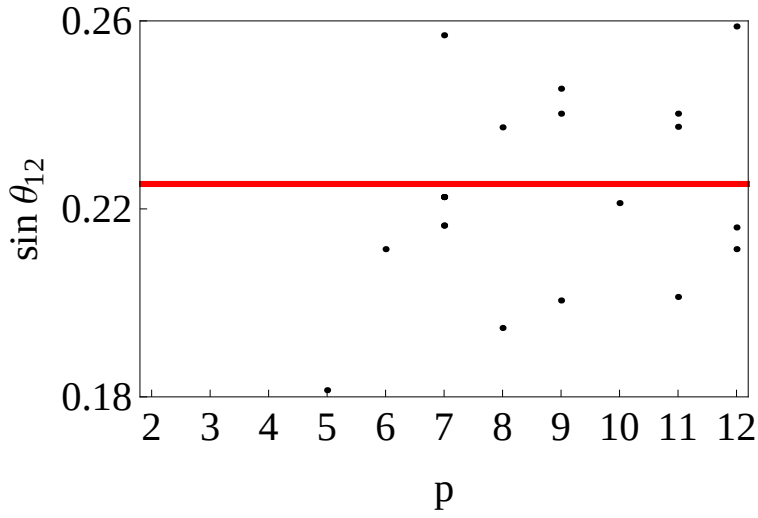

Figure 6.1: Distribution of $\sin\theta_{12}$ as a function of p upto $(n, m, p) = (6, 6, 12)$ while setting $\theta_{23} = \theta_{13} = 0$. The bold line is the experimental value, $\sin\theta_{12} = 0.225$.

$\sin\theta_{12}$	n	m	p	k_u	k_c	k_d	k_s	q_1	q_2	(Re[a], Im[a])
0.223	2	2	7	0	1	1	0	0	3	$(-0.802, 0)$
0.211	2	5	6	0	1	1	4	1	2	$(-1.00, 1.73)$
0.240258	3	4	9	0	1	3	1	5	6	$(-1.27, -2.19)$
0.2165	3	5	7	1	2	1	4	0	3	$(-0.802, 0)$
0.2160	3	5	12	0	1	3	2	7	8	$(-1.37, -2.37)$
0.2374	3	6	11	0	1	1	3	0	2	$(1.83, 0)$
0.246	4	4	9	0	1	2	1	0	4	$(-0.88, 0)$
0.221	4	4	10	0	1	1	0	2	3	$(-1.00, 1.90)$
0.240264	4	5	11	1	3	4	1	0	1	$(2.68, 0)$
0.2373	5	5	8	0	2	3	0	0	3	$(-0.414, 0)$

Table 6.1: While setting $\theta_{23} = \theta_{13} = 0$ and upto $(n, m, p) = (6, 6, 12)$, we pick out some solutions close to the experimental value; all of them are within the range of $0.21 < \sin\theta_{12} < 0.24$. Integer sets which give the same $\sin\theta_{12}$ displayed here are omitted.

solutions close to the experimental values in Table 6.2. All the solutions in Table 6.2 satisfy $0.15 < \sin\theta_{12} < 0.30$ and $0.05 < \sin\theta_{23} < 0.10$. From Figure 6.2, it can be seen that $\sin\theta_{12}$ can be near the experimental value, whereas most of the obtained $\sin\theta_{23}$ are much larger than its experimental value. Moreover, solutions which are marginally consistent with the experimental value of $\sin\theta_{23}$ are obtained for relatively large $(n,\, m,\, p)$. These tendencies may suggest that larger $(n,\, m,\, p)$ are necessary for reproducing a realistic $\sin\theta_{23}$ as well as $\sin\theta_{12}$.

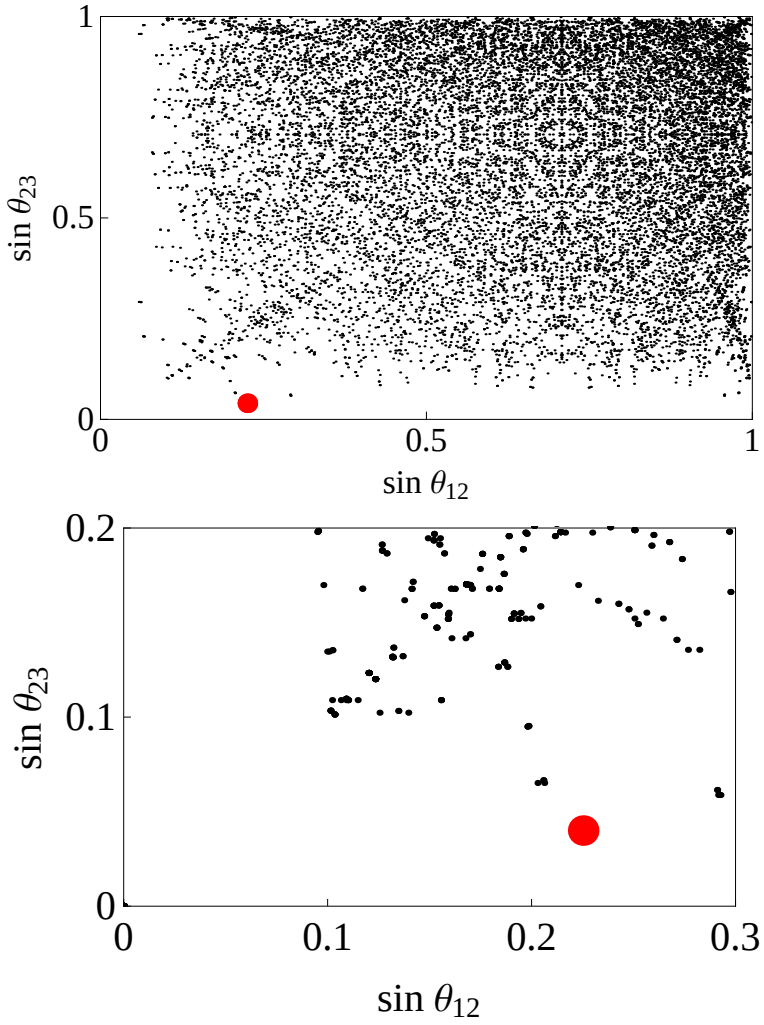

Figure 6.2: Distribution of $\sin\theta_{23}$ as a function of $\sin\theta_{12}$ upto $(n,\, m,\, p) = (6,\, 6,\, 12)$ while setting $\theta_{13} = 0$. The upper diagram is a sketch of entire region and the lower diagram is closeup one. Their experimental values are depicted as the large red point at $(\sin\theta_{12}, \sin\theta_{23}) = (0.225,\, 0.0412)$.

$(\sin\theta_{12}, \sin\theta_{23})$	n	m	p	k_u	k_c	k_d	k_s	q_1	q_2	(Re[a], Im[a])
(0.206, 0.0666)	4	5	11	0	1	4	2	6	7	$(-1.20, -1.95)$
(0.206, 0.0652)	5	4	11	1	3	0	3	2	4	$(-1.20, 1.95)$
(0.203, 0.0652)	5	4	11	4	2	0	1	6	7	$(-1.20, -1.95)$
(0.291, 0.0588)	5	6	11	1	3	0	5	2	4	$(-1.20, 1.95)$
(0.198, 0.0950)	5	6	11	2	0	2	1	1	2	(1.11, 0.460)
(0.293, 0.0588)	5	6	11	4	2	0	1	6	7	$(-1.20, -1.95)$
(0.291, 0.0615)	6	5	11	0	1	4	2	6	7	$(-1.20, -1.95)$
(0.198, 0.0953)	6	5	11	2	1	2	0	1	2	(1.11, 0.460)

Table 6.2: While setting $\theta_{13} = 0$ and upto $(n, m, p) = (6, 6, 12)$, we pick out solutions close to the experimental values. The solutions are all within $0.15 < \sin\theta_{12} < 0.30$ and $0.05 < \sin\theta_{23} < 0.10$. Solutions predicting $\sin\theta_{23} = 0$ are excluded.

6.2.3 Setting θ_{13} and δ to the experimental values

In the previous subsections, we set the small CKM angles to zero. We here consider a more realistic case by setting θ_{13} and δ to their experimental values: $(\sin\theta_{13}, \cos\delta) = (0.00341, 0.355)$. The results upto $(n, m, p) = (6, 6, 12)$ are displayed in Figure 6.3. Comparing with Figure 6.2, one can find that some of the solutions appear in both figures. In addition to such solutions, there also exist solutions which do not appear in Figure 6.2. Solutions close to the experimental values are picked up in Table 6.3. It seems that the tendency for large groups to generate realistic values still holds, while the combination $(p, q_2) = (7, 3)$ is included as one of the simplest ones again. Nevertheless, as variety has come to the solution, one can find favorable solutions more easily.

6.2.4 Setting θ_{23} and δ to the experimental values

In the previous subsections, we fix (θ_{13}, δ) and observe patterns of $(\theta_{12}, \theta_{23})$. Here, we fix (θ_{23}, δ) and observe $(\theta_{12}, \theta_{13})$. We calculate upto $(n, m, p) = (6, 6, 12)$ and show the results in Figure 6.4 and Table 6.4. The result should not be drastically different from that of the previous subsections. We find some solutions which also appearing in the Table 6.3. Note that similar results are obtained in the cases of fixing other two CKM parameters.

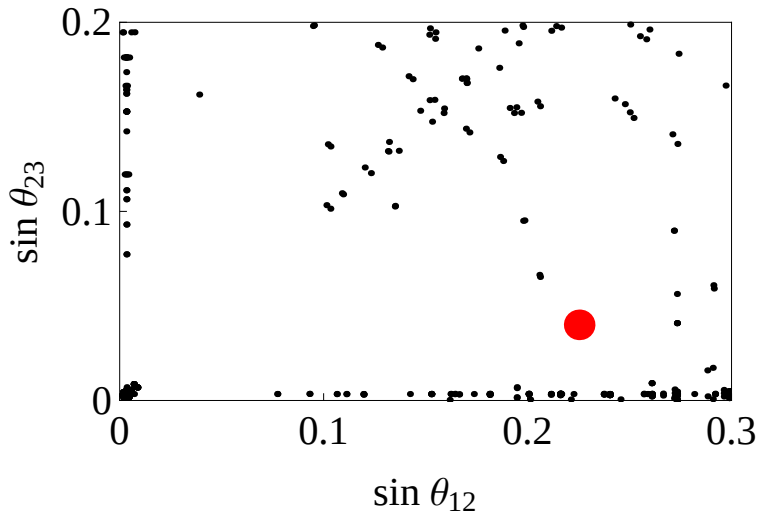

Figure 6.3: Distribution of $\sin\theta_{23}$ as a function of $\sin\theta_{12}$ upto $(n,\ m,\ p) = (6,\ 6,\ 12)$ while setting $(\sin\theta_{13},\ \cos\delta) = (0.00341,\ 0.355)$. Their experimental values are depicted as the large red point at $(\sin\theta_{12}, \sin\theta_{23}) = (0.225,\ 0.0412)$.

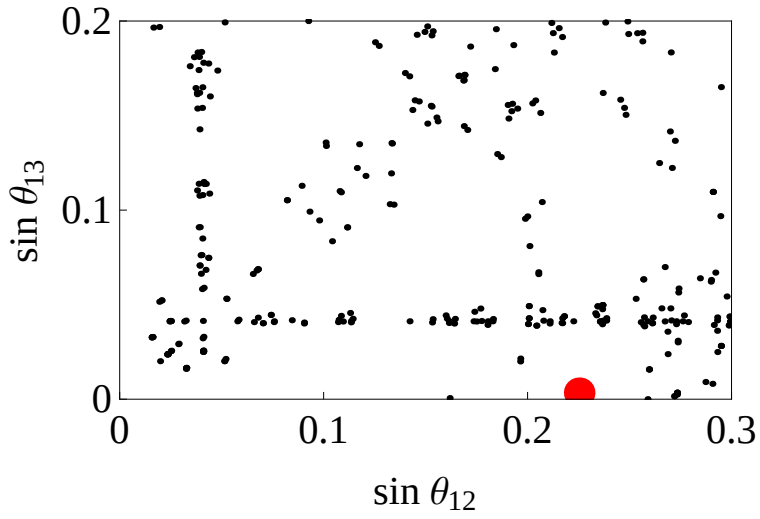

Figure 6.4: Distribution of $\sin\theta_{13}$ as a function of $\sin\theta_{12}$ upto $(n,\ m,\ p) = (6,\ 6,\ 12)$ while setting $(\sin\theta_{23},\ \cos\delta) = (0.0412,\ 0.355)$. Their experimental values are depicted as the large red point at $(\sin\theta_{12},\ \sin\theta_{13}) = (0.2253,\ 0.00341)$.

$(\sin\theta_{12}, \sin\theta_{23})$	n	m	p	k_u	k_c	k_d	k_s	q_1	q_2	$(\mathrm{Re}[a], \mathrm{Im}[a])$
(0.216, 0.00328)	3	5	7	1	2	1	4	0	3	$(-0.80, 0)$
(0.216, 0.00348)	5	3	7	1	4	1	2	0	3	$(-0.80, 0)$
(0.216, 0.00361)	3	5	12	0	1	3	2	7	8	$(-1.37, -2.37)$
(0.216, 0.00281)	5	3	12	2	3	0	2	3	4	$(-1.37, 2.37)$
(0.223, 0.00341)	4	4	7	1	3	1	3	0	3	$(-0.802, 0)$
(0.221, 0.000522)	4	4	10	1	2	0	3	2	3	$(-1.00, 1.90)$
(0.216, 0.00321)	2	3	12	5	5	6	12	0	5	$(-0.732051, 0)$
(0.216, 0.00349)	6	5	12	1	3	3	2	4	9	$(0.37, -0.63)$
(0.206, 0.0664)	4	5	11	0	1	4	2	6	7	$(-1.20, -1.95)$
(0.206, 0.0653)	5	4	11	1	3	0	3	2	4	$(-1.20, 1.95)$
(0.198, 0.0950)	5	6	11	2	0	2	1	1	2	$(1.11, 0.46)$
(0.198, 0.0952)	6	5	11	2	1	2	0	1	2	$(1.11, 0.46)$
(0.273, 0.0408)	2	5	12	0	1	2	3	1	5	$(-1.00, 1.00)$
(0.273, 0.0563)	5	4	10	2	4	1	3	5	7	$(-1.00, -1.90)$
(0.272, 0.08979)	5	6	10	1	2	2	1	5	6	$(-1.00, -1.18)$
(0.272, 0.08980)	5	6	10	1	2	5	4	0	1	$(2.62, 0)$
(0.291, 0.0592)	5	6	11	1	3	0	5	2	4	$(-1.20, 1.95)$
(0.291, 0.0609)	6	5	11	0	1	4	2	6	7	$(-1.20, -1.95)$
(0.273, 0.0409)	6	5	12	2	5	2	3	5	10	$(-0.37, -1.37)$
(0.291, 0.0173)	2	6	11	0	1	1	2	0	2	$(1.83, 0)$
(0.288, 0.0159)	5	6	11	1	4	5	1	0	1	$(2.68, 0)$

Table 6.3: While setting $(\sin\theta_{13}, \cos\delta) = (0.00341, 0.355)$ and upto $(n, m, p) = (6, 6, 12)$, we pick out solutions close to the experimental values. Solutions with small θ_{23} are in the upper box while solutions with large θ_{23} are in the lower box.

$(\sin\theta_{12}, \sin\theta_{13})$	n	m	p	k_u	k_c	k_d	k_s	q_1	q_2	(Re[a], Im[a])
(0.234, 0.0491)	3	4	9	0	1	3	1	5	6	$(-1.27, -2.19)$
(0.217, 0.0428)	3	5	7	1	2	1	4	0	3	$(-0.80, 0)$
(0.217, 0.0404)	5	3	7	1	4	1	2	0	3	$(-0.80, 0)$
(0.233, 0.0454)	3	6	11	0	1	1	3	0	9	$(1.83, 0)$
(0.222, 0.0412)	4	4	7	1	3	1	3	0	3	$(-0.80, 0)$
(0.218, 0.0438)	5	6	12	2	3	1	5	0	5	$(-0.73, 0)$
(0.217, 0.0402)	6	5	12	1	3	3	2	4	9	$(0.37, -0.63)$
(0.234, 0.0444	6	3	11	1	3	0	1	0	9	$(1.83, 0)$
(0.273, 0.00344)	2	5	12	0	1	2	3	1	5	$(-1, 1)$
(0.273, 0.00250)	5	4	10	2	4	1	3	5	7	$(-1, -1.90)$
(0.269, 0.0238)	5	5	12	2	0	3	0	1	0	$(2.73, 0)$
(0.260, 0.0157)	5	6	12	1	4	1	3	3	4	$(-1.37, 2.37)$
(0.196, 0.0200)	5	6	8	1	4	1	2	1	3	$(-1, 1.41)$
(0.196, 0.0215)	6	5	8	1	2	1	4	1	3	$(-1, 1.41)$

Table 6.4: While setting $(\sin\theta_{23}, \cos\delta) = (0.0412, 0.355)$ and upto $(n, m, p) = (6, 6, 12)$, we pick out solutions near to the experiments . Solutions with large θ_{13} are in the upper box while solutions with small θ_{13} are in the lower box.

6.2.5 $m = 2$ case

We consider the case of $m = 2$ as the situation is slightly different from the other cases. In this case, Eq. (6.16) turns out to be

$$\begin{aligned}
|V_{ui}|^2 &= \frac{\mathrm{Re}[a]\cos\frac{\phi_c+\phi_t}{2} + \cos\frac{\phi_c+\phi_t-2\phi_u}{2} + \mathrm{Im}[a]\sin\frac{\phi_c+\phi_t}{2}}{4\sin\frac{\phi_c-\phi_u}{2}\sin\frac{\phi_u-\phi_t}{2}}\,, \\
|V_{ci}|^2 &= \frac{\mathrm{Re}[a]\cos\frac{\phi_u+\phi_t}{2} + \cos\frac{\phi_u+\phi_t-2\phi_c}{2} + \mathrm{Im}[a]\sin\frac{\phi_u+\phi_t}{2}}{4\sin\frac{\phi_u-\phi_c}{2}\sin\frac{\phi_c-\phi_t}{2}}\,, \\
|V_{ti}|^2 &= \frac{\mathrm{Re}[a]\cos\frac{\phi_u+\phi_c}{2} + \cos\frac{\phi_u+\phi_c-2\phi_t}{2} + \mathrm{Im}[a]\sin\frac{\phi_u+\phi_c}{2}}{4\sin\frac{\phi_t-\phi_u}{2}\sin\frac{\phi_c-\phi_t}{2}}\,,
\end{aligned} \tag{6.22}$$

as derived in Ref. [26] for the lepton sector. As a result, one can directly constrain the i-th column of the CKM matrix without inputting the CKM parameters by hand. Note that the unitary condition,

$$|V_{ui}|^2 + |V_{ci}|^2 + |V_{ti}|^2 = 1\,, \tag{6.23}$$

has been used, and the subscript i reflects the position of a positive sign in S_0, e.g. $S_0 = \mathrm{diag}\{1, -1, -1\}$ for $i = d$. In the following, we take $i = s$, for the experimental values of the corresponding column are slightly large.

Results upto $(n,\ p) = (6,\ 12)$ are similar to those in Subsection 6.2.3. Thus, we here vary $(n,\ p)$ upto $(20,\ 20)$ and show that large groups can derive a much more realistic CKM mixing. For each n, in Figure 6.5, we pick out a solution which best reproduces the observed CKM mixing. Furthermore, we pick out solutions near to the experiments from Figure 6.5 and list them in Table 6.5. As can be seen, one can easily find solutions near the experimental values with large n and p.

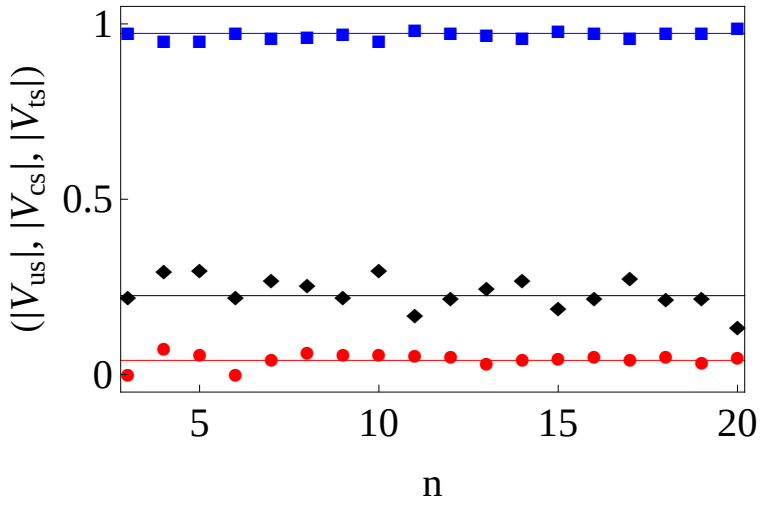

Figure 6.5: $|V_{us}|$, $|V_{cs}|$, and $|V_{ts}|$ are plotted as a function of n upto $(n,\ p) = (20,\ 20)$ while assuming $m = 2$. The black diamonds, blue squares, and red circles represent $|V_{us}|$, $|V_{cs}|$, and $|V_{ts}|$, respectively. The horizontal lines describe the experimental values: $(|V_{us}|,\ |V_{cs}|,\ |V_{ts}|) = (0.225,\ 0.973,\ 0.0404)$. For each n, we pick out a solution which derives the nearest mixing to the experimental values.

6.2.6 Klein group

We consider the case that the residual symmetry in the down sector is the Klein group $Z_2 \times Z_2$. In this case, the situation is the same as that in 5.3. The formulae Eq. (6.22) with two a_1 and a_2 determine two columns and the other column is determined by the unitarity condition. Under the necessary condition that the residual symmetries are included in a flavor group

$$-a_1 - a_2 - \sum_{\alpha=u,c,t} e^{i\phi_\alpha} = a_3\,, \tag{6.24}$$

we systematically search the possible CKM pattern from $(n,\ p_1,\ p_2,\ p_3) = (3,\ 2,\ 2,\ 2)$ to $(8,\ 8,\ 8,\ 8)$.

In results, we do not find any pattern with small mixing angles θ_{23}, θ_{13}. We find several patterns to generate the Cabibbo angle. We list them in the followings. We find

$(\lvert V_{us}\rvert, \lvert V_{cs}\rvert, \lvert V_{ts}\rvert)$	n	p	k_u	k_c	q_1	q_2	$(\mathrm{Re}[a], \mathrm{Im}[a])$
(0.269, 0.962, 0.0444)	7	19	0	2	4	5	$(-0.823, 1.80)$
(0.218, 0.975, 0.0510)	12	19	3	8	11	12	$(-1.31, -2.18)$
(0.248, 0.968, 0.0322)	13	19	5	7	10	11	$(-1.08, -1.25)$
(0.190, 0.981, 0.0468)	15	13	1	10	7	9	$(-1.21, -2.17)$
(0.275, 0.960, 0.0444)	17	18	5	11	10	11	$(-1.21, -1.85)$
(0.215, 0.975, 0.0507)	18	20	6	11	11	12	$(-1.17, -1.71)$
(0.219, 0.975, 0.0345)	19	15	6	1	1	2	$(1.89, 0.199)$

Table 6.5: From Figure 6.5, we pick out solutions close to the experimental values.

a pattern as

$$\begin{pmatrix} 0.95 & 0.30 & 0 \\ 0.30 & 0.95 & 0 \\ 0 & 0 & 1 \end{pmatrix}, \tag{6.25}$$

with $(n,\, p_1,\, p_2;\, k_u,\, k_c,\, a_1,\, a_2) = (3,\, 8,\, 8;\, 1,\, 2,\, -1+\sqrt{2}i,\, -1-\sqrt{2}i)$. We find a pattern as

$$\begin{pmatrix} 0.97 & 0.26 & 0 \\ 0.26 & 0.97 & 0 \\ 0 & 0 & 1 \end{pmatrix}, \tag{6.26}$$

with $(n,\, p_1,\, p_2;\, k_u,\, k_c,\, a_1,\, a_2) = (4,\, 6,\, 6;\, 1,\, 3,\, -1+\sqrt{3}i,\, -1-\sqrt{3}i)$. We find a pattern as

$$\begin{pmatrix} 0.92 & 0.38 & 0 \\ 0.38 & 0.92 & 0 \\ 0 & 0 & 1 \end{pmatrix}, \tag{6.27}$$

with $(n,\, p_1,\, p_2;\, k_u,\, k_c,\, a_1,\, a_2) = (4,\, 8,\, 8;\, 1,\, 3,\, -1+\sqrt{2}i,\, -1-\sqrt{2}i)$.

In our calculation, we do not find any other sets which generate small mixing angles from $(n,\, p_1,\, p_2,\, p_3) = (3,\, 2,\, 2,\, 2)$ to $(8,\, 8,\, 8,\, 8)$. However, if we consider larger $(n,\, p_1,\, p_2,\, p_3)$, it is expected that small mixing angles are also generated.

Chapter 7

Toward GUT

It is an ambitious matter to build a model for the grand unification theory (GUT). Components of the SM and the RG flows of the gauge couplings imply that three gauge symmetries $\mathrm{SU}(3)_C \times \mathrm{SU}(2)_W \times \mathrm{U}(1)_Y$ may unify to a GUT symmetry G_{GUT} such as SU(5) and SO(10) at the high energy scale $M_{\mathrm{GUT}} \sim 10^{16}$ GeV. Although the direct evidence of the GUT such as the proton decay has not been observed yet, the GUT has a various theoretical merits to predict physics at the electroweak scale and beyond. For example, the small neutrino masses can be naturally derived with the see-saw mechanism in a SO(10) GUT model [47].

Some flavor symmetries can exist together with the grand unification. In these cases, models often have the $G_{\mathrm{GUT}} \times G_f$ structure. For the tri-bimaximal lepton mixing, models have been proposed with $G_f = SU(3)_f$[48], $\Delta(27)$[14], A_4[49], S_4[50] and $PSL(2, Z_7)$[11].

To realize a GUT model with a flavor symmetry, all the fermions must be in the same representation of the flavor symmetry. In the purpose of generating both the lepton mixing and quark mixing, the flavor symmetry must break while leaving the residual symmetries in both the lepton sector and quark sector. In general, these residual symmetries could be different from each other. However, it is expected that some simple models have the same residual symmetry in the lepton and quark sectors because many Higgs fields are often need for the different residual symmetries.

Then in the chapter, we consider cases that some residual symmetries in the lepton sector and quark sector are the same. By using the method in the previous chapters, we search residual symmetries for generating both the lepton mixing and the quark mixing. In detail, we consider the following two cases[1]

1. $S_1,\ S_2 \in G_d = G_\nu = Z_2 \times Z_2$
   $T \in G_u = Z_{n_1}$
   $T' \in G_l = Z_{n_2}$.

2. $S_1,\ S_2 \in G_\nu = Z_2 \times Z_2$
   $S' \in G_d = Z_m$
   $T \in G_u = G_l = Z_n$.

[1]Other cases such as $G_d = G_l$ is also possible, which give similar results as those of the above two cases in our discussion.

In the Case 1, the residual symmetries of the down-type quark and neutrino mass terms are the same $S \in Z_2 \times Z_2$ while the symmetries of the up-type quark and charged lepton mass terms are diffetent T and T', respectively. In the case, the PMNS matrix and the CKM matrix are fully generated. However, the choice of S_1 and S_2 just influences to the positions of columns to be generated. It implies that the derived patterns are not changed from those of in Section 5.3 and Subsection 6.2.6, and no new information is obtained.

In the Case 2, the up-type quark and charged lepton mass terms have the same residual symmetry of $T \in Z_n$ while the other residual symmetires are different, i.e. S_1, $S_2 \in G_\nu = Z_2 \times Z_2$ and $S' \in G_d$, respectively. The symmetries satisfy the following relations

$$\begin{aligned} & S_1^2 = S_2^2 = S'^m = T^n \\ & = (S'T)^{p_1} = (S_1T)^{p_2} = (S_2T)^{p_3} = (S_1S_2T)^{p_4} = 1\,. \end{aligned} \tag{7.1}$$

As discussed in Subsection 5.3, the PMNS matrix is fully generated while the CKM matrix is generated by fixing some parameters in the CKM matrix. From Chapter 6, we find that the Cabibbo angle can be generated by a flavor symmetry. Then we focus on the Cabibbo angle. For each $S' \in G_d$ and $T \in G_u = G_l$, we calculate the Cabibbo angle by fixing other mixing angles to zero, $\theta_{23} = \theta_{13} = 0$, in the CKM matrix. If the derived Cabibbo angle is near to the experiments, $0.18 < \sin\theta_C < 0.26$, we next calculate the PMNS matrix by using the method discussed in Subsection 5.3.

We change integer sets from $(n,\, m,\, p_{1,2,3,4}) = (2,\, 2,\, 2)$ to $(8,\, 8,\, 8)$. The resulting patterns should be combinations of the PMNS matrix appearing in Subsection 5.3 and the Cabibbo angle. We have already known that the patterns of the PMNS matrix near to the experiments are given by the tri-bimaximal and from Eq. (5.43) to Eq. (5.49) in Subsection 5.3. Then we list the result for each useful pattern of the PMNS matrix given in Subsection 5.3. The results are in Table 7.1, Table 7.2, Table 7.3 and Table 7.4.

From the result, we can find the Cabibbo angles near to the experiments for almost all patterns of the PMNS matrix. However, we can not find any sets to generate the Cabibbo angle near to the experiments with the tri-bimaximal pattern of the PMNS matrix. If we expand the allowed region of the Cabibbo angle, we can find more sets.

It is another problem whether these residual symmetries are directly realized by a finite flavor symmetry. The search for the detailed finite group is to be done in future work.

PMNS	$\sin\theta_C$	n	m	$\begin{pmatrix} p_1 \\ p_2 \\ p_3 \end{pmatrix}$	k_u	k_c	k_d	k_s	$\begin{pmatrix} a_1 \\ a_2 \\ a_3 \end{pmatrix}$
$\begin{pmatrix} 0.82 & 0.58 & 0 \\ 0.42 & 0.58 & 0.71 \\ 0.42 & 0.58 & 0.71 \end{pmatrix}$	–	–	–	–	–	–	–	–	–
$\begin{pmatrix} 0.93 & 0.36 & 0 \\ 0.25 & 0.66 & 0.71 \\ 0.25 & 0.66 & 0.71 \end{pmatrix}$	0.2569	3	6	$\begin{pmatrix} 7 \\ 5 \\ 5 \end{pmatrix}$	0	1	3	1	$\begin{pmatrix} -0.8 \\ 1.6 \\ -0.6 \end{pmatrix}$
$\begin{pmatrix} 0.89 & 0.41 & 0.19 \\ 0.41 & 0.82 & 0.41 \\ 0.19 & 0.41 & 0.89 \end{pmatrix}$	0.2569	3	6	$\begin{pmatrix} 7 \\ 7 \\ 4 \end{pmatrix}$	1	0	1	3	$\begin{pmatrix} -0.8 \\ -0.5+1.3i \\ 1 \end{pmatrix}$
$\begin{pmatrix} 0.79 & 0.58 & 0.21 \\ 0.58 & 0.58 & 0.58 \\ 0.21 & 0.58 & 0.79 \end{pmatrix}$	0.2569	3	6	$\begin{pmatrix} 7 \\ 8 \\ 3 \end{pmatrix}$	1	0	1	3	$\begin{pmatrix} -0.8 \\ i \\ 0 \end{pmatrix}$

Table 7.1: Under the condition $G_u = G_l$, we list integer sets which generate the Cabibbo angle between $0.18 < \sin\theta_C < 0.26$ for each pattern of the PMNS matrix in Subsection 5.3. We search integer sets from $(n,\, m,\, p_{1,2,3,4}) = (2,\, 2,\, 2)$ to $(8,\, 8,\, 8)$. The results are continue to Table 7.2, 7.3 and 7.4.

PMNS	$\sin\theta_C$	n	m	$\begin{pmatrix} p_1 \\ p_2 \\ p_3 \end{pmatrix}$	k_u	k_c	k_d	k_s	$\begin{pmatrix} a_1 \\ a_2 \\ a_3 \end{pmatrix}$
$\begin{pmatrix} 0.71 & 0.71 & 0 \\ 0.5 & 0.5 & 0.71 \\ 0.5 & 0.5 & 0.71 \end{pmatrix}$	0.2432	4	8	$\begin{pmatrix} 7 \\ 3 \\ 3 \end{pmatrix}$	0	1	1	5	$\begin{pmatrix} 2.2 \\ 0 \\ 0 \end{pmatrix}$
	0.2055	8	3	$\begin{pmatrix} 8 \\ 3 \\ 3 \end{pmatrix}$	2	5	2	1	$\begin{pmatrix} 2.4 \\ 0 \\ 0 \end{pmatrix}$
	0.2039	8	5	$\begin{pmatrix} 8 \\ 3 \\ 3 \end{pmatrix}$	2	5	1	4	$\begin{pmatrix} -1+1.4i \\ 0 \\ 0 \end{pmatrix}$
	0.1855	8	7	$\begin{pmatrix} 8 \\ 3 \\ 3 \end{pmatrix}$	2	5	5	2	$\begin{pmatrix} 2.4 \\ 0 \\ 0 \end{pmatrix}$

Table 7.2: Continuation of Table 7.1.

PMNS	$\sin\theta_C$	n	m	$\begin{pmatrix} p_1 \\ p_2 \\ p_3 \end{pmatrix}$	k_u	k_c	k_d	k_s	$\begin{pmatrix} a_1 \\ a_2 \\ a_3 \end{pmatrix}$
$\begin{pmatrix} 0.84 & 0.5 & 0.21 \\ 0.5 & 0.71 & 0.5 \\ 0.21 & 0.5 & 0.84 \end{pmatrix}$	0.2432	4	8	$\begin{pmatrix} 7 \\ 7 \\ 3 \end{pmatrix}$	1	0	5	1	$\begin{pmatrix} 2.25 \\ -0.5+1.3i \\ 0 \end{pmatrix}$
$\begin{pmatrix} 0.85 & 0.53 & 0 \\ 0.37 & 0.60 & 0.71 \\ 0.37 & 0.60 & 0.71 \end{pmatrix}$	0.2373	5	5	$\begin{pmatrix} 8 \\ 5 \\ 3 \end{pmatrix}$	0	2	3	0	$\begin{pmatrix} -0.4 \\ 1.6 \\ 0 \end{pmatrix}$
	0.2469	5	8	$\begin{pmatrix} 5 \\ 5 \\ 3 \end{pmatrix}$	0	2	5	3	$\begin{pmatrix} -1.3-2.1i \\ 1.6 \\ 0 \end{pmatrix}$

Table 7.3: Continuation of Table 7.2.

PMNS	$\sin\theta_C$	n	m	$\begin{pmatrix} p_1 \\ p_2 \\ p_3 \end{pmatrix}$	k_u	k_c	k_d	k_s	$\begin{pmatrix} a_1 \\ a_2 \\ a_3 \end{pmatrix}$
$\begin{pmatrix} 0.81 & 0.36 & 0.45 \\ 0.45 & 0.81 & 0.36 \\ 0.36 & 0.45 & 0.81 \end{pmatrix}$	0.2547	7	3	$\begin{pmatrix} 7 \\ 3 \\ 7 \end{pmatrix}$	2	4	2	1	$\begin{pmatrix} 2.2 \\ 0 \\ -0.5-1.3i \end{pmatrix}$
	0.1948	7	4	$\begin{pmatrix} 7 \\ 7 \\ 4 \end{pmatrix}$	3	6	1	3	$\begin{pmatrix} -1.3-2.4i \\ -0.5+1.3i \\ 1 \end{pmatrix}$
	0.2263	7	5	$\begin{pmatrix} 7 \\ 7 \\ 4 \end{pmatrix}$	3	6	1	4	$\begin{pmatrix} -1.3-2.4i \\ -0.5+1.3i \\ 1 \end{pmatrix}$
	0.2456	7	7	$\begin{pmatrix} 5 \\ 3 \\ 7 \end{pmatrix}$	2	4	2	6	$\begin{pmatrix} -0.6 \\ 0 \\ -0.5-1.3i \end{pmatrix}$
	0.2199	7	7	$\begin{pmatrix} 5 \\ 7 \\ 4 \end{pmatrix}$	3	6	1	4	$\begin{pmatrix} -0.6 \\ -0.5+1.3i \\ 1 \end{pmatrix}$

Table 7.4: Continuation of Table 7.3.

Chapter 8

Models for Lepton Mixing and Quark Mixing

8.1 Embedding into $\Delta(6N^2)$

We have considered the von Dyck group. Constraining to some special cases, it is possible to embed the obtained residual symmetries into a finite group, for example, $\Delta(6N^2)$. We stress that this group is also useful to provide the mixing angles of leptons under the experimentally allowed region.

In this section, we focus on the case with $\theta_{13} = \theta_{23} = 0$ as studied in Subsection 6.2.1. For the purpose of embedding residual symmetries into a smaller $\Delta(6N^2)$ series, we redraw the plots in Figure 6.1 as a function of the least common multiples (LCMs) of (n, m, p) to Figure 8.1.

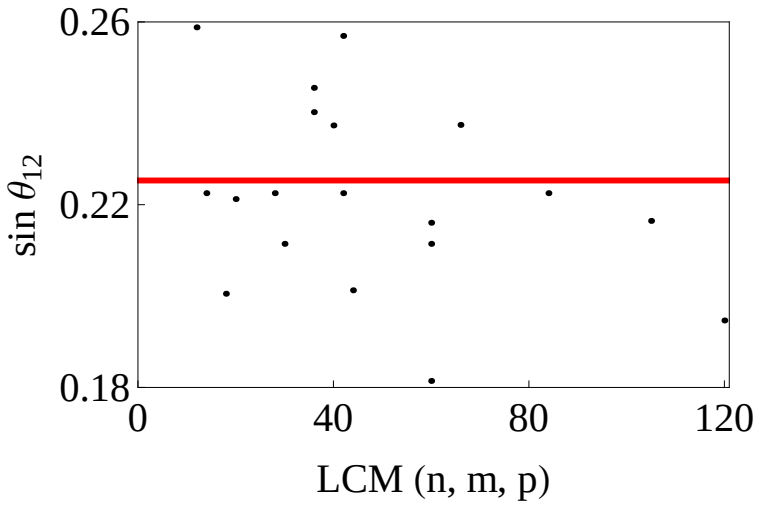

Figure 8.1: Distribution of $\sin\theta_{12}$ as a function of the least common multiples of (n, m, p) upto (6, 6, 12) in the case of $\theta_{13} = \theta_{23} = 0$.

For example, in Figure 8.1, the solution with LCM(n, m, p) = 12 corresponds to

$$(\sin\theta_{12},\, n,\, m,\, p) \;=\; (0.259,\, 2,\, 2,\, 12)\,, \tag{8.1}$$

which is also found in Table.I of Ref. [51]. This solution can be derived by $\Delta(6 \times 12^2)$ and it realizes the value by

$$\sin\theta_{12} = \frac{1}{2}|e^{2\pi\frac{i}{12}} + e^{\pi i}|\,. \tag{8.2}$$

Another example is LCM(n, m, p) = 14 with

$$(\sin\theta_{12},\, n,\, m,\, p) = (0.223,\, 2,\, 2,\, 7)\,. \tag{8.3}$$

We can derive it by $\Delta(6 \times 7^2)$ with the value of

$$\sin\theta_{12} = \frac{1}{2}|e^{2\pi\frac{i}{7}} + e^{8\pi\frac{i}{7}}|\,. \tag{8.4}$$

In the following subsections, we show how these results are gained by the analysis of $\Delta(6N^2)$ and propose a useful $\Delta(6N^2)$ symmetry for both the lepton mixing and the Cabibbo angle.

8.1.1 Z_2 elements in $\Delta(6N^2)$

Before deriving the above Cabibbo angles from $\Delta(6N^2)$, we review properties of $\Delta(6N^2)$ [52, 17].

The generators of $\Delta(6N^2)$ denoted by a, a', b and c satisfies the following algebraic relations

$$a^N = a'^N = b^3 = c^2 = 1\,, \tag{8.5}$$

and other relations. The detailed algebraic relation of $\Delta(6N^2)$ is written in the appendix. All the group elements are expressed by $g = b^z c^w a^x a'^y$.

For the purpose of later use, we see that the generators of $\Delta(6N^2)$ obey the following relations

$$ba^x a'^y b^2 = a^{-x+y} a'^{-x}\,, \qquad b^2 a^x a'^y b = a^{-y} a'^{x-y}\,, \tag{8.6}$$

$$cb^z c = b^{2z}\,. \tag{8.7}$$

To derive the Cabibbo angle, we use the Z_2 elements of $\Delta(6N^2)$; namely elements satisfying $g^2 = 1$. Then, we write down the Z_2 elements in the followings.

We write down Z_2 elements for fixed z and w. By definition, the possible combinations of (z, w) are

$$(z,\, w) = (0,\, 0),\, (1,\, 0),\, (2,\, 0),\, (0,\, 1),\, (1,\, 1),\, (2,\, 1)\,. \tag{8.8}$$

For $(z,\, w) = (0,\, 0)$, the square of elements are written by

$$g^2_{(z,w)=(0,0)} = a^{2x} a'^{2y} \,. \tag{8.9}$$

As both x and y take values from 0 to $\frac{N}{2}$, elements for satisfing $g^2 = 1$ are derived by

$$a^{\frac{N}{2}} \,, \qquad a'^{\frac{N}{2}} \,, \qquad a^{\frac{N}{2}} a'^{\frac{N}{2}} \,, \tag{8.10}$$

if N is even. For $(z,\, w) = (1,\, 0)$, the square of elements are written by

$$g^2_{(z,w)=(1,0)} = b^2 a^{x-y} a'^{x} \,. \tag{8.11}$$

Then, Z_2 elements do not exist for $(z,\, w) = (1,\, 0)$. For $(z,\, w) = (2,\, 0)$, the square of elements are written by

$$g^2_{(z,w)=(2,0)} = b a^{y} a'^{y-x} \,. \tag{8.12}$$

Then, Z_2 elements do not exist for $(z,\, w) = (2,\, 0)$. For $(z,\, w) = (0,\, 1)$, the square of elements are written by

$$g^2_{(z,w)=(0,1)} = a^{x-y} a'^{-x+y} \,. \tag{8.13}$$

When $x = y$, the above equation satisfy $g^2 = 1$. Then,

$$c a^{x} a'^{x} \tag{8.14}$$

are elements of Z_2. For $(z,\, w) = (1,\, 1)$, the square of elements are written by

$$g^2_{(z,w)=(1,1)} = a^{y} a'^{2y} \,. \tag{8.15}$$

When $y = 0$, the above equation satisfy $g^2 = 1$. As the x is arbitrary,

$$b c a^{x} \tag{8.16}$$

are elements of Z_2. For $(z,\, w) = (2,\, 1)$, the square of elements are written by

$$g^2_{(z,w)=(2,1)} = a^{2x} a'^{x} \,. \tag{8.17}$$

When $x = 0$, the above equation satisfy $g^2 = 1$. As the y is arbitrary,

$$b^2 c a'^{y} \tag{8.18}$$

are elements of Z_2. As a result, all the Z_2 elements can be written down by

$$a^{\frac{N}{2}} \,, \qquad a'^{\frac{N}{2}} \,, \qquad a^{\frac{N}{2}} a'^{\frac{N}{2}} \,, \tag{8.19}$$

$$c a^{x} a'^{x} \,, \qquad b c a^{x} \,, \qquad b^2 c a'^{y} \,. \tag{8.20}$$

8.1.2 Embedding

Here we identify Z_2 symmetries in down and up quark mass terms with bca^x and bca^y, respectively.

$$S = bca^x = \begin{pmatrix} 0 & -e^{-\frac{2\pi i}{N}x} & 0 \\ -e^{\frac{2\pi i}{N}x} & 0 & 0 \\ 0 & 0 & -1 \end{pmatrix}, \tag{8.21}$$

$$T = bca^y = \begin{pmatrix} 0 & -e^{-\frac{2\pi i}{N}y} & 0 \\ -e^{\frac{2\pi i}{N}y} & 0 & 0 \\ 0 & 0 & -1 \end{pmatrix}. \tag{8.22}$$

In the diagonalizing basis of the up quark mass terms[1], matrix representations are expressed as

$$S_D = \begin{pmatrix} \cos\left[\frac{2\pi}{N}(x-y)\right] & i\sin\left[\frac{2\pi}{N}(x-y)\right] & 0 \\ -i\sin\left[\frac{2\pi}{N}(x-y)\right] & -\cos\left[\frac{2\pi}{N}(x-y)\right] & 0 \\ 0 & 0 & 1 \end{pmatrix}, \tag{8.23}$$

and $T = \mathrm{diag}\{1, -1, -1\}$. Setting $S_0 = \mathrm{diag}\{-1, 1, -1\}$, the CKM matrix is obtained as

$$V_{\rm CKM} = \begin{pmatrix} (1-\rho^{x-y})/2 & (1+\rho^{x-y})/2 & 0 \\ (1+\rho^{x-y})/2 & (1-\rho^{x-y})/2 & 0 \\ 0 & 0 & 1 \end{pmatrix}, \tag{8.24}$$

where $\rho = e^{2\pi i/N}$. Since the overall phase is irrelevant, we obtain

$$\sin\theta_{12} = \cos\left[\frac{\pi(x-y)}{N}\right]. \tag{8.25}$$

This formula is the same as the one derived in Subsection 6.2.1 i.e.,

$$\sin\theta_{12} = \cos\frac{\pi q_2}{p}. \tag{8.26}$$

When $N = 12$ and $x - y = 5$, it yields

$$|V_{us}| = \sin\theta_{12} = 0.259, \tag{8.27}$$

which is the same as in the case of Eq. (8.3). When $N = 7$ and $x - y = 3$, it yields

$$|V_{us}| = \sin\theta_{12} = 0.223, \tag{8.28}$$

which is very close to the experimental value. As commented in Subsection 6.2.1, there is no integer N for $N < 89$, which fits better than $N = 7$ except $(N, x-y) = (7r, 3r)$.

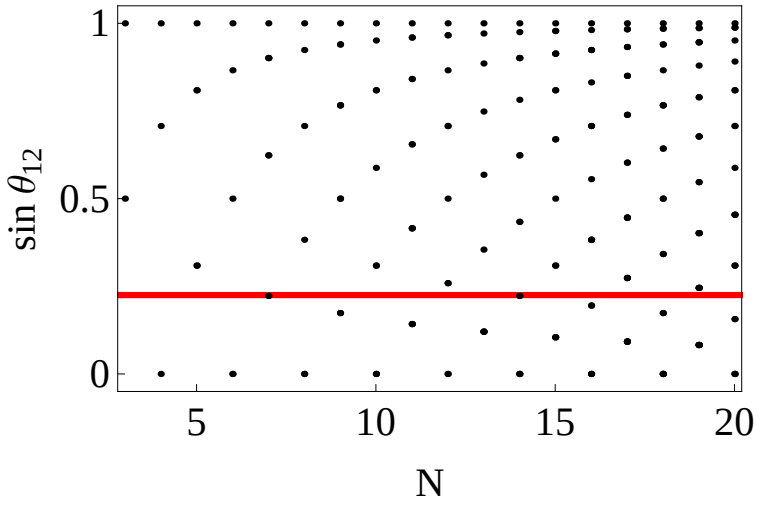

Figure 8.2: $\sin\theta_{12}$ versus N are plotted. N is the number of $\Delta(6N^2)$ that is taken from 3 to 20. The continuous line describes the experimental value, $\sin\theta_{12} = 0.225$.

Thus, the $\Delta(6N^2)$ with $N = 7r$ seems favorable. Figure 6 shows $\sin\theta_{12}$ for several values of N and $x - y$.

Next, we consider mixing angles of the lepton sector by using other group elements. We find that Z_3 elements are useful to explain large mixing angles of leptons. Through the similar discussion of Z_2, all the Z_3 elements of the group are explicitly written in the form of

$$\begin{gathered} a^{\alpha N/3}\,, \qquad a'^{\alpha N/3}\,, \qquad a^{\alpha N/3}a'^{\beta N/3}\,, \\ ba^x a'^y\,, \qquad b^2 a^x a'^y\,, \end{gathered} \tag{8.29}$$

where $\alpha, \beta = 0, 1, 2$, and $N/3$ is assumed to be integer. This time, we take the charged lepton Z_3 symmetry as $T' \equiv ba^{-x}a'^{-x-y}$. This representation can be written and diagonalized by

$$T' = \begin{pmatrix} 0 & \rho^{-y} & 0 \\ 0 & 0 & \rho^{x+y} \\ \rho^{-x} & 0 & 0 \end{pmatrix} = U_{T'} \begin{pmatrix} 1 & 0 & 0 \\ 0 & \omega & 0 \\ 0 & 0 & \omega^2 \end{pmatrix} U_{T'}^\dagger\,, \tag{8.30}$$

$$U_{T'} = \frac{1}{\sqrt{3}} \begin{pmatrix} \rho^x & \omega\rho^x & \omega^2\rho^x \\ \rho^{x+y} & \omega^2\rho^{x+y} & \omega\rho^{x+y} \\ 1 & 1 & 1 \end{pmatrix}\,, \tag{8.31}$$

[1]As discussed before, we need two Z_2 symmetries to uniquely determine the U_S and U_T, respecitvely. Here, we assume that the diagonal third element in each S and T is not mixed with another eigenvector with eigenvalue -1.

where $\omega = e^{2\pi i/3}$. For the neutrino Z_2 symmetry, we choose $S' \equiv b^2 c a'^{x'}$ so that

$$S' = \begin{pmatrix} -1 & 0 & 0 \\ 0 & 0 & -\rho^{-x'} \\ 0 & -\rho^{x'} & 0 \end{pmatrix} = U_{S'} \begin{pmatrix} 1 & 0 & 0 \\ 0 & -1 & 0 \\ 0 & 0 & -1 \end{pmatrix} U_{S'}^\dagger \,, \tag{8.32}$$

$$U_{S'} = \begin{pmatrix} 0 & 1 & 0 \\ -\rho^{-x'}/\sqrt{2} & 0 & 1/\sqrt{2} \\ 1/\sqrt{2} & 0 & \rho^{x'}/\sqrt{2} \end{pmatrix} . \tag{8.33}$$

Then the mixing matrix of the lepton sector becomes

$$U_{\rm PMNS} \,=\, U_{T'}^\dagger U_{S'} \,=\, \begin{pmatrix} \frac{1-\rho^{-x-y-x'}}{\sqrt{6}} & \frac{\rho^{-x}}{\sqrt{3}} & \frac{\rho^{-x-y}+\rho^{x'}}{\sqrt{6}} \\ \frac{1-\omega\rho^{-x-y-x'}}{\sqrt{6}} & \frac{\omega^2\rho^{-x}}{\sqrt{3}} & \frac{\omega\rho^{-x-y}+\rho^{x'}}{\sqrt{6}} \\ \frac{1-\omega^2\rho^{-x-y-x'}}{\sqrt{6}} & \frac{\omega\rho^{-x}}{\sqrt{3}} & \frac{\omega^2\rho^{-x-y}+\rho^{x'}}{\sqrt{6}} \end{pmatrix} . \tag{8.34}$$

The same mixing matrix has been analyzed by [53, 54] and it predicts the sum rules $\theta_{23} \approx 45^\circ \mp \theta_{13}/\sqrt{2}$. Also, it realizes the trimaximal mixing $\sin^2\theta_{12} \approx 1/3$ for small θ_{13}. In particular, since $\sin\theta_{13}$ can be written as

$$\sin\theta_{13} = \sqrt{\frac{2}{3}} \cos\left[\frac{\pi(x+y+x')}{N}\right] , \tag{8.35}$$

small θ_{13} is realized by $(x+y+x')/N \approx 1/2$. When $N = 7$ and $x+y+x' = 3$, we have

$$\sin^2 2\theta_{13} = 0.128 \,, \tag{8.36}$$

which is close to the experimental value. As a result, the $\Delta(6N^2)$ for $N = 7r$ is interesting to realize the mixing angles for both the quark and lepton sectors.

Chapter 9

Summary

In this thesis, we first review the fundamental topics about the SM, neutrino mass and lepton mixing. Then, we discuss relations between the lepton mixing and a flavor symmetry to generate the tri-bimaximal PMNS matrix and review on a simple model with A_4 flavor symmetry breaking as an example.

For searching flavor symmetries to generate patterns near to the experiments, we review the model-independent formalism, which was recently developed by Hernandez and Smirnov. We revisit their results and derive some additional results. Especially, by applying their method to a $Z_2 \times Z_2$ Klein group, we confirm all the patterns generated by flavor symmetries from $(n,\, p_1,\, p_2,\, p_3) = (3,\, 2,\, 2,\, 2)$ to $(8,\, 8,\, 8,\, 8)$.

Next, we have applied the Hernandez-Smirnov method to the quark sector and sought possible residual symmetries with a focus on the von Dyck groups. In the case of $\theta_{13} = \theta_{23} = 0$, the Cabibbo angle θ_{12} can be close to its experimental values for small n, m, and p. In particular, the combination between the Z_2 and Z_7 symmetries seems favorable to realize the realistic value of θ_{12}. Furthermore, these residual symmetries can orginate from finite groups such as D_N and $\Delta(6N^2)$ with $N = 7r$.

We have also discussed possibilities of embedding the obtained residual symmetries into the $\Delta(6N^2)$ series. It is found that $\Delta(6N^2)$ for $N = 7r$ would be favorable to realize the Cabibbo angle and also interesting from the viewpoint of the mixing angles for the lepton sector.

On the other hand, in the sense of GUT, we have discussed special cases that some residual symmetries in the lepton sector and the quark sector are the same. By searching flavor symmetries, we find some favorable patterns for both the PMNS matrix and the Cabibbo angle, which could be used for models of GUT.

In contrast, relatively large n, m, and p are needed in order to reproduce all the quark mixing parameters at the same time. The von Dyck groups with such large integers correspond to not finite groups, but infinite ones. However, they may be embedded into finite subgroups of infinite von Dyck groups (see e.g. Ref. [40]). The work is in progress, and we would like to postpone this issue to our next study. At any rate, we have shown which combinations of residual symmetries lead to favorable results. That can become a starting point to investigate the full flavor symmetry hiding behind the quark and lepton mass matrices.

Acknowledgements

I would like to thank Tatsuo Kobayashi for his great support to my study from my master's course. Also I would like to thank Hajime Ishimori, Takeshi Araki and Hiroyuki Ishida for collaborating with me. I have frequently put Hiroyuki Hata, a supervisor, to trouble. I appreciate it. I would like to thank Humihiro Takayama, Yuta Hamada, Daiki Yasuhara for useful discussions. This work was supported in part by the Grant-in-Aid for Scientific Research No. 25.1146 from the Ministry of Education, Culture, Sports, Science and Technology of Japan.

Appendix A

Non-Abelian Discrete Symmetries

In the appendix, following Ref. [17], we list properties of non-Abelian discrete symmetries such as A_4, S_4, $\Delta(6N^2)$, $PSL(2, Z_7)$ and the von Dyck group.

A.1 S_N, A_N

S_N is defined by permutations of N components, and A_N is defined by all elements of even permutations in S_N. For, example, S_3 include permutations of the triplet (x_1, x_2, x_3) as follows

$$\begin{aligned} a_1 &\quad (x_1, x_2, x_3) \to (x_2, x_1, x_3) \\ a_2 &\quad (x_1, x_2, x_3) \to (x_3, x_2, x_1) \\ a_3 &\quad (x_1, x_2, x_3) \to (x_1, x_3, x_2) \end{aligned}$$

$$\begin{aligned} a_4 &\quad (x_1, x_2, x_3) \to (x_3, x_1, x_2) \\ a_5 &\quad (x_1, x_2, x_3) \to (x_2, x_3, x_1) \\ e &\quad (x_1, x_2, x_3) \to (x_1, x_2, x_3) \end{aligned}$$

where the upper three a_1, a_2, a_3 are the odd permutations while the lower three a_4, a_5, e are the even permutations. Then, by definition, A_3 is generated by the $\{a_4, a_5, e\}$. However, as $a_4^2 = a_5$, $a_4^3 = e$ the A_3 is Abelian symmetry and equal to the Z_3 symmetry. Therefore, it is known that the smallest non-Abelian group is A_4.

A.1.1 S_4

S_4 is the permutations of (x_1, x_2, x_3, x_4) such as

$$(x_1, x_2, x_3, x_4) \to (x_i, x_j, x_k, x_l)\,. \tag{A.1}$$

The number of the elements is $4! = 24$. Under the transformation Eq. (A.1), $x_1 + x_2 + x_3 + x_4$ behaves as a trivial singlet. Then, we can extend other representations in the

orthogonal space of $x_1 + x_2 + x_3 + x_4$, which span in the three dimensional space,

$$\begin{pmatrix} x_1 + x_2 - x_3 - x_4 \\ x_1 - x_2 + x_3 - x_4 \\ x_1 - x_2 - x_3 + x_4 \end{pmatrix} \tag{A.2}$$

Therefore, repsentations of S_4 are in the triplet space. The detail of S_4 is discussed in later.

A.1.2 A_4

A_4 is constrcuted by elements of even permutations in S_4. Using the representation of Eq. (A.2), all the $24/2 = 12$ elements in A_4 are written down by

$$\begin{gathered} a_1 = \begin{pmatrix} 1 & 0 & 0 \\ 0 & 1 & 0 \\ 0 & 0 & 1 \end{pmatrix}, \quad a_2 = \begin{pmatrix} 1 & 0 & 0 \\ 0 & -1 & 0 \\ 0 & 0 & -1 \end{pmatrix}, \quad a_3 = \begin{pmatrix} -1 & 0 & 0 \\ 0 & 1 & 0 \\ 0 & 0 & -1 \end{pmatrix}, \\ a_4 = \begin{pmatrix} -1 & 0 & 0 \\ 0 & -1 & 0 \\ 0 & 0 & 1 \end{pmatrix}, \quad b_1 = \begin{pmatrix} 0 & 0 & 1 \\ 1 & 0 & 0 \\ 0 & 1 & 0 \end{pmatrix}, \quad b_2 = \begin{pmatrix} 0 & 0 & 1 \\ -1 & 0 & 0 \\ 0 & -1 & 0 \end{pmatrix}, \\ b_3 = \begin{pmatrix} 0 & 0 & -1 \\ 1 & 0 & 0 \\ 0 & -1 & 0 \end{pmatrix}, \quad b_4 = \begin{pmatrix} 0 & 0 & -1 \\ -1 & 0 & 0 \\ 0 & 1 & 0 \end{pmatrix}, \quad c_1 = \begin{pmatrix} 0 & 1 & 0 \\ 0 & 0 & 1 \\ 1 & 0 & 0 \end{pmatrix}, \\ c_2 = \begin{pmatrix} 0 & 1 & 0 \\ 0 & 0 & -1 \\ -1 & 0 & 0 \end{pmatrix}, \quad c_3 = \begin{pmatrix} 0 & -1 & 0 \\ 0 & 0 & 1 \\ -1 & 0 & 0 \end{pmatrix}, \quad c_4 = \begin{pmatrix} 0 & -1 & 0 \\ 0 & 0 & -1 \\ 1 & 0 & 0 \end{pmatrix} \end{gathered} \tag{A.3}$$

It is known that the above elements are generated by the following relations,

$$S^2 = T^3 = (ST)^3 = 1\,, \tag{A.4}$$

where $S = a_2$, $T = b_1$. In other words, A_4 symmetry can be regarded as a symmetry in tetrahedron, which is sketched in Figure A.1.

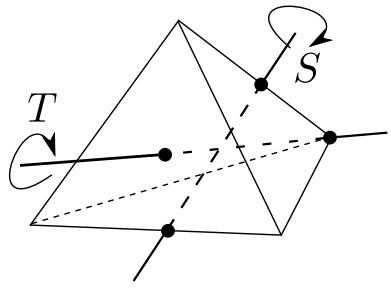

Figure A.1: The A_4 symmetry is sketched in a tetrahedron. $T \in Z_3$ and $S \in Z_2$.

Let us find all the irreducible representations of A_4. First, we consider the conjugacy class, which is defined by the group of elements generated from $a \in G$ through $\{g^{-1}ag,\ g \in G\}$, i.e. the conjugate of a. The elements in the same conjugacy class have the same character, $\chi_D \equiv \mathrm{tr}D(g)$, where the $D(g)$ is a representation of $g \in G$. Then, the elements of Eq. (A.3) are classified in Table A.1. The h is called "order", which represents that

name	elements	order
C_1	$\{a_1\}$	$h = 1$
C_3	$\{a_2,\ a_3,\ a_4\}$	$h = 2$
C_4	$\{b_1,\ b_2,\ b_3,\ b_4\}$	$h = 3$
C_4'	$\{c_1,\ c_2,\ c_3,\ c_4\}$	$h = 3$

Table A.1: The conjugacy classes of A_4.

$a^h = 1$. The number of the conjugacy class is the same as the number of the irreducible representation. Then,

$$\sum_n m_n = m_1 + m_2 + m_3 + \cdots = 4\,, \tag{A.5}$$

where m_n is the number of n dimensional irreducible representations, On the other hand, the orthogonality gives a relation on the character as the following

$$\sum_\alpha \chi_{D_\alpha}(g_i)^* \chi_{D_\alpha}(g_j) = \frac{N_G}{n_i}\delta_{C_iC_j}\,, \tag{A.6}$$

where n_i is the number of the elements in the conjugacy class C_i, and N_G is the number of elements in G. We can get a requirement on m_n by considering

$$\sum_\alpha |\chi_\alpha(C_1)|^2 = \sum_n m_n n^2 = m_1 + 4m_2 + 9m_3 + \cdots = 12\,. \tag{A.7}$$

From Eq. (A.5) and Eq. (A.7), we find $(m_1,\ m_2,\ m_3) = (3,\ 0,\ 1)$.

A brief sketch of proof to the above number relations

The story of the proof on the orthogonality relation Eq. (A.6) and the sum rule Eq. (A.5) are the following. We consider

$$A_{\alpha\beta} \equiv \sum_{a\in G} D_\alpha(a) B D_\beta(a^{-1})\,. \tag{A.8}$$

In the matrix representation, B is a $d_\alpha \times d_\beta$ matrix. We find that

$$D(g)A_{\alpha\alpha} = A_{\alpha\alpha}D(g) \qquad \forall g \in G\,, \tag{A.9}$$

$$D_\alpha(g)A_{\alpha\beta} = A_{\alpha\beta}D_\beta(g) \qquad \forall g \in G\,. \tag{A.10}$$

Using the Shur's lemma, they imply that $A_{\alpha\beta}$ is proportional to the identity matrix iff $\alpha = \beta$, and otherwise 0. Inserting $B = \delta_{il}\delta_{jm}$,

$$\sum_{a\in G} D_\alpha(a)_{il} D_\beta(a^{-1})_{mj} = \lambda(l,m)\delta_{\alpha\beta}\delta_{ij}\,, \tag{A.11}$$

By considering the trace, λ is determined by

$$\lambda(l,\,m) = \frac{\sum_{a\in G} D_\alpha(aa^{-1})_{lm}}{\mathrm{tr}\delta_{ij}} = \frac{N_G\delta_{lm}}{d_\alpha}\,. \tag{A.12}$$

The equality of the number of conjugacy classes and irreducible representations is proved by considering the class function $F(a) \quad \{F(g^{-1}ag) = F(a)\,, \quad \forall g \in G\}$ expanded in terms of the irreducible representations.

$$\begin{aligned} F(a) &= \frac{1}{N_G}\sum_{g\in G}\sum_{\alpha,j,l} c^\alpha_{j,k}(D_\alpha(g^{-1})D_\alpha(a)D_\alpha(g))_{jk} \\ &= \sum_{\alpha,j,k} c^\alpha_{j,j} D_\alpha(a)_{ll} = \sum_{\alpha,j}\frac{1}{d_\alpha} c^\alpha_{j,j}\chi_\alpha(a)\,. \end{aligned} \tag{A.13}$$

At the first equality on the second line, we use the orthogonal relation (A.11). The equation implies that any class function $F(a)$, which is constant in each conjugacy classes, are expanded by the characters $\chi_\alpha(a)$. To realize the situation, the number of α must be the same to the number of conjugacy classes. Therefore, the equality of the number of conjugacy classes and irreducible representations is proved.

Then, back to Eq. (A.11), setting $l = i$, $m = j$ and summing over i, j, we find the orthogonality relation over the characters,

$$\sum_{g\in G} \chi_{D_\alpha}(g)^*\chi_{D_\beta}(g) = N_G\delta_{\alpha\beta}\,. \tag{A.14}$$

As we know that the number of conjugacy classes and irreducible representations are the same, we rewrite Eq. (A.14) by the following squre matrix $V_{i\alpha}$

$$V_{i\alpha} = \sqrt{\frac{n_i}{N_G}}\chi_\alpha(C_i)\,, \tag{A.15}$$

$$V^\dagger V = V^*_{\alpha i}V_{i\beta} = 1\,, \tag{A.16}$$

where n_i is the number of the elements of the conjugacy class C_i. It leads to $VV^\dagger = 1$, which is exactly Eq. (A.6).

□

As we derive the species of representations, we next discuss the specific matrix representations. The triplet representation **3** is just Eq. (A.3). The three singlet representations can be derived from Eq. (A.4). We call them as **1**, **1′**, **1″**, respectively. Before deriving

name	elements
C_1	$\{e\}$
C_3	$\{S,\, TST^2,\, T^2ST\}$
C_4	$\{T,\, TS,\, ST,\, STS\}$
C_4'	$\{T^2,\, ST^2,\, T^2S,\, TST\}$

Table A.2: Elements of A_4 in terms of S and T.

singlet	S	T
$\mathbf{1}$	1	1
$\mathbf{1}'$	1	ω
$\mathbf{1}''$	1	ω^2

Table A.3: 1 dimensional representations of A_4.

representations of singlets, we classify the conjugacy class in terms of t and s by using known triplet representation. The result is in Table A.2. As the conjugacy class is independent of representations, we can find the singlets with considering the above table. From $S^2 = 1$, $S = \pm 1$. As T and TS are in the same C_4, it is found that $S = 1$ in all singlets. T could be 1, ω, ω^2, all are consistent to the conjugacy class. Then, all $\mathbf{1}$, $\mathbf{1}'$, $\mathbf{1}''$ are written down in Table A.3. Characters depend on the representations. We list in Table A.4.

	C_1	C_3	C_4	C_4'
$\chi_{\mathbf{1}}$	1	1	1	1
$\chi_{\mathbf{1}'}$	1	1	ω	ω^2
$\chi_{\mathbf{1}''}$	1	1	ω^2	ω
$\chi_{\mathbf{3}}$	3	-1	0	0

Table A.4: Characters of A_4.

name	elements	order
C_1	$\{a_1\}$	$h=1$
C_3	$\{a_2,\, a_3,\, a_4\}$	$h=2$
C_6	$\{d_1,\, d_2,\, e_1,\, e_4,\, f_1,\, f_3\}$	$h=2$
C_8	$\{b_1,\, b_2,\, b_3,\, b_4,\, c_1,\, c_2,\, c_3,\, c_4\}$	$h=3$
C_6'	$\{d_3,\, d_4,\, e_2,\, e_3,\, f_2,\, f_4\}$	$h=4$

Table A.5: The conjugacy classes of S_4.

A.1.3 Properties of S_4

The elements of S_4 are Eq. (A.3) and the following 12 matrices,

$$
\begin{aligned}
d_1 &= \begin{pmatrix} 1 & 0 & 0 \\ 0 & 0 & 1 \\ 0 & 1 & 0 \end{pmatrix}, \quad
d_2 = \begin{pmatrix} 1 & 0 & 0 \\ 0 & 0 & -1 \\ 0 & -1 & 0 \end{pmatrix}, \quad
d_3 = \begin{pmatrix} -1 & 0 & 0 \\ 0 & 0 & 1 \\ 0 & -1 & 0 \end{pmatrix}, \\
d_4 &= \begin{pmatrix} -1 & 0 & 0 \\ 0 & 0 & -1 \\ 0 & 1 & 0 \end{pmatrix}, \quad
e_1 = \begin{pmatrix} 0 & 1 & 0 \\ 1 & 0 & 0 \\ 0 & 0 & 1 \end{pmatrix}, \quad
e_2 = \begin{pmatrix} 0 & 1 & 0 \\ -1 & 0 & 0 \\ 0 & 0 & -1 \end{pmatrix}, \\
e_3 &= \begin{pmatrix} 0 & -1 & 0 \\ 1 & 0 & 0 \\ 0 & 0 & -1 \end{pmatrix}, \quad
e_4 = \begin{pmatrix} 0 & -1 & 0 \\ -1 & 0 & 0 \\ 0 & 0 & 1 \end{pmatrix}, \quad
f_1 = \begin{pmatrix} 0 & 0 & 1 \\ 0 & 1 & 0 \\ 1 & 0 & 0 \end{pmatrix}, \\
f_2 &= \begin{pmatrix} 0 & 0 & 1 \\ 0 & -1 & 0 \\ -1 & 0 & 0 \end{pmatrix}, \quad
f_3 = \begin{pmatrix} 0 & 0 & -1 \\ 0 & 1 & 0 \\ -1 & 0 & 0 \end{pmatrix}, \quad
f_4 = \begin{pmatrix} 0 & 0 & -1 \\ 0 & -1 & 0 \\ 1 & 0 & 0 \end{pmatrix}. \qquad \text{(A.17)}
\end{aligned}
$$

The conjugacy classes and their order are in Table A.5. The relations of orthogonality and the total number of the conjugacy classes are written by

$$m_1 + 4m_2 + 9m_3 + \cdots = 24\,, \qquad \text{(A.18)}$$

$$m_1 + m_2 + m_3 + \cdots = 5\,. \qquad \text{(A.19)}$$

The solution of the above equations is $(m_1,\, m_2,\, m_3) = (2,\, 1,\, 2)$. Therefore, the representations of S_4 are two singlets $\mathbf{1}$, $\mathbf{1'}$, a doublet $\mathbf{2}$ and two triplets $\mathbf{3}$, $\mathbf{3'}$.

As examples, some of the elements of representation $\mathbf{2}$ are written down in the following

$$
\begin{aligned}
a_2 &= \begin{pmatrix} 1 & 0 \\ 0 & 1 \end{pmatrix}, \quad
b_1 = \begin{pmatrix} \omega & 0 \\ 0 & \omega^2 \end{pmatrix}, \\
d_1 &= d_3 = d_4 = \begin{pmatrix} 0 & 1 \\ 1 & 0 \end{pmatrix}. \qquad \text{(A.20)}
\end{aligned}
$$

	C_1	C_3	C_6	C'_6	C_8
$\chi_{\mathbf{1}}$	1	1	1	1	1
$\chi_{\mathbf{1'}}$	1	1	-1	-1	1
$\chi_{\mathbf{2}}$	2	2	0	0	-1
$\chi_{\mathbf{3}}$	3	-1	1	-1	0
$\chi_{\mathbf{3'}}$	3	-1	-1	1	0

Table A.6: Characters of S_4.

Some elements of the representation $\mathbf{3'}$ are

$$a_2 = \begin{pmatrix} 1 & 0 & 0 \\ 0 & -1 & 0 \\ 0 & 0 & -1 \end{pmatrix}, \qquad b_1 = \begin{pmatrix} 0 & 0 & 1 \\ 1 & 0 & 0 \\ 0 & 1 & 0 \end{pmatrix},$$
$$d_1 = \begin{pmatrix} -1 & 0 & 0 \\ 0 & 0 & -1 \\ 0 & -1 & 0 \end{pmatrix}, \qquad d_3 = \begin{pmatrix} 1 & 0 & 0 \\ 0 & 1 & 0 \\ 0 & 0 & -1 \end{pmatrix}, \qquad d_4 = \begin{pmatrix} 1 & 0 & 0 \\ 0 & -1 & 0 \\ 0 & 0 & 1 \end{pmatrix}. \tag{A.21}$$

Differences between $\mathbf{3}$ and $\mathbf{3'}$ come from the overall phase of d_4. The elements of the representation $\mathbf{3}$ are in Eq. (A.17). The characters of S_4 are listed in Table A.6.

A.2 $\Delta(6N^2)$

$\Delta(6N^2)$ is the discrete group, which is isomorphic to $(Z_N \times Z'_N) \rtimes S_3$. The number of the elements is $6N^2$. We define the generators as follows,

$$a \in Z_N\,, \qquad a' \in Z'_N\,, \qquad b \in Z_3 \qquad c \in Z_2\,. \tag{A.22}$$

The algebraic relations are given by

$$\begin{gathered} a^N = a'^N = b^3 = c^2 = (bc)^2 = e\,, \\ aa' = a'a\,, \\ bab^{-1} = a^{-1}a'^{-1}\,, \qquad ba'b^{-1} = a\,, \\ cac^{-1} = a'^{-1}\,, \qquad ca'c^{-1} = a^{-1}\,. \end{gathered} \tag{A.23}$$

The elements of $\Delta(6N^2)$ are derived by $g = b^k c^l a^m a'^m$.

In this thesis, we consider the case that $N \neq 3Z$. The conjugacy classes are in the Table A.7 [52]. Note that in Table A.7, C_3^z with $z = 0$ reduces to C_1, and $C_6^{x,y}$ with $\{x \equiv -y,\, 2x \equiv y,\, x \equiv 2y \pmod N\}$ are identified to C_3^z or C_1. The sum of the irreducible representations is

$$\begin{aligned} m_1 + m_2 + m_3 + \cdots &= 1 + \frac{N^2 - 3(N-1) - 1}{6} + (N-1) + 1 + N \\ &= \frac{N^2 - 3N + 2}{6} + 2N + 1\,. \end{aligned} \tag{A.24}$$

Name	Elements
C_1	$\{e\}$
$C_6^{x,y}$	$\{a^x a'^y,\ a^{y-x}a'^{-x},\ a^{-y}a'^{x-y},\ a^{-y}a'^{-x},\ a^{y-x}a'^{y},\ a^x a'^{x-y}\}$
C_3^z	$\{a^z a'^z,\ a^{-2z}a'^{-z},\ a^z a'^{2z}\}$
C_{4N^2}	$\{ba^p a'^q,\ b^2 a^{-q}a'^{-p} \mid (p,\ q) = 0, 1, \cdots, N-1\}$
C_{9N}^w	$\{ca^{w+p}a'^p,\ b^2 ca^{-w}a'^{-p-w},\ bca^{-p}a'^w \mid p = 0, 1, \cdots, N-1\}$

Table A.7: Th conjugacy classes of $\Delta(6N^2)$ $(N \neq 3Z)$. $(x, y, z, w) = \{0, 1, \cdots, N-1\}$.

From the relation between the number of irreducible representations and the number of elements,

$$m_1 + 2^2 m_2 + 3^2 m_3 + \cdots = 6N^2\,. \tag{A.25}$$

It is found that the solution of Eq. (A.24) and Eq. (A.25) is $(m_1,\ m_2,\ m_3,\ m_6) = (2,\ 1,\ 2(N-1),\ \frac{(N-1)(N-2)}{6})$. Then, the irreducible representations are two singlets $\mathbf{1}$, $\mathbf{1}'$, a doublet $\mathbf{2}$, $2(N-1)$ tripletes $\mathbf{3}_j$, $\mathbf{3}'_j$ and $\frac{(N-1)(N-2)}{6}$ of 6 dimensional representations $\mathbf{6}_{j,k}$. One singlet $\mathbf{1}$ is written by $a = a' = b = c = 1$, and another singlet $\mathbf{1}'$ is $a = a' = b = 1$, $c = -1$. The doublet $\mathbf{2}$ representation is

$$a = a' = \begin{pmatrix} 1 & 0 \\ 0 & 1 \end{pmatrix}, \qquad b = \begin{pmatrix} \omega & 0 \\ 0 & \omega^2 \end{pmatrix}, \qquad c = \begin{pmatrix} 0 & 1 \\ 1 & 0 \end{pmatrix}. \tag{A.26}$$

The triplet representations $\mathbf{3}_j$ is the following

$$a = \begin{pmatrix} e^{2\pi i \frac{j}{N}} & 0 & 0 \\ 0 & e^{-2\pi i \frac{j}{N}} & 0 \\ 0 & 0 & 1 \end{pmatrix}, \qquad a' = \begin{pmatrix} 1 & 0 & 0 \\ 0 & e^{2\pi i \frac{j}{N}} & 0 \\ 0 & 0 & e^{-2\pi i \frac{j}{N}} \end{pmatrix} \tag{A.27}$$

$$b = \begin{pmatrix} 0 & 1 & 0 \\ 0 & 0 & 1 \\ 1 & 0 & 0 \end{pmatrix}, \qquad c = \begin{pmatrix} 0 & 0 & 1 \\ 0 & 1 & 0 \\ 1 & 0 & 0 \end{pmatrix}, \tag{A.28}$$

where $j = 1, 2, \cdots, N-1$. The other triplets $\mathbf{3}'_j$ are the same as $\mathbf{3}_j$ except for the sign of the b i.e. $b(\mathbf{3}'_j) = -b(\mathbf{3}_j)$. The 6 dimensional representations $\mathbf{6}_{j,k}$ is written by

$$a = \begin{pmatrix} a_1 & 0 \\ 0 & a_2 \end{pmatrix}, \qquad a' = \begin{pmatrix} a_2^{-1} & 0 \\ 0 & a_1^{-1} \end{pmatrix}, \qquad b = \begin{pmatrix} b_1 & 0 \\ 0 & b_2 \end{pmatrix}, \qquad c = \begin{pmatrix} 0 & 1 \\ 1 & 0 \end{pmatrix}, \tag{A.29}$$

where

$$a_1 = \begin{pmatrix} e^{2\pi i \frac{j}{N}} & 0 & 0 \\ 0 & e^{2\pi i \frac{k}{N}} & 0 \\ 0 & 0 & e^{-2\pi i \frac{j+k}{N}} \end{pmatrix}, \qquad a_2 = \begin{pmatrix} e^{2\pi i \frac{j+k}{N}} & 0 & 0 \\ 0 & e^{-2\pi i \frac{j}{N}} & 0 \\ 0 & 0 & e^{-2\pi i \frac{k}{N}} \end{pmatrix}, \tag{A.30}$$

$$b_1 = \begin{pmatrix} 0 & 1 & 0 \\ 0 & 0 & 1 \\ 1 & 0 & 0 \end{pmatrix}, \qquad b_2 = \begin{pmatrix} 0 & 0 & 1 \\ 1 & 0 & 0 \\ 0 & 1 & 0 \end{pmatrix}, \tag{A.31}$$

name	typical element	number of elements	order
C_1	1	1	$h = 1$
C_2	S	21	$h = 2$
C_3	T	56	$h = 3$
C_4	$S^{-1}T^{-1}ST$	42	$h = 4$
C_5	ST	24	$h = 7$
C_6	ST^2	24	$h = 7$

. (A.34)

Table A.8: The conjugacy classes of $PSL(2, Z_7)$.

where $(j, k) = 1, 2, \cdots, N-1$. Note that the above representation is reducible if $j \equiv k$ or ($j \equiv 0$, $k \not\equiv 0$) or ($k \equiv 0$, $j \not\equiv 0$) under mod N. Moreover, there are duplication of the representations. The representations of exchanging (j, k) as $\{(-j-k, j), (k, -j-k), (-k, -j), (j+k, -k), (-j, j+k)\}$ lead to the same irreducible representation. Omitting these defective ones, we obtain all representations of $\Delta(6N^2)$.

A.3 $PSL(2, Z_7)$

Properties of $PSL(2, Z_7)$ are listed in Ref. [10].

The algebraic relations of $PSL(2, Z_7)$ are written by

$$S^2 = T^3 = (ST)^7 = (S^{-1}T^{-1}ST)^4 = 1\,. \tag{A.32}$$

We can find a 2-dimensional representation with the following generators

$$S = \begin{pmatrix} 0 & -1 \\ 1 & 0 \end{pmatrix}\,, \qquad T = \begin{pmatrix} 0 & -1 \\ 1 & 1 \end{pmatrix}\,. \tag{A.33}$$

By calculating all 168 elements from S and T, we can find six conjugacy classes in Table A.8. Then, from the following relations of the orthogonality and conjugacy classes,

$$m_1 + 4m_2 + 9m_3 + \cdots = 168\,, \tag{A.35}$$

$$m_1 + m_2 + m_3 + \cdots = 6\,, \tag{A.36}$$

we find the solutions as (m_1, m_3, m_6, m_7, m_8) = (1, 2, 1, 1, 1).

The characters of $PSL(2, Z_7)$ is listed in Table A.9. In Table A.9,

$$b_7 = \frac{1}{2}(-1 + i\sqrt{7})\,, \qquad \bar{b}_7 = \frac{1}{2}(-1 - i\sqrt{7})\,, \tag{A.38}$$

which are following from the notation of "Atlas of Finite Groups" [55].

	C_1	C_2	C_3	C_4	C_5	C_6
$\chi_{\mathbf{1}}$	1	1	1	1	1	1
$\chi_{\mathbf{3}}$	3	-1	0	1	b_7	$\bar{b}_7$
$\chi_{\mathbf{3'}}$	3	-1	0	1	$\bar{b}_7$	b_7
$\chi_{\mathbf{6}}$	6	2	0	0	-1	-1
$\chi_{\mathbf{7}}$	7	-1	1	-1	0	0
$\chi_{\mathbf{8}}$	8	0	-1	0	1	1

, (A.37)

Table A.9: Characters of $PSL(2, Z_7)$.

Generators in the 3-dimensional representation **3** are explicitly written by

$$S = \frac{i}{\sqrt{7}} \begin{pmatrix} \eta^2 - \eta^5 & \eta - \eta^6 & \eta^4 - \eta^3 \\ \eta - \eta^6 & \eta^4 - \eta^3 & \eta^2 - \eta^5 \\ \eta^4 - \eta^3 & \eta^2 - \eta^5 & \eta - \eta^6 \end{pmatrix} , \tag{A.39}$$

$$T = \frac{i}{\sqrt{7}} \begin{pmatrix} \eta^3 - \eta^6 & \eta^3 - \eta & \eta - 1 \\ \eta^2 - 1 & \eta^6 - \eta^5 & \eta^6 - \eta^2 \\ \eta^5 - \eta^4 & \eta^4 - 1 & \eta^5 - \eta^3 \end{pmatrix} , \tag{A.40}$$

where $\eta \equiv e^{2\pi i/7}$. Generators of another 3-dimensional representation $\mathbf{3'}$ is written by the conjugates of Eq. (A.39) and Eq. (A.40).

A.4 von Dyck group

The von Dyck group is a discrete group generating from X, Y, Z satisfying the following relation,

$$X^p = Y^q = Z^r = XYZ = 1 \qquad p,\, q,\, r \in Z\,. \tag{A.41}$$

The algebraic relation is fundamentally equivalent to that of Eq. (5.13).

The von Dyck group can be regarded as a extension of the symmetry of regular polyhedrons in R^3. We define the number of edges, faces, vertices as e, f, v, and the number of symmetry elements of each as r_e, r_f, r_v, respectively. We consider the projection of the regular polyhedron to S^2, and also its barycentric subdivisions. The three vertices of a triangle of the barycentric subdivision correspond to the edge, face and vertex of a polyhedron, respectively. We focus on a triangle in S^2. We call three vertices of the triangle by $P(e)$, $P(f)$, $P(v)$ corresponding to the barycentric subdivision. In the barycentric subdivision, an angle around a vertex in a boundary is divided into $r_{e,f,v}$ equal parts. Then, the angles of the triangle with vertices $P(e)$, $P(f)$, $P(v)$ in S^2 are $\frac{\pi}{r_e}$, $\frac{\pi}{r_f}$, $\frac{\pi}{r_v}$. We introduce A_e, A_f, $A_v \in SO(3)$ as rotations around $P(e)$, $P(f)$, $P(v)$ by $\frac{\pi}{r_e}$, $\frac{\pi}{r_f}$, $\frac{\pi}{r_v}$. The As transfrom Ps to vertices in the other triangles and satisfy the relation

$$A_e^{r_e} = A_f^{r_f} = A_v^{r_v} = A_e A_v A_f = 1\,. \tag{A.42}$$

Then, we expand the situation and define Eq. (A.41) as the relation of the von Dyck group.

From the above discussion, the generators of the von Dyck group X, Y, Z seems to be rotations around points $P(X)$, $P(Y)$, $P(Z)$ in S^2 and form a triangle. In truth, that is correct only if

$$\frac{1}{p}+\frac{1}{q}+\frac{1}{r}>1\,. \tag{A.43}$$

We can derive the condition from evaluating the area of the triangle. For simplicity, we set $P(X)$, $P(Y)$ on the equator and $P(Z)$ in the upper hemisphere with radius R. By extending edges of the triangle, we can divide the area of the upper hemisphere into four regions as in Figure A.2. Summing the areas, we get

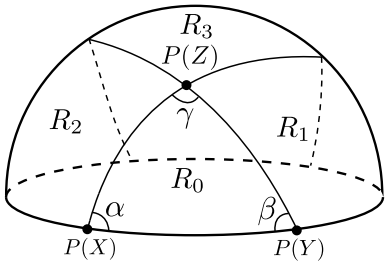

Figure A.2: The hemisphere is divided into four regions $R_{0,1,2,3}$. The angles α, β, γ are $\frac{\pi}{p}$, $\frac{\pi}{q}$, $\frac{\pi}{r}$, respectively.

$$\begin{aligned}2\pi R^2 &= \sigma(R_0)+\sigma(R_1)+\sigma(R_2)+\sigma(R_3)\\ &= \sigma(R_0)+(2\frac{\pi}{p}R^2-\sigma(T))+(2\frac{\pi}{q}R^2-\sigma(T))+(2\frac{\pi}{r}R^2-\sigma(T))\end{aligned} \tag{A.44}$$

It leads

$$\sigma(T)=(\frac{\pi}{p}+\frac{\pi}{q}+\frac{\pi}{r}-\pi)R^2>0\,. \tag{A.45}$$

The last inequality comes from the positivity of the area. Therefore, the von Dyck group must satisfy Eq. (A.43) if it could embed into S^2.

The sets of $(p,\,q,\,r)$ satisfying Eq. (A.43) can be written down as

$$(p,\,q,\,r)=(2,\,2,\,n),\,(2,\,3,\,3),\,(2,\,3,\,4),\,(2,\,3,\,5)\,, \tag{A.46}$$

and their exchanges. All the regular polyhedrons are included in the above list Eq. (A.46). We list the polyhedrons in Table A.10. The von Dyck group with

$$\frac{1}{p}+\frac{1}{q}+\frac{1}{r}\leq 0\,. \tag{A.48}$$

is infinite group [56].

Name	$(r_e,\, r_f,\, r_v)$	$(e,\, f,\, v)$	order
Dihedral	(2,n,2)		
Tetrahedron	(2,3,3)	(6,4,4)	12
Cube	(2,4,3)	(12,6,8)	24
Octahedron	(2,3,4)	(12,8,6)	24
Icosahedron	(2,3,5)	(30,20,12)	60
Dodecahedron	(2,5,3)	(30,12,20)	60

(A.47)

Table A.10: List of polyhedrons.

Bibliography

[1] G. Aad *et al.* [ATLAS Collaboration], Phys. Lett. B **716**, 1 (2012) [arXiv:1207.7214 [hep-ex]]; S. Chatrchyan *et al.* [CMS Collaboration], Phys. Lett. B **716**, 30 (2012) [arXiv:1207.7235 [hep-ex]].

[2] J. Beringer et al. (Particle Data Group), Phys. Rev. D **86**, 010001 (2012).

[3] P. F. Harrison, D. H. Perkins and W. G. Scott, Phys. Lett. B **530**, 167 (2002) [arXiv:hep-ph/0202074]; Z. Z. Xing, Phys. Lett. B **533**, 85 (2002) [arXiv:hep-ph/0204049]; P. F. Harrison and W. G. Scott, Phys. Lett. B **535**, 163 (2002) [arXiv:hep-ph/0203209]; Phys. Lett. B **557** (2003) 76 [arXiv:hep-ph/0302025].

[4] W. Grimus, A. S. Joshipura, S. Kaneko, L. Lavoura and M. Tanimoto, JHEP **0407**, 078 (2004) [hep-ph/0407112].

[5] A. Blum, C. Hagedorn and M. Lindner, Phys. Rev. D **77**, 076004 (2008) [arXiv:0709.3450 [hep-ph]].

[6] J. Kubo, A. Mondragon, M. Mondragon and E. Rodriguez-Jauregui, Prog. Theor. Phys. **109**, 795 (2003) [Erratum-ibid. **114**, 287 (2005)] [hep-ph/0302196].

[7] R. N. Mohapatra, M. K. Parida and G. Rajasekaran, Phys. Rev. D **69**, 053007 (2004) [hep-ph/0301234].

[8] E. Ma and G. Rajasekaran, Phys. Rev. D **64**, 113012 (2001) [hep-ph/0106291].

[9] P. H. Frampton and T. W. Kephart, Int. J. Mod. Phys. A **10**, 4689 (1995) [hep-ph/9409330].

[10] C. Luhn, S. Nasri and P. Ramond, J. Math. Phys. **48**, 123519 (2007) [arXiv:0709.1447 [hep-th]].

[11] S. F. King and C. Luhn, Nucl. Phys. B **820**, 269 (2009) [arXiv:0905.1686 [hep-ph]]; S. F. King and C. Luhn, Nucl. Phys. B **832**, 414 (2010) [arXiv:0912.1344 [hep-ph]].

[12] L. L. Everett and A. J. Stuart, Phys. Rev. D **79**, 085005 (2009) [arXiv:0812.1057 [hep-ph]].

[13] C. Luhn, S. Nasri and P. Ramond, Phys. Lett. B **652**, 27 (2007) [arXiv:0706.2341 [hep-ph]].

[14] I. de Medeiros Varzielas, S. F. King and G. G. Ross, Phys. Lett. B **648**, 201 (2007) [hep-ph/0607045].

[15] S. F. King and G. G. Ross, Phys. Lett. B **574**, 239 (2003) [hep-ph/0307190].

[16] G. Altarelli and F. Feruglio, Rev. Mod. Phys. **82**, 2701 (2010) [arXiv:1002.0211 [hep-ph]].

[17] H. Ishimori, T. Kobayashi, H. Ohki, Y. Shimizu, H. Okada and M. Tanimoto, Prog. Theor. Phys. Suppl. **183**, 1 (2010) [arXiv:1003.3552 [hep-th]]; Lect. Notes Phys. **858**, pp.1 (2012); Fortsch. Phys. **61**, 441 (2013).

[18] S. F. King and C. Luhn, Rept. Prog. Phys. **76**, 056201 (2013) [arXiv:1301.1340 [hep-ph]].

[19] C. S. Lam, Phys. Lett. B**656**, 193 (2007) [arXiv:0708.3665 [hep-ph]]; Phys. Rev. Lett. **101**, 121602 (2008) [arXiv:0804.2622 [hep-ph]]; Phys. Rev. D**78**, 073015 (2008) [arXiv:0809.1185 [hep-ph]]; W. Grimus, L. Lavoura and P. O. Ludl, J. Phys. G**36**, 115007 (2009) [arXiv:0906.2689 [hep-ph]].

[20] K. Abe *et al.* [T2K Collaboration], Phys. Rev. Lett. **107**, 041801 (2011) [arXiv:1106.2822 [hep-ex]].

[21] P. Adamson *et al.* [MINOS Collaboration], Phys. Rev. Lett. **107**, 181802 (2011) [arXiv:1108.0015 [hep-ex]].

[22] Y. Abe *et al.* [DOUBLE-CHOOZ Collaboration], Phys. Rev. Lett. **108**, 131801 (2012) [arXiv:1112.6353 [hep-ex]].

[23] F. P. An *et al.* [DAYA-BAY Collaboration], Phys. Rev. Lett. **108**, 171803 (2012) [arXiv:1203.1669 [hep-ex]].

[24] J. K. Ahn *et al.* [RENO Collaboration], Phys. Rev. Lett. **108**, 191802 (2012) [arXiv:1204.0626 [hep-ex]].

[25] S. -F. Ge, D. A. Dicus and W. W. Repko, Phys. Rev. Lett. **108**, 041801 (2012) [arXiv:1108.0964 [hep-ph]]; Phys. Lett. B **702**, 220 (2011) [arXiv:1104.0602 [hep-ph]].

[26] D. Hernandez and A. Y. Smirnov, Phys. Rev. D **86**, 053014 (2012) [arXiv:1204.0445 [hep-ph]]; Phys. Rev. D **87**, 053005 (2013) [arXiv:1212.2149 [hep-ph]]; arXiv:1304.7738 [hep-ph].

[27] B. Hu, Phys. Rev. D **87**, no. 3, 033002 (2013) [arXiv:1212.2819 [hep-ph]]; C. S. Lam, [arXiv:1301.3121 [hep-ph]];

P. Ballett, S. F. King, C. Luhn, S. Pascoli and M. A. Schmidt, arXiv:1308.4314 [hep-ph].

[28] T. Araki, H. Ishida, H. Ishimori, T. Kobayashi and A. Ogasahara, Phys. Rev. D **88**, 096002 (2013) [arXiv:1309.4217 [hep-ph]].

[29] K. S. Babu, Z. Phys. C **35**, 69 (1987).

[30] D. Espriu, J. Manzano and P. Talavera, Phys. Rev. D **66**, 076002 (2002) [hep-ph/0204085].

[31] D. Buttazzo, G. Degrassi, P. P. Giardino, G. F. Giudice, F. Sala, A. Salvio and A. Strumia, JHEP **1312**, 089 (2013) [arXiv:1307.3536].

[32] S. Eliezer and A. R. Swift, Nucl. Phys. B **105**, 45 (1976).

[33] B. T. Cleveland, T. Daily, R. Davis Jr., J. R. Distel, K. Lande, C. K. Lee, P. S. Wildenhain and J. Ullman, Astrophys. J. **496**, 505, (1998).

[34] Y. Fukuda *et al.* [Super-Kamiokande Collaboration], Phys. Rev. Lett. **81**, 1562 (1998) [hep-ex/9807003].

[35] K. Eguchi *et al.* [KamLAND Collaboration], Phys. Rev. Lett. **90**, 021802 (2003) [hep-ex/0212021].

[36] K. S. Babu, C. N. Leung and J. T. Pantaleone, Phys. Lett. B **319**, 191 (1993) [hep-ph/9309223]; P. H. Chankowski and Z. Pluciennik, Phys. Lett. B **316**, 312 (1993) [hep-ph/9306333]; J. A. Casas, J. R. Espinosa, A. Ibarra and I. Navarro, Nucl. Phys. B **573**, 652 (2000) [hep-ph/9910420].

[37] M. Lindner, M. Ratz and M. A. Schmidt, JHEP **0509**, 081 (2005) [hep-ph/0506280]; S. Antusch, J. Kersten, M. Lindner, M. Ratz and M. A. Schmidt, JHEP **0503**, 024 (2005) [hep-ph/0501272].

[38] G. Altarelli and F. Feruglio, Nucl. Phys. B **741**, 215 (2006) [hep-ph/0512103].

[39] B. Schoeneberg, "Elliptic Modular Functions - An Introduction", Springer-Verlag 1974; R.C. Gunning, "Lectures on Modular Forms", Princeton University Press 1962.

[40] R. de Adelhart Toorop, F. Feruglio and C. Hagedorn, Nucl. Phys. B **858**, 437 (2012) [arXiv:1112.1340 [hep-ph]].

[41] C. S. Lam, Phys. Rev. D **83**, 113002 (2011) [arXiv:1104.0055 [hep-ph]].

[42] R. d. A. Toorop, F. Feruglio and C. Hagedorn, Phys. Lett. B **703**, 447 (2011) [arXiv:1107.3486 [hep-ph]].

[43] F. Feruglio and A. Paris, JHEP **1103**, 101 (2011) [arXiv:1101.0393 [hep-ph]].

[44] G. -J. Ding, L. L. Everett and A. J. Stuart, Nucl. Phys. B **857**, 219 (2012) [arXiv:1110.1688 [hep-ph]].

[45] T. Araki, Prog. Theor. Phys. **117**, 1119 (2007) [arXiv:hep-ph/0612306]; T. Araki, T. Kobayashi, J. Kubo, S. Ramos-Sanchez, M. Ratz and P. K. S. Vaudrevange, Nucl. Phys. B **805**, 124 (2008) [arXiv:0805.0207 [hep-th]]; C. Luhn and P. Ramond, JHEP **0807**, 085 (2008) [arXiv:0805.1736 [hep-ph]].

[46] A. Blum, C. Hagedorn, M. Lindner, Phys. Rev. D **77**, 076004 (2008) [arXiv:0709.3450 [hep-ph]]; A. Blum, C. Hagedorn and A. Hohenegger, JHEP **0803**, 070 (2008) [arXiv:0710.5061 [hep-ph]]; C. Hagedorn and D. Meloni, Nucl. Phys. B **862**, 691 (2012) [arXiv:1204.0715 [hep-ph]].

[47] K. S. Babu and R. N. Mohapatra, Phys. Rev. Lett. **70**, 2845 (1993) [hep-ph/9209215].

[48] I. de Medeiros Varzielas and G. G. Ross, Nucl. Phys. B **733**, 31 (2006) [hep-ph/0507176]; B. Dutta, Y. Mimura and R. N. Mohapatra, Phys. Rev. D **80**, 095021 (2009) [arXiv:0910.1043 [hep-ph]].

[49] S. F. King, JHEP **1401**, 119 (2014) [arXiv:1311.3295 [hep-ph]].

[50] C. Hagedorn, M. Lindner and R. N. Mohapatra, JHEP **0606**, 042 (2006) [hep-ph/0602244].

[51] M. Holthausen and K. S. Lim, [arXiv:1306.4356 [hep-ph]].

[52] J. A. Escobar and C. Luhn, J. Math. Phys. **50**, 013524 (2009) [arXiv:0809.0639 [hep-th]].

[53] H. Ishimori and T. Kobayashi, Phys. Rev. D **85**, 125004 (2012) [arXiv:1201.3429 [hep-ph]].

[54] S. F. King, T. Neder and A. J. Stuart, arXiv:1305.3200 [hep-ph].

[55] J. H. Conway et. al., "Atlas of Finite Groups", Oxford University Press, 1985.

[56] H. S. M. Coxeter and W. O.J. Moser, "Generators and Relations for Discrete Groups", Springer-Verlag 1980.